Cathepsin G: A Novel Gene for the Regulation of Pain

LIU, Xiaodong

A Thesis Submitted in Partial Fulfilment

of the Requirements for the Degree of

Doctor of Philosophy

in

Anaesthesia and Intensive Care

The Chinese University of Hong Kong

September 2011

ProQuest LLC.
789 East Eisenhower Parkway
P.O. Box 1346
Ann Arbor, MI 48106 - 1346

Thesis/Assessment Committee

Professor Anna LEE (Chair)

Professor Matthew Tak-Vai CHAN (Thesis Supervisor)

Professor Christopher Hon-Ki CHENG (Committee Member)

Professor Wing-Ho YUNG (Committee Member)

Professor Karl Wah-Keung TSIM (External Examiner)

Abstract

Abstract of thesis entitled: **Cathepsin G: A Novel Gene for the Regulation of Pain**

Submitted by **LIU, Xiaodong**

For the degree of Doctor of Philosophy in Anaesthesia and Intensive Care

At the Chinese University of Hong Kong in September, 2011.

Objective: Spinal cord is an important part of the pain pathway. Nociceptive transmission is regulated by the ascending and descending neurons, local interneurons and glial cells within the dorsal horn of the spinal cord. Under pathological condition, transcriptional regulations in these cells cause synaptic plasticity in the spinal cord and contribute to the classical symptoms of chronic pain (e.g. hyperalgesia, allodynia and paresthesia). The purpose of this study was to identify differential gene expressions within spinal dorsal horn that contribute to the development and maintenance of chronic pain. The role of new nociceptive candidate gene was also evaluated using a series of *in vivo* and *in vitro* functional experiments and clinical association study.

Methods: Chronic pain was induced by intraplantar injection of complete Freund's adjuvant (CFA) into the hind paw of Sprague Dawley rats. Ipsilateral lumbar dorsal horn from control rats and rats with CFA induced pain were harvested for microarray analysis. A cutoff of 1.5-fold change and $p<0.05$ (Student's t test) was set for identifying the differential genes between rats with and without chronic pain. Functional annotation of differential genes was analyzed using Genomatix software suite (Genomatix Software GmbH, Michigan, USA). A new candidate gene was selected from the list of differential genes by literature research and quantitative real time polymerase chain reaction (RT PCR). Cellular and molecular experiments as well as *in vivo* animal studies were performed to investigate the molecular function of the candidate gene.

Genotyping of related single nucleotide polymorphisms (SNPs) was performed to explore their association with postoperative pain in patients undergoing major abdominal surgery.

Results: CFA caused heat hyperalgesia in the ipsilateral paw after injection. The microarray analysis revealed 391 genes with at least 1.5-fold changes in messenger ribonucleic acid (mRNA) level after CFA induced chronic pain. A total of 188 (48%) genes were up-regulated and 203 (52%) genes were down-regulated in rats with chronic pain. 169 (43%) genes were known genes according to the National Center for Biotechnology Information gene database. Cluster analysis showed that 25 of 169 (15%) known genes were involved in the regulation of gene expression and 10 of 169 (6%) were known genes that belonged to the proteases or protease inhibitors family. Also, genes involved in the endogenous pain control system such as cytokine production, cellular biogenic amine metabolic process and glucocorticoid receptor related signaling pathway were identified in this study. Literature research and quantitative RT PCR suggested cathepsin G was a candidate gene expressed in the spinal cord that is important in the regulation of pain. Functional study showed that cathepsin G activated signaling pathways for p38 mitogen-activated protein kinase (p38MAPK)-cAMP response element-binding (CREB), inhibitor of kappa B (IκB)-nuclear factor kappa light chain enhancer of activated B cells (NFκB). Cathepsin G also up-regulated the mRNA expressions of interleukin 6 (IL6) and matrix metallopeptidase 9 (MMP9) in C6 glioma cells. Treatment of Cathepsin G increased phosphorylation of p38MAPK, IκB and signal transducer and activator of transcription 3 (STAT3) in primary spinal astrocytes. Quantitative RT PCR studies showed that cathepsin G promoted p38MAPK dependent gene expressions of IL6 and MMP in primary astrocytes. Blockade of cathepsin G using subcutaneous injection of cathepsin G inhibitor however, attenuated heat hyperalgesia after CFA induced pain in rats. Finally, in a cohort of patients undergoing major abdominal surgery, mutation of

rs2237642 in cathepsin G gene was associated with the occurrence of severe postoperative pain.

Conclusions: Transcriptional regulation is an important event in the dorsal horn of the spinal cord during the development and maintenance of chronic pain. Cathepsin G is a key element in this transcriptional process. The microarray analysis, *in vitro* and *in vivo* experiments and clinical association study demonstrate that cathepsin G is a novel gene involved in the development of chronic pain.

中文摘要

目的: 脊髓是疼痛通路的重要組成部分。痛覺的傳導受脊髓內上行神經元、下行神經元、中間神經元以及膠質細胞共同調控。在病理性疼痛條件下,基因轉錄水準的改變可調節神經突觸可塑性並參與產生疼痛症狀(如痛覺過敏、痛覺超敏及感覺異常)。 本研究的目的是鑒定脊髓中負責慢性痛建立和維持的差異基因,同時通過一系列體內、體外功能學實驗和臨床關聯研究對新的疼痛候選基因進行功能評價。

方法:福氏完全佐劑 （CFA）注射大鼠左後腳腳掌誘導慢性疼痛。疼痛行為學檢驗後,分別從對照大鼠和慢性疼痛大鼠中截取左側腰椎背角脊髓,並進行基因表達晶片分析。在兩組大鼠中平均表達水準相差至少 1.5 倍且 p 值小於 0.05(Student's t test)者定義為差異基因。差異基因的功能注釋用 Genomatix 套裝軟體進行(Genomatix Software GmbH, Michigan, USA)。一個新的候選基因通過文獻研究和即時定量聚合酶鏈式反應(PCR)選定,並通過細胞和分子生物學以及動物實驗評價其功能。同時對相關單核苷酸多態性位點進行基因型的分析,並比較其與實施腹部手術病人產生術後疼痛的相關性。

結果: CFA 注射 4 天後導致大鼠對熱的痛覺過敏。基因晶片分析鑒定出 391 個差異基因。在疼痛大鼠脊髓中,共有 188(48%)個差異基因表達被上調,203(52%)個差異基因表達被下調。

根據 NCBI 基因數據庫,總共有 169 個基因屬於已知基因。歸類分析表明,169 個已知基因中有 25(15%)個基因屬於基因表達調控亞群,10(6%)個基因屬於蛋白酶或蛋白酶抑制劑家族。另外,還有相當一部分基因歸屬於內源性疼痛調節系統,如參與細胞因數產生和細胞生物合成單胺物質代謝過程的基因,以及糖皮質激素受體信號通路相關的基因。文獻研究和即時定量 PCR 研究表明 cathepsin G 是一個候選疼痛相關基因。功能研究表明 cathepsin G 可以啟動 C6 膠質細胞內 p38MAPK-CREB 以及 IκB- NFκB 信號通路,並上調 IL6 和 MMP9 mRNA 水準的表達。同時,cathepsin G 也可以上調元代脊髓星狀膠質細胞中 p38MAPK, IκB 和 STAT3 的磷酸化水準。即時定量 PCR 分析表明 cathepsin G 也可以促進元代細胞中 IL6 和 MMP9 的表達,並且這種作用是依賴 p38MAPK 活性的。 動物實驗則表明,皮下注射 cathepsin G 抑制劑可以減輕 CFA 導致的疼痛。最後, 臨床研究表明 cathepsin G rs2237642 位點的基因型與腹部手術後病人產生急性疼痛成顯著性相關。

結論:脊髓中的轉錄調控是慢性疼痛建立和維持的重要環節,而 cathepsin G 則是轉錄調節過程中的關鍵因素之一。基因表達晶片分析、體內體外實驗, 以及臨床關聯研究的結果表明 cathepsin G 是一個新的促進炎症痛的基因。

Declaration of origination

The work contained in this thesis is the original research carried out by the author in the Department of Anaesthesia and Intensive Care, Faculty of medicine, The Chinese University of Hong Kong. No part of the work described in this dissertation has already been or is being submitted to any other degree, diploma or other qualification at this or any other institution.

Abstract

Objective: Spinal cord is an important part of the pain pathway. Nociceptive transmission is regulated by the ascending and descending neurons, local interneurons and glial cells within the dorsal horn of the spinal cord. Under pathological condition, transcriptional regulations in these cells cause synaptic plasticity in the spinal cord and contribute to the classical symptoms of chronic pain (e.g. hyperalgesia, allodynia and paresthesia). The purpose of this study was to identify differential gene expressions within spinal dorsal horn that contribute to the development and maintenance of chronic pain. The role of new nociceptive candidate gene was also evaluated using a series of *in vivo* and *in vitro* functional experiments and clinical association study.

Methods: Chronic pain was induced by intraplantar injection of complete Freund's adjuvant (CFA) into the hind paw of Sprague Dawley rats. Ipsilateral lumbar dorsal horn from control rats and rats with CFA induced pain were harvested for microarray analysis. A cutoff of 1.5-fold change and $p<0.05$ (Student's t test) was set for identifying the differential genes between rats with and without chronic pain. Functional annotation of differential genes was analyzed using Genomatix software suite (Genomatix Software GmbH, Michigan, USA). A new candidate gene was selected from the list of differential genes by literature research and quantitative real

time polymerase chain reaction (RT PCR). Cellular and molecular experiments as well as *in vivo* animal studies were performed to investigate the molecular function of the candidate gene. Genotyping of related single nucleotide polymorphisms (SNPs) was performed to explore their association with postoperative pain in patients undergoing major abdominal surgery.

Results: CFA caused heat hyperalgesia in the ipsilateral paw after injection. The microarray analysis revealed 391 genes with at least 1.5-fold changes in messenger ribonucleic acid (mRNA) level after CFA induced chronic pain. A total of 188 (48%) genes were up-regulated and 203 (52%) genes were down-regulated in rats with chronic pain. 169 (43%) genes were known genes according to the National Center for Biotechnology Information gene database. Cluster analysis showed that 25 of 169 (15%) known genes were involved in the regulation of gene expression and 10 of 169 (6%) were known genes that belonged to the proteases or protease inhibitors family. Also, genes involved in the endogenous pain control system such as cytokine production, cellular biogenic amine metabolic process and glucocorticoid receptor related signaling pathway were identified in this study. Literature research and quantitative RT PCR suggested cathepsin G was a candidate gene expressed in the spinal cord that is important in the regulation of pain. Functional study showed that cathepsin G activated signaling pathways for p38 mitogen-activated protein kinase

(p38MAPK)-cAMP response element-binding (CREB), inhibitor of kappa B (IκB)-nuclear factor kappa light chain enhancer of activated B cells (NFκB). Cathepsin G also up-regulated the mRNA expressions of interleukin 6 (IL6) and matrix metallopeptidase 9 (MMP9) in C6 glioma cells. Treatment of Cathepsin G increased phosphorylation of p38MAPK, IκB and signal transducer and activator of transcription 3 (STAT3) in primary spinal astrocytes. Quantitative RT PCR studies showed that cathepsin G promoted p38MAPK dependent gene expressions of IL6 and MMP in primary astrocytes. Blockade of cathepsin G using subcutaneous injection of cathepsin G inhibitor however, attenuated heat hyperalgesia after CFA induced pain in rats. Finally, in a cohort of patients undergoing major abdominal surgery, mutation of rs2237642 in cathepsin G gene was associated with the occurrence of severe postoperative pain.

Conclusions: Transcriptional regulation is an important event in the dorsal horn of the spinal cord during the development and maintenance of chronic pain. Cathepsin G is a key element in this transcriptional process. The microarray analysis, *in vitro* and *in vivo* experiments and clinical association study demonstrate that cathepsin G is a novel gene involved in the development of chronic pain.

中文摘要

目的: 脊髓是疼痛通路的重要組成部分。痛覺的傳導受脊髓內上行神經元、下行神經元、中間神經元以及膠質細胞共同調控。在病理性疼痛條件下,基因轉錄水準的改變可調節神經突觸可塑性並參與產生疼痛症狀(如痛覺過敏、痛覺超敏及感覺異常)。 本研究的目的是鑒定脊髓中負責慢性痛建立和維持的差異基因,同時通過一系列體內、體外功能學實驗和臨床關聯研究對新的疼痛候選基因進行功能評價。

方法:福氏完全佐劑 （CFA）注射大鼠左後腳腳掌誘導慢性疼痛。疼痛行為學檢驗後,分別從對照大鼠和慢性疼痛大鼠中截取左側腰椎背角脊髓,並進行基因表達晶片分析。在兩組大鼠中平均表達水準相差至少 1.5 倍且 p 值小於 0.05(Student's t test)者定義為差異基因。差異基因的功能注釋用 Genomatix 套裝軟體進行(Genomatix Software GmbH, Michigan, USA)。一個新的候選基因通過文獻研究和即時定量聚合酶鏈式反應(PCR)選定,並通過細胞和分子生物學以及動物實驗評價其功能。同時對相關單核苷酸多態性位點進行基因型的分析,並比較其與實施腹部手術病人產生術後疼痛的相關性。

結果: CFA 注射 4 天後導致大鼠對熱的痛覺過敏。基因晶片分析鑒定出 391 個差異基因。在疼痛大鼠脊髓中,共有 188(48%)個差異基因表達被上調,203(52%)個差異基因表達被下調。根據 NCBI 基因數據庫,總共有 169 個基因屬於已知基因。歸類分析表明,169 個已知基因中有 25(15%)個基因屬於基因表達調控亞群,10(6%)

個基因屬於蛋白酶或蛋白酶抑制劑家族。另外,還有相當一部分基因歸屬於內源性疼痛調節系統,如參與細胞因數產生和細胞生物合成單胺物質代謝過程的基因,以及糖皮質激素受體信號通路相關的基因。文獻研究和即時定量 PCR 研究表明 cathepsin G 是一個候選疼痛相關基因。功能研究表明 cathepsin G 可以啟動 C6 膠質細胞內 p38MAPK-CREB 以及 IκB- NFκB 信號通路,並上調 IL6 和 MMP9 mRNA 水準的表達。同時,cathepsin G 也可以上調元代脊髓星狀膠質細胞中 p38MAPK, IκB 和 STAT3 的磷酸化水準。即時定量 PCR 分析表明 cathepsin G 也可以促進元代細胞中 IL6 和 MMP9 的表達,並且這種作用是依賴 p38MAPK 活性的。 動物實驗則表明,皮下注射 cathepsin G 抑制劑可以減輕 CFA 導致的疼痛。最後, 臨床研究表明 cathepsin G rs2237642 位點的基因型與腹部手術後病人產生急性疼痛成顯著性相關。

結論:脊髓中的轉錄調控是慢性疼痛建立和維持的重要環節,而 cathepsin G 則是轉錄調節過程中的關鍵因素之一。基因表達晶片分析、體內體外實驗, 以及臨床關聯研究的結果表明 cathepsin G 是一個新的促進炎症痛的基因。

Acknowledgements

I would like to express my sincere appreciation to Professor Matthew Chan for giving me the precious chance to join in this interesting research. I would like to thank his valuable time, enduring patience, inspiring guidance, sustained support and encouragement through all the stages of my study. I would also like to thank Professor Christopher Cheng from the School of Biomedical Sciences, the Chinese University of Hong Kong, who had introduced me to this project, for his valuable time, enlightening discussion and technical supports in the past three years.

I would like to extend thanks to my beloved families; their support and understanding are source of my energy. In particular, I must give my whole-hearted thanks to my wife, Yujuan Dong, for her technical suggestion and support.

I wish to thank all my colleagues in the Department of Anaethesia and Intensive care. I would like to give my gratitude to my fellow classmates, Yan Chen, Qinzhou Wang and Quanmeng Liu, for their advice and support in the animal studies. I would like to thank Amy Meng and Yuanyuan Tian for their help in the clinical study and data analysis. Also, I am grateful to Dr Belinda Wong and all the research assistants, Matthew Tsang, Joy Yip, Angela Miu and Ming Wai Tsang, for all their hard work in patient recruitment and clinical data collection. Finally, I thank Pet Tan for sharing the laboratory with us and keeping it clean and tidy.

Table of Contents

List of Tables

List of Figures

Abbreviations

Ace2	angiotensin I converting enzyme (peptidyl-dipeptidase A) 2
ACTB	β-actin
AIF1L	allograft inflammatory factor 1-like
ANOVA	analysis of variance
ATF2	activating transcription factor 2
BDNF	brain derived neurotrophic factor
BSA	bovine serum albumin
CCI	chronic constriction injury
CCL5	chemokine (C-C motif) ligand 5
cDNA	complimentary deoxyribonucleic acid
CFA	complete Freund's adjuvant
c-fos	FBJ osteosarcoma oncogene
CGRP	calcitonin gene related peptide
CI	confidence interval
CNS	central nervous system
COMT	catechol-*O*-methyltransferase
CREB	cAMP response element-binding
CRH	corticotropin-releasing hormone
Ct	cycle threshold
CTSG	cathepsin G
Cy3-CTP	cyanine 5-cytosine triphosphate
DAPI	4',6-diamidino-2-phenylindole
DEPC	diethylpyrocarbonate
DLF	dorsolateral fasciculus

DMEM	Dulbecco's modified Eagle medium
DMSO	dimethyl sulfoxide
dNTPs	deoxyribonucleotide triphosphastes
DREAM	downstream regulatory element antagonist modulator
DRG	dorsal root ganglion
EDTA	ethylenediaminetetraacetic acid
EGF	epidermal growth factor
Erk1/2	extracellular signal regulated kinases 1/2
FBS	fetal bovine serum
GABA	gamma-aminobutyric acid
GATA3	GATA binding protein 3
GFAP	glial fibrillary acidic protein
GluR1	glutamate receptor 1
GPCR	G protein-coupled receptor
HBSS	Hank's balanced salt solution
HCL	hierarchical cluster
HWE	Hardy-Weinberg equilibrium
ICAM	intercellular adhesion molecule
IL	interleukin
IκB	inhibitor of kappa B
JNK	c-Jun N-terminal kinase
LPS	lipopolysaccharide
mBPI	modified brief pain inventory
MMP	matrix metallopeptidase
NCBI	National Center for Biotechnology Information

NFκB	nuclear factor kappa light chain enhancer of activated B cells
NMDAR	*N*-methyl-*D*-asparate receptor
p38MAPK	p38 mitogen-activated protein kinase
PAG	periaqueductal gray
PAR	protease-activated receptor
PBS	phosphate buffered saline
PDYN	prodynorphin
PFA	paraformaldehyde
PKC	protein kinase C
PSD	post-synaptic density
PTPRC	protein tyrosine phosphatase receptor type C
PWL	paw withdrawal latency
RANKL	receptor activator of nuclear factor-κB ligand
RIN	RNA integrity number
RIPA	radio-immunoprecipitation assay
rRNA	ribosomal ribonucleic acid
RT	real time
RT PCR	Reverse transcription polymerase chain reaction
RVM	rostral ventral medulla
S100	S100 calcium binding protein
SEM	Standard error of the mean
SERPINE1	serpin peptidase inhibitor clade E member 1
slc18a2	solute carrier family 18 (vesicular monoamine) member 2
SNPs	single nucleotide polymorphisms
STAT3	signal transducer and activator of transcription 3

TBST	tris-buffered saline containing Tween-20
TIMP1	tissue inhibitor of metalloproteinases 1
TLRs	toll-like receptors
TNFα	tumor necrosis factor alpha
TPCK	tosyl phenylalanyl chloromethyl ketone
TRPV1	transient receptor potential vanilloid 1
VAS	visual analogue scale

Part 1 Mechanism of pain: A Review

Chapter 1-1 Background

1.1.1 Pain pathways

Pain is a protective mechanism to prevent individuals from further damage. After a noxious stimulus, nociceptive signal travels from peripheral tissue to the somatosensory cortex of the brain through the ascending pain pathway (Basbaum et al., 2009). In humans, the ascending pathway consists of three orders of neurons (Purves et al., 2001). The first order neurons, known as the nociceptors, are initiated from peripheral tissue with their dendrites connecting with the peripheral tissue and receive noxious stimuli from the environment. The cell bodies of many nociceptors join together to form the dorsal root ganglion (DRG). The axons of nociceptors are derived from the DRG and terminate in the grey matter of spinal cord dorsal horn where they synapse on to the second order neurons. The second order neuron fibers send their axons into spinothalamic tract in the contralateral anterolateral column of the spinal cord and project to the thalamus. The third order neurons after synapse with the second order axons in the thalamus, project their fibers into somatosensory cortex where the nociceptive perception is formed (Figure 1-1a).

In addition to ascending pain pathway, the nociceptive transmission is also regulated by descending pain pathways (Ossipov et al., 2010). After activation, the ascending second order neurons also send signals to the neurons of descending pain

pathways and therefore activate descending pain control systems (Basbaum et al., 2009). In contrast to ascending pathway, the neurons in descending modulatory pathways include the inhibitory and the facilitatory pathways. Both of them have inputs from multiple areas in brain such as the periaqueductal gray (PAG) and the rostral ventral medulla (RVM). Descending pathways then project down along the dorsolateral fasciculus (DLF) to the spinal cord dorsal horn where they modulate the signals from the ascending neurons by making synaptic connection with the neurons in the spinal cord (Ossipov et al., 2010). The descending neurons then produce neuromodulators such as gamma-aminobutyric acid (GABA), glycine, serotonin and norepinephrine which exert either pro- or anti-nociceptive effects (Ossipov et al., 2010).

Finally, the local nerve cells including interneurons and glial cells are also regulators of nociceptive transmission in the spinal cord. The interneurons are small neurons in the grey matter of spinal cord where they synapse with the descending neurons, the second order neurons and the central terminus of the nociceptors. The inhibitory interneurons decrease the firing rate of ascending neurons either by attenuating the excitatory neurotransmitters release from nociceptors or increasing the release of inhibitory neurotransmitters (e.g. GABA and glycine) and endogenous opioid peptides (e.g. enkephalin) (Pertovaara and Almeida, 2006). The glial cells,

especially astrocytes, are major cell pools in the spinal cord. Glial cells does not seem to participate during "normal" nociception, because neither microglial cells nor astrocytes inhibitors affects nociceptive response (Padi and Kulkami 2008; Wei et al., 2008). However, during chronic pain, changes on glial cells lead to abnormal neurotransmitter metabolism and inflammatory molecules release, by then, they play important roles in nociceptive transmission (Milligan and Watkins et al., 2009).

In summary, spinal cord dorsal horn is an important part of nociceptive transmission. Both pro-nociceptive and anti-nociceptive signals from nociceptors, descending neurons, local glial cells and local interneurons are integrated in the spinal cord. Only the "net" signals were transmitted to the third-order neurons and contribute to the final extent of pain perception (Figure 1-1b).

Figure 1-1. Schematic representation of the pain pathways. a: Ascending pain pathway and descending pain pathways. Nociceptors (first order neurons) from ascending pain pathway transform environmental noxious stimulus to action potentials in their receptors. The noxious signals are then conveyed to the ascending second order neurons in the spinal cord. The second order neurons synapse with the third order neurons in the thalamus. The third order neurons convey the noxious signals to the somatosensory cortex where pain is perceived. In contrast, neurons from descending pain pathway arise from several areas of brain (e.g. periaqueductal gray and rostral ventral medulla), and then project to the spinal cord where they synapse with the ascending second order neurons. **b:** Cell-cell communication within superficial spinal cord dorsal horn. The ascending second order neurons receive signals from nociceptors, descending neurons, interneurons, microglial cells, astrocytes and infiltrated immune cells. The integration of multiple signals decides the final output of second order neurons in the thalamus.

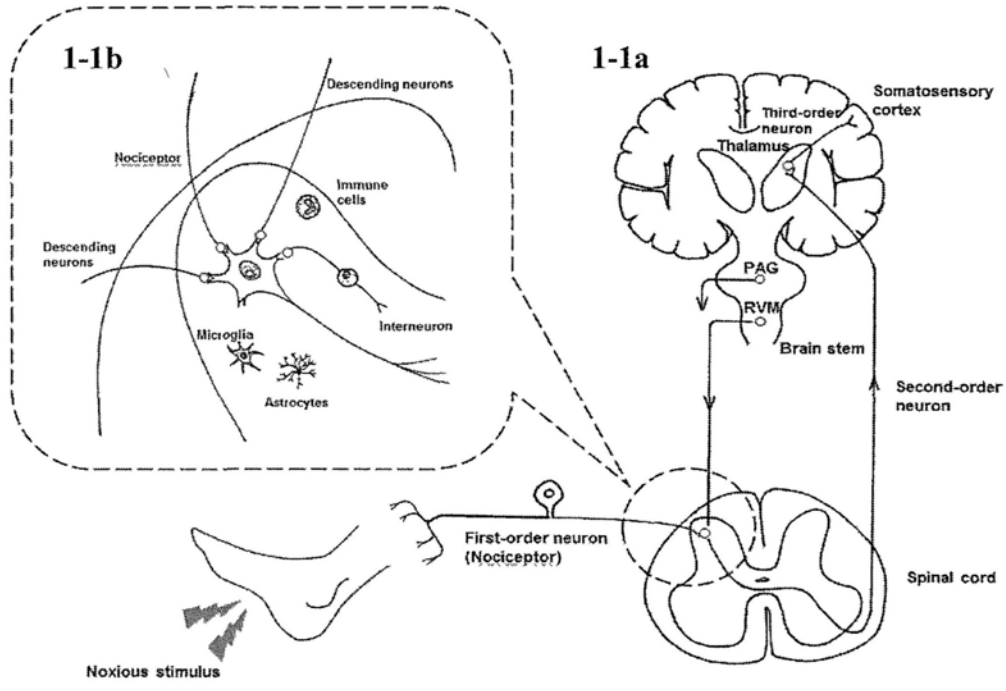

PAG = periaqueductal gray; RVM = rostral ventral medulla

1.1.2 Chronic pain syndrome

Abnormal regulation on either inhibitory signals or facilitation signals may result in chronic pain. Clinically, this is commonly defined as pain >3-6 months in duration. Chronic pain syndromes are usually characterized by any of the following features:

(1) Hyperalgesia: increased response to a painful stimulus;

(2) Allodynia: pain from stimuli which are not normally painful;

(3) Paresthesia: spontaneous perception of tingling, pricking or numbness of the skin.

1.1.3 Mechanisms of chronic pain syndrome

A number of mechanisms of chronic pain syndrome have been proposed.

1.1.3.1 Peripheral sensitization

This refers to the change in the characteristics of nociceptors. Following local inflammation, a large number of immune cells, including neutrophils, macrophages, mast cells and T cells are recruited. Once activated these immune cells release a battery of pro-inflammatory mediators such as cytokines and chemokines. These molecules subsequently act on receptors of the peripheral nerve endings, leading to sensitization of nociceptor. For example, tumor necrosis factor alpha (TNFα) binds to

TNF receptors and increases the amplitudes of transient receptor potential vanilloid 1 (TRPV1) current (p38MAPK and protein kinase C (PKC) dependent process) in the nociceptors (Constantin et al., 2008). This may lead to an increase in the firing rate of the nociceptors, resulting in an increase in signal output. Other cytokines such as IL1β and IL6, as well as chemokine (e.g. fractalkine and chemokine (C-C motif) ligand 5 (CCL5)) are well-known triggers of pain hypersensitivity because of their direct effects in the nociceptors (Binshtok et al., 2008; Obreja et al., 2002; Melemedjian et al., 2010; Oh et al., 2001). Moreover proteases, as another subset of inflammatory mediators, are released from immune cells and are important in the peripheral sensitization. For example, matrix metalloproteinases (MMP), such as MMP9, sensitize nociceptors by processing IL1β in DRG or facilitating macrophages migration (Kawasaki et al., 2008; Shubayev et al., 2006).

1.1.3.2 Central sensitization

In contrast to peripheral sensitization, central sensitization refers to the change in the characteristics of ascending neurons, leading to an increase in excitability (hyperalgesia) or a decrease in excitatory threshold (allodynia) of these neurons in the nervous system. In the spinal cord, this mainly refers to the changes of second order neurons as a result of abnormal regulations from other cells:

1. Increased nociceptive transmission in second order neurons may be caused by abnormal release of neurotransmitters and neuromodulators from nociceptors. For example, up-regulated messenger ribonucleic acid (mRNA) of pro-nociceptive neuropeptides (e.g. calcitonin gene related peptide (CGRP) and substance P) could lead to direct nociceptive transmission of ascending neurons (Priestley et al., 2002). Dysfunctional calcium channels on the central terminal of nociceptors lead to an increase in the release of glutamate and neuropeptides which in turn, increase the firing rate of second order neurons (Fukuizumi et al., 2003; Pietrobon 2010).
2. Spinal inhibitory interneurons are a source of inhibitory neurotransmitters and other endogenous analgesic peptides. Loss of inhibitory interneurons, as a result of apoptosis, increases the firing rate of second order neurons. There is also a decrease in the level of inhibitory neurotransmitters such as GABA and glycine in spinal cord. Blockade of apoptosis has been shown to reverse chronic pain in animals (Scholz et al., 2005; Meisner et al., 2010).
3. Abnormal descending pain pathways contribute to central sensitization in spinal cord. In this regard, a decrease in serotonin level from descending inhibitory neurons has been observed in many neuropathic pain studies (Goettl et al., 2002; Hains et al., 2002; Sounvoravong et al., 2004; Liu et al., 2010). Consistent with

these findings, the mRNA expression of spinal serotonin receptor isoform was down-regulated in neuropathic pain model (Nakae et al., 2008). Induction of inflammation on neonatal rats also causes changes in descending modulation from RVM and may contribute to hyperalgesia (Zhang et al., 2010).

4. Activation of spinal glial cells after pain may be important in central sensitization. Glial cells are required for the development and maintenance of chronic pain following initial tissue inflammation and damage. The most important role of the glial cells after activation is the regulation of inflammatory milieu in the nervous system (Watkins et al., 2001). The glial cells, including microglial cells and astrocyte, release a large number of pro-inflammatory mediators in the spinal cord. The mediators include small molecular chemicals (e.g. nitric oxide), cytokines (e.g. IL1β, TNFα and IL6), chemokines (e.g. monocyte chemoattractant protein-1 (MCP-1)) and extracellular proteases (e.g. MMP2 and MMP9). Similar to the situation in the peripheral tissue, inflammatory mediators can also sensitize the second order neurons, leading to central sensitization. A study using spatial knockout of the *N*-methyl-D-asparate receptor (NMDAR) in the spinal dorsal horn neurons (including second order neurons) revealed that addition of IL1β and its downstream signaling transduction on spinal neurons could still produce nociceptive transmission. This study suggested that inflammatory mediators are

important in the maintenance of allodynia (Weyerbacher et al., 2009). IL1β was also thought to be responsible for the phosphorylation of NMDAR subunit and may increase NMDAR activity and result in hyperalgesia (Zhang et al., 2008). Similarly, in response to peripheral tissue inflammation, TNFα was rapidly released from spinal glial cells. TNFα facilitates glutamate receptor 1 (GluR1) subunit insertion in the post-synaptic density (PSD) of the second order neurons, and is responsible for pain hypersensitivity (Choi et al., 2010). Finally, proteases derived from activated glial cells are also important because of their roles in cytokines processing. It was reported that MMP2 and MMP9 were responsible for IL1β cleavage in spinal cord and this activity was required for the development and maintenance of spinal nerve ligation induced chronic pain (Kawasaki et al., 2008). All these data show that glial cells derived inflammatory mediators can directly regulate the second order neurons in the spinal cord and thus contribute to central sensitization during chronic pain.

5. Migration of blood borne immune cells in the spinal cord after inflammation or nerve injury may regulate the nociceptive transmission of second order neurons. Depending on the pain model, different immune cells have been shown to migrate into the spinal cord (Ren and Dubner 2010). Following partial sciatic nerve ligation, peripheral macrophages or monocytes migrate into the spinal cord and

differentiate into microglial-like cells, contributing to chronic pain (Zhang et al., 2007). Large number of T cells is seen in spinal cord in response to spared nerve injury and contribute to interferon-γ dependent chronic pain syndrome (Costigan et al., 2009). In another model producing inflammatory pain, the neutrophils migration has been observed in response to peripheral inflammation (Mitchell et al., 2008). However, the role of neutrophils is not clear.

In summary, the nociceptive transmission of ascending pain pathway can be regulated under a number of pathological conditions. The altered endogenous pain control system causes changes in descending neurons, local interneurons, glial cells and migrated immune cells. These changes act on ascending second order neurons in the spinal cord. All these events lead to either an increase in excitability (hyperalgesia) or a decrease in excitatory threshold (allodynia) of the neurons. Study on spinal cord using genome wide method may reveal the alterations of the endogenous pain control system and is helpful in identifying new candidate for analgesic development.

Chapter 1-2 Hypothesis and objectives

Current data suggest that genes involved in endogenous pain control system such as endogenous analgesics and regulatory genes of neuromodulators play an important role in the development of chronic pain. Also, proteases from glial cells are recently identified as a new subset of genes involved in the mechanism of central sensitization during the development of chronic pain. However, no genome wide studies have specifically focused on these two subsets of genes in the spinal cord during the development and maintenance of chronic pain. Furthermore, the immune cells, which might be the source of endogenous analgesics and proteases, are largely excluded with perfusion during tissues harvest in many recent microarray studies. This will result in data loss. In this study, I hypothesized that:

1. Endogenous analgesic molecules such as opioid peptides could be transcriptionally regulated during chronic pain;
2. The level of modulators derived from descending pain pathways could be regulated by genes controlling metabolic pathway and membrane transporters in the spinal cord, and such genes could be transcriptionally regulated during chronic pain;
3. Proteases or proteases inhibitors may alter the development of chronic pain due to their inflammatory regulation within spinal cord.

To identify these differential genes, microarray analysis on lumbar dorsal horn from rats with and without chronic pain was planned. To preserve all the differential genes, including those introduced by immune cells migration, tissues were harvested without perfusion. After microarray analysis, bioinformatics analysis was done to cluster the differential genes involved in endogenous pain control system or belong to proteases and protease inhibitors family. Literature research and quantitative RT PCR were done to select new nociceptive gene during chronic pain. The selected candidate was evaluated using molecular and cellular biology methods (Quantitative reverse transcription polymerase chain reaction (RT PCR), Western blot, Taqman genotyping and primary cell culture), as well as pain behavioral testing in animals (Figure 1- 2). The main objectives were:

1. to identify differential genes involved in endogenous pain control system during chronic pain;
2. to identify new proteases and protease inhibitors within the spinal cord during chronic pain, including those introduced by immune cells migration;
3. to examine whether the new candidate exerts pro-inflammatory potentials on spinal astrocytes *in vitro*;
4. to validate the pro-nociceptive effects of the new candidate gene on animals;
5. to investigate the clinical implications of this candidate gene.

Figure 1-2. Flow chart on identification of differential genes and evaluation of new nociceptive gene.

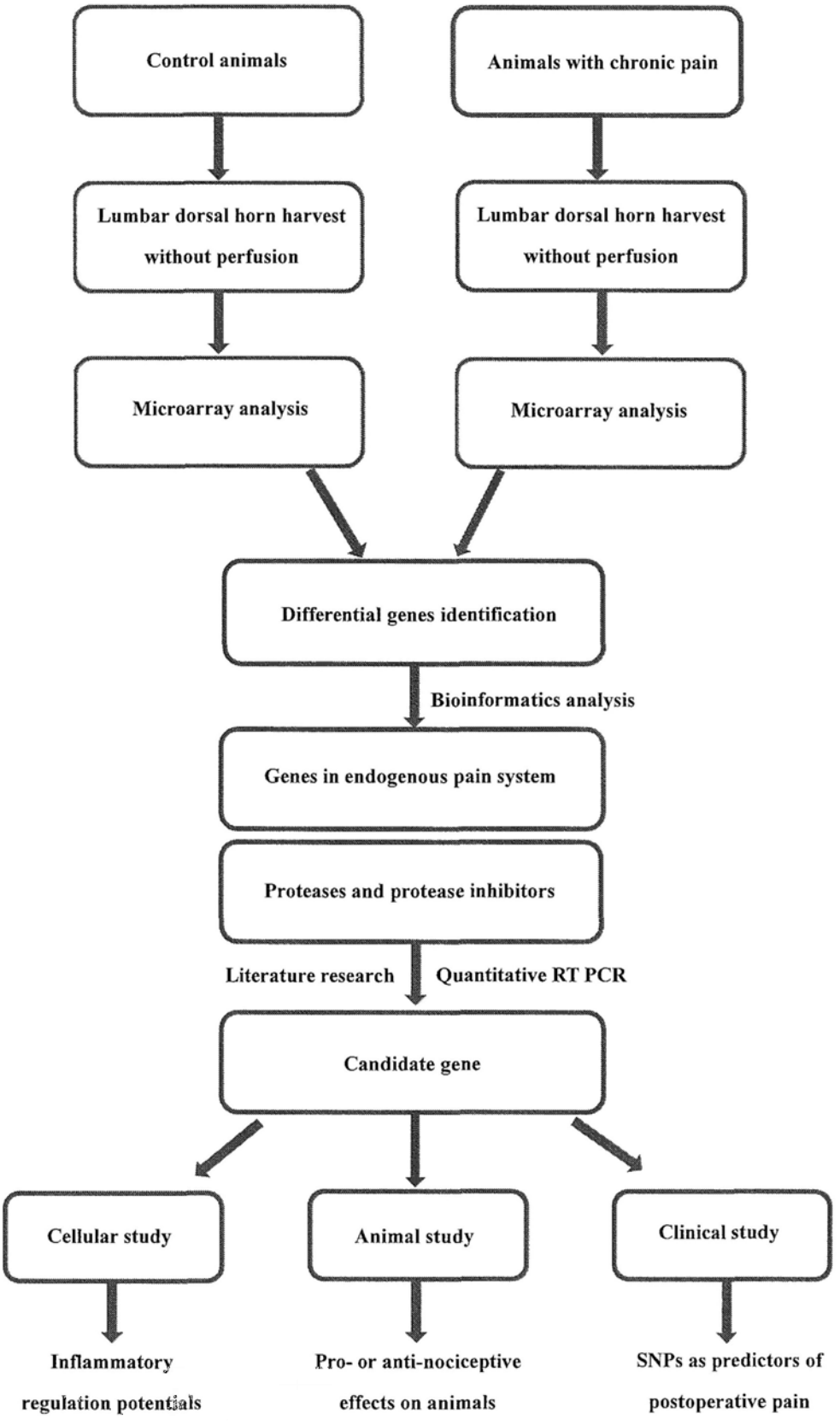

Part 2 Genome wide transcription profile of the dorsal horn in complete Freund's adjuvant induced chronic pain

Chapter 2-1 Introduction

Spinal cord is an essential part of the pain pathway. As the second order of ascending pain pathway, the wide range dynamic type of neurons in the spinal cord dorsal horn receives both anti-nociceptive and pro-nociceptive signals, coming from peripheral nociceptors (first order), local interneurons, glial cells and descending modulatory cells (Kuner 2010). Only the net signals after integration of all these signals will be sent to the third order neurons of the pain pathway in the somatosensory cortex where the pain is perceived. Therefore, the study on spinal cord may reveal the control of pain pathway.

Transcriptional regulation is an important event in the spinal cord during the development of chronic pain syndrome (Woolf and Costigan 1999). In response to peripheral tissue or nerve injury, there is release of neurotransmitters or neuromodulators from nociceptors, glial cells or descending neurons. These molecules activate the receptors in the neurons and glial cells, leading to the downstream signal transduction, transcription, and changes of gene expression in the spinal cord. The change of gene expression will further contribute to synapse plasticity and central sensitization in spinal cord (Kuner 2010).

Endogenous pain control system is important during the development of chronic pain. The neurons in the spinal cord dorsal horn such as inhibitory interneurons

release a large number of molecules that can inhibit nociceptive transmission of ascending pain pathway. One example is prodynorphin (PDYN), the expression of which is regulated by transcription repressor downstream regulatory element antagonist modulator (DREAM). Knockout of DREAM attenuates pain perception in almost all animal models for chronic pain, presumably based on the PDYN dependent mechanism (Cheng et al., 2002). In addition, it has been shown that leukocytes migration provided analgesia by producing opioid peptides (Rittner et al., 2005). The latter experiment indicated that immune cells could be another source of modulators for endogenous pain control. Therefore, further studies to identify such endogenous modulators will be helpful to understand the mechanism of chronic pain and may highlight new candidates of analgesics. Descending pain pathways derived from cerebral cortex have also been shown to modulate chronic pain. The neurons in the cortex are able to release different neuromodulators such as endogenous cannabinoids and neurotransmitters (such as GABA, glycine, norepinephrine and serotonin), all of which may interfere with nociceptive transmission (Michael et al., 2010). The levels of these modulators in spinal cord can be regulated by either the modulator synthesis pathways or the membrane transporters (including re-uptake channels or secretion channels). Therefore, it is reasonable to consider that altered expression of such channels or modulators synthesis pathway genes will contribute to the pain control.

Identification of these differential genes would offer insights for the new targets in the development of analgesics.

In addition, proteases are important inflammatory mediators (Pham 2006; Sharony et al., 2010). Recently, several proteases were identified as important pain modulators in the spinal cord. These proteases include the cysteine protease cathepsin S, MMP2 and MMP9. Cathepsin S is up-regulated in the spinal microglial cells (or macrophages) and contributes to the transmembrane chemokine (fractalkine) release. Based on a p38MAPK dependent mechanism, cathepsin S induces allodynia in mice after peripheral nerve injury (Clark et al., 2006). MMP2 and MMP9 are up-regulated in the astrocytes and microglial cells, respectively. The up-regulation of both MMP2 and MMP9 could lead to IL1β cleavage in the spinal cord and thus produce pain in the animals (Kawasaki et al., 2008). These results strongly suggest that proteases are involved in chronic pain because of their proteolytic activities. On the other hand, as the counterparts, endogenous proteases inhibitors may act in the opposite fashion during chronic pain. Therefore, identification of differential expressions of proteases and protease inhibitors in the spinal cord during the development of chronic pain would reveal promising targets of pain control.

Maintenance of inflammatory milieu within spinal cord is a key feature of central sensitization during chronic pain. The inflammatory regulation is mediated not only

by local glial cells but also by the migration of blood borne immune cells. The latter has been observed in many different animal pain models (Ren and Dubner, 2010). These immune cells release several molecules during chronic pain. The molecules, including cytokines and proteases, could exert effects on inflammation and nociception. For example, macrophages migrate to the spinal cord where they differentiate into microglial-like cells (Zhang et al., 2007). After that, these macrophages become the sources of pro-nociceptive molecules (e.g. cathepsin S and MMP9) and are involved in the central sensitization of chronic pain. However, the roles of other immune cells such as neutrophils which could be found in spinal cord during induction of chronic pain are unclear (Mitchell et al., 2008). Systematic biological study using microarray and bioinformatics analysis will be able to identify the genes introduced by such immune cells and should improve our understanding on the roles of these cells in the spinal cord during the development of chronic pain. Although microarray has been done to characterize the differential gene expression in the spinal cord during chronic pain (Nesic et al., 2005), perfusion before tissue harvest washes out the migrated immune cells attached to the spinal cord vasculature (Mitchell et al., 2008). This will introduce bias in the experiment because an unknown amount of immune cells is lost.

In this study, we focus on the gene expression pattern of spinal cord after

inflammation induced chronic pain, using genome wide microarray study. To preserve all the differential genes involved in chronic pain, the dorsal part of lumbar spinal cord was harvested without perfusion. The aim of this study was to identify new genes that are involved in the endogenous pain control system at the level of the spinal cord.

Chapter 2-2 Materials and methods

2.2.1 A chronic pain model induced by peripheral inflammation

All animal experiments were performed in accordance with the Hong Kong Animals Act [no. (10-3) in DH/HA&P/8/2/1 Pt.10] and were approved by the Animal Experimentation Ethics Committee of the Chinese University of Hong Kong. Adult male Sprague Dawley rats (200 g) were used. Before induction of peripheral inflammation, the normal nociceptive responses were recorded by measuring the paw withdrawal latency (PWL) to noxious heat (See below). A total of 12 rats were then randomly assigned to three groups. There were two groups of rats that received peripheral inflammation and one control group was used. Peripheral inflammation was induced by intraplantar injection of either pure (100%) complete Freund's adjuvant (CFA), 25 μL/rat, (Sigma, St. Louis, MO), n = 4 or 25% (v/v) CFA in incomplete Freund's adjuvant, 100 μL/rat, n = 4, into the left hind paw of rats during isoflurane anesthesia. Rats in the control group were injected with 100 μL of normal saline under the same experimental condition, n = 4.

2.2.2 Behavioral testing

All animals were allowed to recover from anesthesia. Pain response was measured regularly up to five days after CFA or saline injection. We tested thermal

hyperalgesia with a plantar analgesia meter (Model 390G, IITC Life Science, Woodland Hills, CA). Each rat was placed in a plexiglas chamber on a glass plate located above a light box. A beam of innoxious light was aimed onto the middle plantar skin surface of left hind paw. After this, the noxious heat to the hind paw was generated by turning on the light box. When the animal withdrew its hind paw, the light beam was turned off immediately. The duration between the start of the noxious heating and the paw withdrawal was recorded and was defined as the PWL. A cutoff (maximum) time of 20 sec was used to prevent paw tissue damage. The PWL for each rat at one time point was averaged from at least three tests separated by 2 min intervals. Changes of PWL were tested among groups using factorial analysis of variance (ANOVA) with repeated measures. Inter-group difference was tested by Student's *t* test.

2.2.3 Total RNA extraction

For microarray study, the total RNA was extracted with RNeasy lipid tissue mini kit according to manufacturer's instruction (QIAGEN, Hilden, Germany). Four days after CFA injection in the left hind paw, ipsilateral lumbar dorsal horn (L4-L6) was harvested without perfusion. The tissues were then homogenized in 1 ml of QIAzol lysis reagent using tissuelyser (QIAGEN, Hilden, Germany). The homogenate was

incubated at 22°C for 5 min to dissociate the nucleoprotein complexes. 0.2 ml of chloroform was then added to the homogenate and vortex vigorously for 15 sec. The samples were incubated at 22°C for another 3 min, followed by centrifugation at 12,000×g for 15 min at 4°C. After centrifugation, two phases could be observed. The upper, aqueous phase was then carefully transferred to a new tube. 1 volume (600 μL) of 70% (v/v) ethanol in diethylpyrocarbonate (DEPC) treated water was added and mixed thoroughly by vortexing. The mixtures were transferred to the RNeasy mini spin column and centrifuged for 15 sec at 8,000×g at 22°C. After centrifugation, all the samples were treated with DNase I column at 22°C for 15 min. The columns were then washed three times with following procedures: (1) 700 μL of buffer RW1 added and centrifuged at 8,000×g for 15 sec; (2) 500 μL of buffer RPE added and centrifuged at 8,000×g for 15 sec; (3) 500 μL of buffer RPE added and centrifuged at 8,000×g for 2 min. After washing, the columns were centrifuged at 16,000×g for 1 min to remove all the residual liquid. 50 μL of RNase free water were applied to the column to wash out the total RNA samples by centrifuging at 1 min at 8,000×g. The total RNA samples were quantified using Nanodrop 1000 spectrophotometer (Nanodrop, Wilmington, DE). The RNA integrity was monitored with Agilent Bioanalyzer (Agilent Technologies, Santa Clara, CA).

For quantitative RT PCR study, total RNA was extracted using Trizol (Life

Technologies, Carlsbad, CA). Tissues were harvested as above and were immediately transferred to the 1 ml TRIzol in 1.5 ml tube. The tissues were then homogenized in the TRIzol reagent using the Tissuelyser (QIAGEN, Hilden, Germany). The homogenate was incubated for 5 minutes at 22˚C to allow complete dissociation of the nucleoprotein complex. 0.2 ml of chloroform was added to the homogenate and then vortex for 15 sec. The mixture was incubated for 3 min at 22˚C and the samples were centrifuged at 12,000×g for 15 min at 4˚C. After centrifugation, two phases can be seen. The upper, aqueous phase was transferred into a new RNase free tube. 0.5 ml of 100% isopropanol was then added to the aqueous phase. The mixture was mixed via inversing the tube for several times and incubated at 22˚C for 10 min, following with centrifugation at 12,000×g for 10 minutes at 4˚C. Generally, a white pellet can be seen after centrifugation. The pellet was washed by adding 1 ml of 75% (v/v) ethanol in DEPC treated water, taping and inversing the tube for several times. Afterwards, the tube was centrifuged at 7,400×g for 5 min at 4˚C and the supernatant was then removed completely. The RNA pellet was air dried until the white pellet was turned into transparent appearance. The RNA pellet was re-suspended in 20-50 μL of RNase free water by tapping the tube bottom. The total RNA samples were quantified using Nanodrop spectrophotometer (Nanodrop, Wilmington, DE). 2 μg of total RNA was then used for DNase I (QIAGEN, Hilden, DE) treatment to remove residual DNA

contamination.

2.2.4 Microarray analysis

Total RNA (10 μg) extracted from each tissue was used as templates for complimentary deoxyribonucleic acid (cDNA) synthesis (reverse transcription). In vitro transcription (cRNA synthesis and labeling) was performed using Agilent low RNA input fluorescent linear amplification kit (Agilent Technologies, Santa Clara, CA) in the presence of cyanine 5-cytosine triphosphate (Cy3-CTP). Synthesized fluorescence labeled cRNA (Cy3 labeling) was then used for oligomicroarray hybridization. Hybridization solution was prepared according to in situ hybridization kit plus (Agilent Technologies, Santa Clara, CA). Hybridization was performed using Agilent 4 × 44 k whole rat genome microarray (Agilent Technologies, Santa Clara, CA) in hybridization oven at 60°C for 18 hours. Microarray scanner system (Agilent Technologies, Santa Clara, CA) was used for data analysis. The expression level of specific genes was determined by signal intensities. Fold change of specific gene was made between the average expression level of two saline rats and average expression level of two CFA rats. *A priori* cutoff was set to filter out the differential genes according to the average expression level of each dataset. Accordingly, the differential gene list is selected according to the fold change (≥ 1.5) and the p value (< 0.05) of

unpaired Student's *t* test. Hierarchical cluster analysis (HCL) for the whole datasets and the differential gene list were performed with Genespring software (Agilent Technologies, Santa Clara, CA). Cluster on both entities and condition and Pearson centered distance metric was considered for all the datasets during clustering.

2.2.5 Reverse Transcription PCR

Reverse transcription PCR for quantitative RT PCR study was performed in a final volume of 20 μL using high capacity cDNA reverse transcription kit (Life Technologies, Carlsbad, CA). Briefly, the following solution was added: 2 μL of reverse transcription buffer (10×), 0.8 μL of deoxyribonucleotide triphosphastes (dNTPs, 25×), 2 μL of random primers (50 μM), 1 μL of reverse trancriptase, 0.2 μL of RNase inhibitor, 4 μL of water (DNase and RNase free) and 10 μL of DNase I treated total RNA (0.1 μg/μL) to a 200 μL tube. It was mixed by pipetting up and down for several times. The mixture was then incubated at 25°C for 10 min. Single-strand cDNA synthesis was performed at 37°C for 2 h and the reaction was abolished at 85°C for 5 min. All samples were then diluted for 10 folds with water before PCR application.

2.2.6 Quantitative RT PCR

The primer pairs for quantitative RT PCR were designed with Primer express software (Life Technologies, Carlsbad, CA) and the primers sequences are shown in Table 2-1. All primers were obtained from Invitrogen (Life Technologies, Carlsbad, CA). Quantitative RT PCR was done using the Power SYBR Green PCR master mix kit (Life Technologies, Carlsbad, CA). The reaction was performed in a final volume of 10 μL according to manufacturer's protocol. Briefly, the following solution was added to a well of 384-well real time PCR plate: 5 μL of master mix solution, 0.75 μL of primer pair (mixture of forward and reverse primers, 10 μM each), 1 μL of DNase free water and 2.5 μL of diluted cDNA solution (diluted for 10 folds from original cDNA solution, see above). After incubation at 50°C for 5 min, the reaction mixture was denaturated at 95°C for 10 min, followed by 40 PCR cycles (denaturation at 95°C, 15 sec, primer annealing and extension at 60°C, 1 min). The comparative cycle threshold (Ct) method was used for relative quantification of gene expression. The relative expression level of specific gene in each group was normalized to the housekeeping gene β-actin and given by $2^{-\Delta\Delta Ct}$ method according to manufacture. The Ct value was read according to the number of cycles at which the fluorescence signal passes a manual threshold.

2.2.7 Bioinformatics analysis

Functional annotation for biological processes, cellular components, molecular functions and signal transduction pathways analysis was completed with the Genomatix software (Genomatix Sofrware, München, DE).

Table 2-1. Primer sequences for validated genes.

Gene symbol*	Accession	Primer sequences
PDYN	NM_019374	For: 5'- GCAGACTGCCTGTCCTTGTG-3'
		Rev: 5'- GGCACTCCAGGGAGCAAAT-3'
CRH	NM_031019	For: 5'- CAGCCGTTGAATTTCTTGCA-3'
		Rev: 5'- CTTCACCCATGCGGATCAG-3'
CTSG	NM_001106041	For: 5'- GGAAACCCGAGAGAAAGGAAGT-3'
		Rev: 5'- CCTGGGCCACATTATTACATACC-3'
AIF1L	NM_001108578	For: 5'- GGTGAGTGCCGCCGAGTA-3'
		Rev: 5'- GCTCAATGCTTCCCTGTCTTTC-3'
ACTB	NM_031144	For: 5'-GGGAAATCGTGCGTGACATT-3'
		Rev: 5'-GCGGCAGTGGCCATCTC-3'

*The gene symbol represents the official symbol of specific gene according to the Gene database of National Center for Biotechnology Information;
PDYN = prodynorphin; CRH = corticotropin-releasing hormone;
CTSG = cathepsin G; AIF1L = allograft inflammatory factor 1-like; ACTB = β-actin.
For = Forward primer sequence; Rev = Reverse primer sequence

Chapter 2-3 Results

2.3.1 Inflammatory pain induced heat hyperalgesia

To collect tissue samples for microarray analysis, chronic pain model by intraplantar injection of pure CFA (25 μL/rat) or 25% CFA (100 μL/rat) was established. The results showed that heat hyperalgesia was peaked at 6 hours, and starting to recover from day 1 to day 3. The recovery was partial and finally reached a plateau from day 3 to day 5 (Figure 2-1). This finding suggested the establishment of CFA induced chronic pain model. There was no significant difference between the injection of pure CFA or 25% CFA solution (*post hoc* Student's *t* test). Since 100 μL of injection was more practical and produced more acute effect than 25 μL, all the CFA related pain model experiments were performed using the 25% CFA solution (100 μL/rat).

Figure 2-1. Chronic pain model development. Heat hyperalgesia was developed in a time dependent manner after complete Freund's adjuvant (CFA) injection (n=4, factorial analysis of variance with repeated measures, F=41.703, p<0.001). There was significant difference between saline groups and CFA group (n=4, p<0.001), saline group and 25% CFA group (n=4, p<0.001). However, no difference was observed between CFA group and 25% CFA group (n=4, p=0.45). This pain like response was peaked at 6 hours and partially recovered from day 3 to day 5 (p<0.0001, ANOVA). The difference of PWL between saline group and 25% CFA group was analyzed by *post hoc* Student's t test at each time point (6 h, t=8.391, df=6, p=0.0002; 1 day, t=9.789, df=6, p<0.0001; 3 day, t=3.423, df=6, p=0.014; 4 day, t=3.886, df=6, p=0.008; 5 day, t=7.172, df=6, p=0.0004). Similarly, the difference between saline group and CFA group was also analyzed by Student's t test at each time point (6 h, t=8.642, df=6, p=0.0001; 1 day, t=9.149, df=6, p<0.0001; 3 day, t=3.194, df=6, p=0.019; 4 day, t=7.105, df=6, p=0.0004; 5 day, t=4.010, df=6, p=0.007). *and$^{\#}$, p<0.05; **and$^{\#\#}$, p<0.01, ***and$^{\#\#\#}$, p<0.001 (compared with saline group, Student's t test). Error bars indicate standard error of mean (SEM).

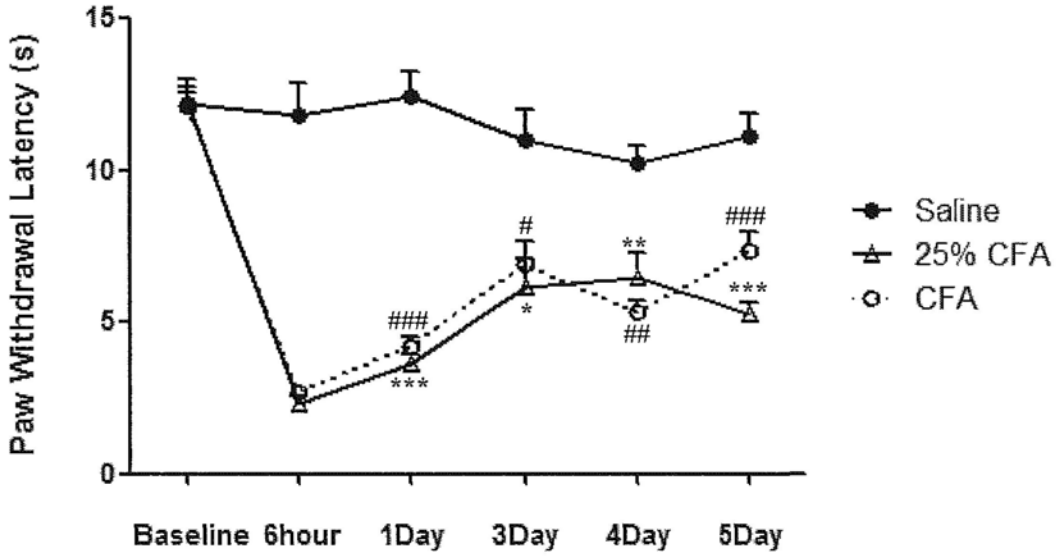

2.3.2 Sample preparation for genome wide profiling of lumbar dorsal horn

Chronic pain was induced in the left hind paw as above (n = 4 for each group). On the fourth day, heat hyperalgesia was again measured to ensure the development of chronic pain (Figure 2-2). CFA injection significantly reduced the PWL on day 4 (t=5.648, df=6, p=0.001), confirming the development of chronic pain. Ipsilateral lumbar dorsal horn (L4-L6) was then harvested (n = 2 for each group). To preserve the migrated blood borne cells, no perfusion was performed before tissue harvest. Total RNA from tissues were extracted and then analyzed for the RNA integrity. For cDNA microarray study, the threshold of ribosomal ribonucleic acid (rRNA) ratio (i.e. the ratio between 28S and 18S RNA) and RNA integrity number was 0.8 and 5.5, respectively. Capillary electrophoresis analysis of total RNA samples showed that RNA extraction fulfilled the standard suggested by the manufacturer (Figure 2-3). The result also showed that all the samples were suitable for cDNA microarray study (Table 2-2).

Figure 2-2. Heat Hyperalgesia response after CFA injection. Saline injection did not cause pain like response on animals on day 4 as compared with baseline (n=4, paired Student's t test, t=1.141, df=3, p=0.34). In the contrast, CFA injection successfully caused heat hyperalgesia on animals on day 4 as compared with baseline (n=4, Student's paired t test, t=6.835, df=3, p=0.006). Decreased paw withdrawal latency was found on day 4 by CFA injection as compared with saline injection (n=4, Student's t test, t=5.648, df=6, p=0.001). Error bars indicated standard error of the means.

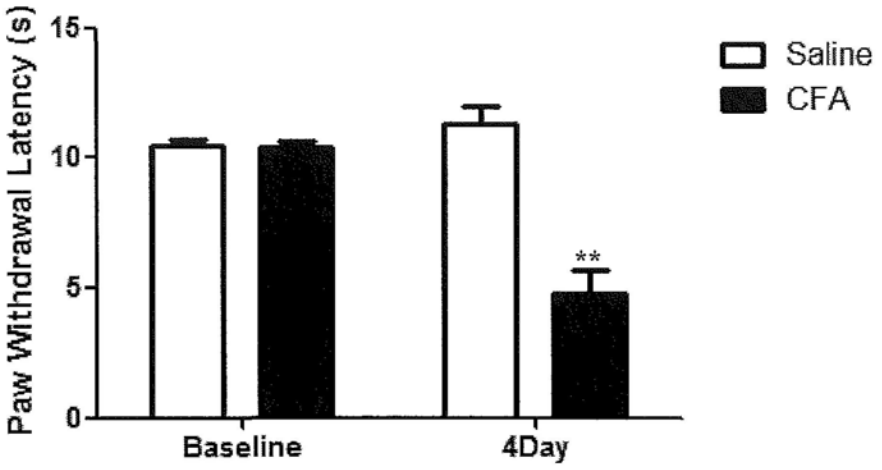

Figure 2-3. Capillary electrophoresis analysis of total RNA samples. The two major peaks indicate 18S and 28S RNA. CFA = complete Freud's adjuvant; CTR = control; $^{**}p<0.01$, Student's *t* test.

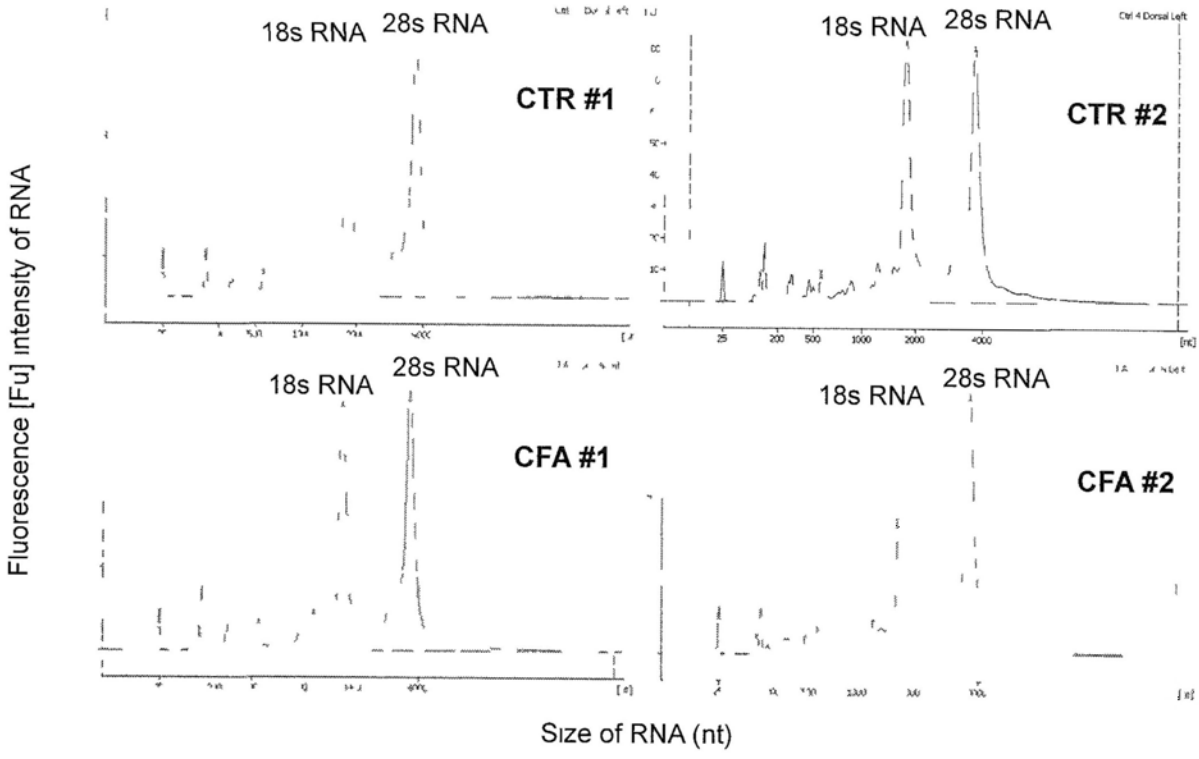

Table 2-2. Total RNA quality analysis.

Sample	260/280[1]	260/230[2]	RIN[3]	rRNA ratio[4]
CTR1	2.08	1.86	8.3	1.3
CTR2	2.06	1.85	8.3	1.2
CFA1	2.07	1.97	8.1	1.1
CFA2	2.11	2.12	8.5	1.4

[1] ratio of Nanodrop readout under 260 nm and 280 nm, good quality $\geq$ 1.80;
[2] ratio of Nanodrop readout under 260 nm and 230 nm, good quality $\geq$ 1.70;
[3] RIN read by Agilent bioanalyzer, value $\geq$ 5.5 indicates good quality;
[4] rRNA ratio read by Agilent bioanalyzer, value $\geq$ 0.8 indicates good quality;
CFA = complete Freud's adjuvant; CTR = control.

2.3.3 Microarray analysis

The expression level of specific genes was determined according to the average signal intensities. HCL analysis was performed to organize the genes in the replicated samples ($n = 2$) for the two conditions (i.e. saline *versus* CFA injections) into clusters, based on the similarity of their abundance profiles. The heat map generated by cluster analysis showed that the HCL identified the differential gene expression patterns for each of the dataset analyzed when comparison was made between saline and CFA treated rats (Figure 2-4a). The two saline samples and two CFA samples were clustered together. This indicated that the gene expression profiles depend on the treatment. We selected out the differential expression of genes with ≥ 1.5 folds of change between saline and CFA treated rats ($p < 0.05$, Student's t test) (Figure 2-4b). There were a total of 391 genes in the list. Among these, 188 genes were up-regulated and 203 genes were down-regulated in the rats after CFA injection. HCL analysis on this differential gene list again identified differential expression pattern between the two treatments.

Figure 2-4. Microarray analysis of lumbar dorsal horn. 4a: Generation of differential gene list. Each point in this graph marks a gene. The horizontal axis indicates the expression level of saline treated (control) rats. The vertical axis indicates the expression level of complete Freud's adjuvant (CFA) treated rats. The color represents the level of expression for a specific gene. The red color indicates the gene is highly expressed in lumbar dorsal part, while blue color indicates low level of expression. The green lines indicate the threshold of gene selection (fold change $\geq$ 1.5). Genes outside of the green lines with $p<0.05$ were selected as the differential genes. **4b:** Hierarchical cluster analysis for the whole datasets (samples clustering). **4c:** Hierarchical cluster analysis for differential gene list.

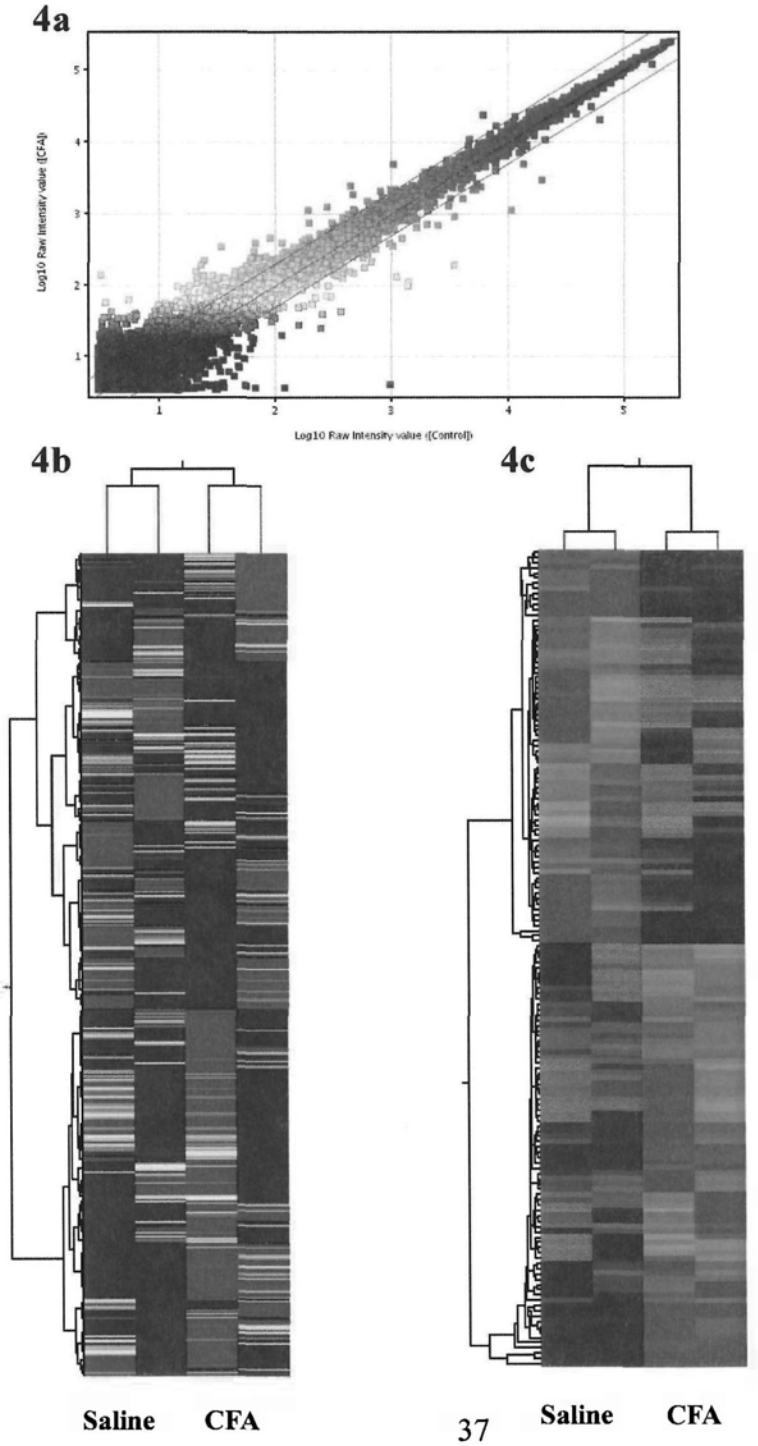

2.3.4 Validation of differential genes

To validate the differential expression of genes, we used quantitative RT PCR methods. The candidate genes with at least 3 folds of change in the microarray analysis were choosen and further selected according to the literature research. Two known pain related genes (i.e. prodynorphin [PDYN] and corticotrophin-releasing hormone [CRH]) and two inflammatory genes (i.e. cathepsin G [CTSG] and allograft inflammatory factor 1-like [AIF1L]) were selected. All the tissue samples were harvested from new experiments. Chronic pain was induced as above (section 2.2.1). On the fourth day, the heat hyperalgesia was measured and confirmed the development of chronic pain (Figure 4a). Lumbar dorsal horn was harvested and applied to RNA extraction and reverse transcription reaction. Quantitative RT PCR confirmed that PDYN (4.7 folds, Student's *t* test, t=7.576, df=6, p=0.0003), CRH (2.4 folds, Student's *t* test, t=4.193, df=5, p=0.0086), AIF1L (1.79 folds, Student's *t* test, t=3.102, df=6, p=0.0211) and CTSG (4.0 folds, Student's *t* test, t=3.115, df=6, p=0.027) were up-regulated in the CFA rats (n=4) compared with control rats (n=4).

Figure 2-5. Validation of differential genes expression. 5a: CFA induced chronic pain development. Saline injection did not cause pain like response on animals on day 4 as compared with baseline (n=4, Student's paired t test, t=1.231, df=3, p=0.3060). In the contrast, CFA injection successfully caused heat hyperalgesia on animals on day 4 as compared with baseline (n=4, Student's paired t test, t=4.865, df=3, p=0.0166). Heat hyperalgesia was induced on day 4 by CFA injection (n=4, Student's t test, t=3.950, df=6, p=0.0075) compared with saline injection; **5b-5e:** Spinal expression of PDYN, 4.7 folds, Student's t test, t=7.576, df=6, p=0.0003, CRH, 2.4 folds, Student's t test, t=4.193, df=5, p=0.0086, AIF1L, 1.79 folds, Student's t test, t=3.102, df=6, p=0.0211 and CTSG, 4.0 folds, Student's t test, t=3.115, df=6, p=0.027, were confirmed to be up-regulated in response to periphery inflammation. n=4, *p<0.05, **p<0.01, ***p<0.001. Error bars indicate standard error of means.

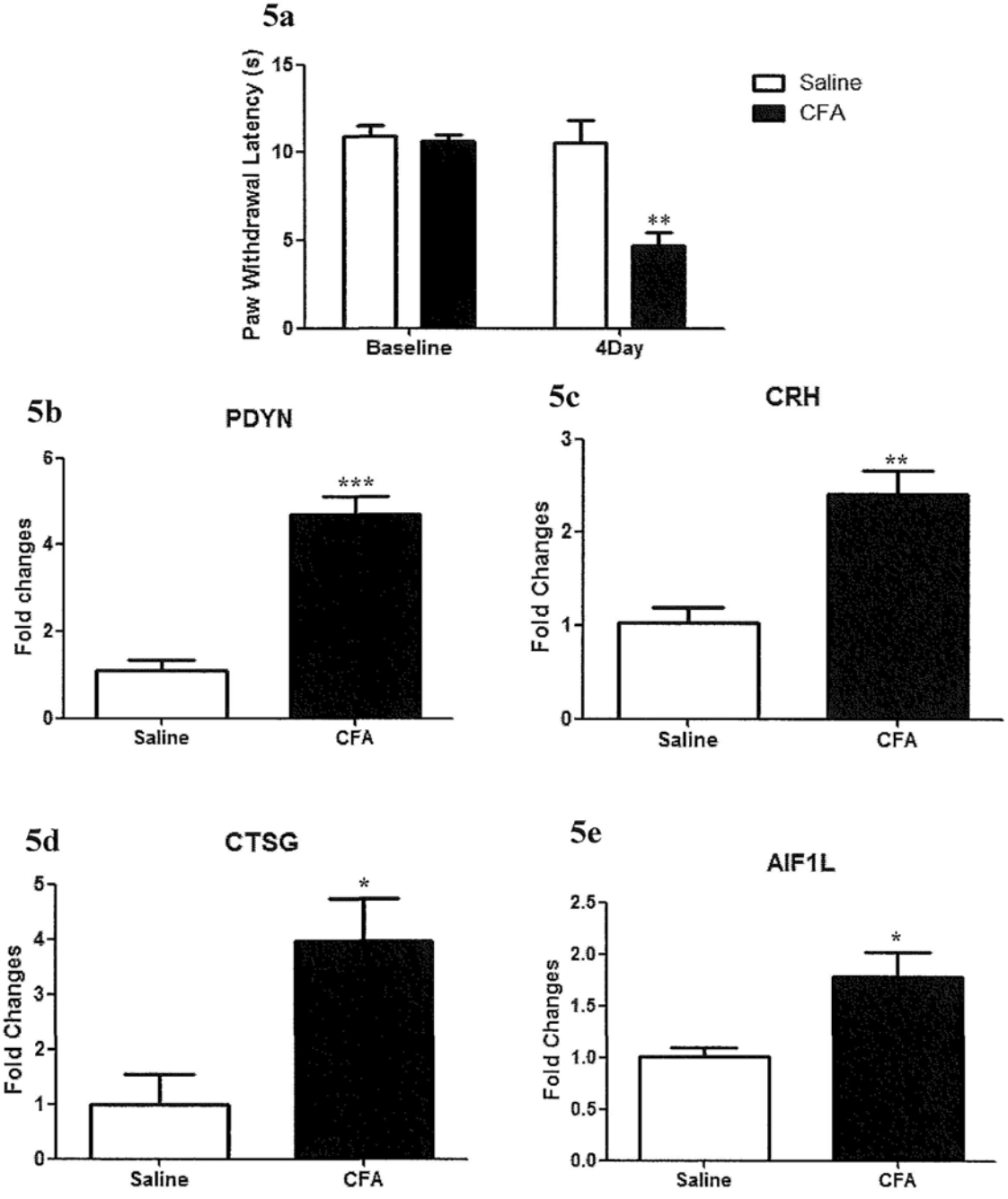

2.3.5 Bioinformatics analysis of differential genes

We then searched all the differential genes which have official gene symbols in the National Center for Biotechnology Information (NCBI) for further bioinformatics study. There were a total of 169 genes being selected (Appendix 1 and 2). These genes were then analyzed by Genomatix software (Fisher's exact test) and clustered on molecular functions (Table 2-3), biological processes (Table 2-4), cellular components (Table 2-5), and signal transduction pathways (Table 2-6).

Table 2-3. Molecular functions among differential genes.

GO-Term*	*p*-value**	Genes (observed)	Genes (total)
Potassium channel regulator activity	4.93E-04	3	19
Kinase regulator activity	5.68E-04	5	81
Protein kinase regulator activity	2.33E-03	4	67
Transcription factor activity	3.67E-03	14	746
Protein serine/threonine kinase inhibitor activity	5.84E-03	2	14
Enzyme inhibitor activity	6.05E-03	7	260
Channel regulator activity	7.81E-03	3	49

*GO = Gene Ontology

***p*-value was determined by Fisher's exact test. $p<0.05$ indicated the gene list is specifically associated in the listed cluster above.

Table 2-4. Biological processes regulated by differential genes.

GO-Term*	*p*-value**	Genes (observed)	Genes (total)
Immune effector process	1.09E-04	8	193
Cytokine production	8.89E-04	7	203
Regulation of gene expression	6.64E-03	25	1989
Adaptive immune response	6.77E-03	4	99
Cellular biogenic amine metabolic process	7.51E-03	4	102

*GO = Gene Ontology

***p*-value was determined by Fisher's exact test. $p<0.05$ indicated the gene list is specifically associated in the listed cluster above.

Table 2-5. Cellular components among differential genes.

GO-Term*	*p*-value**	Genes (observed)	Genes (total)
Stored secretory granule	1.91E-03	7	212
Membrane-bounded vesicle	4.01E-03	12	599
Extracellular region	7.30E-03	20	1349

* GO = Gene Ontology

***p*-value was determined by Fisher's exact test. $p<0.05$ indicated the gene list is specifically associated in the listed cluster above.

Table 2-6. Signal transduction pathways among differential genes.

Pathway	*p*-value*	Genes (observed)	Genes (total)
TGF beta	1.63E-03	26	1307
Dopamine receptor	3.09E-03	3	26
Protein kinase A	3.44E-03	23	1155
Protein phosphatase 5	3.83E-03	3	28
Nuclear receptor subfamily 3, group C, member 1 (Glucocorticoid receptor)	8.51E-03	6	156

**p*-value was determined by Fisher's exact test. $p<0.05$ indicated the gene list is specifically associated in the listed cluster above.

2.3.6 Differential protease and protease inhibitor genes in the lumbar dorsal horn during CFA induced chronic pain.

Our microarray study showed that a subset of proteases and proteases inhibitors were included in the differential gene list during the development of chronic pain (Table 2-7). This indicates that proteolytic activity may play a role in the regulation of central sensitization. MMP2, MMP9 and tissue inhibitor of MMP1 (TIMP1) belong to the protease and protease inhibitor family and is important in the peripheral and central sensitization following peripheral nerve injury. To investigate whether these nociceptive regulators are also regulated during CFA induced chronic pain, we used quantitative RT PCR to examine the expression level of these genes in lumbar dorsal horn from CFA treated (n = 4) and saline treated rats (n = 4). The results showed that MMP9 (1.84 folds, Student's t test, t=2.647, df=6, p=0.038), but not MMP2 and TIMP1 were up-regulated during chronic pain (Figure 2-65). This result suggested that MMP9 may also play a role in the regulation of CFA induced chronic pain. Moreover, this result also suggested that other proteases found in the differential gene list may exert similar effect with MMP9.

Table 2-7. Differential protease and protease inhibitor genes in the lumbar dorsal horn during CFA induced chronic pain by microarray analysis.

Gene symbol	Genebank accession	Description	Fold changes[a]	*p*-Value[b]
Ctsg	NM_001106041	Rattus norvegicus cathepsin G (Ctsg), mRNA	6.17	0.035782
Ace2	NM_001012006	Rattus norvegicus angiotensin I converting enzyme (peptidyl-dipeptidase A) 2 (Ace2), mRNA	1.77	0.01674
Prss21	NM_181477	Rattus norvegicus protease, serine, 21 (Prss21), mRNA	1.55	0.007851
Adamts6	NM_001108544	Rattus norvegicus ADAM metallopeptidase with thrombospondin type 1 motif, 6 (Adamts6), mRNA	-1.85	0.033804
Usp18	NM_001014058	Rattus norvegicus ubiquitin specific peptidase 18 (Usp18), mRNA	-1.74	0.000901
Ctsq	BC107913	Rattus norvegicus cathepsin Q, mRNA (cDNA clone MGC:125032 IMAGE:7460613), complete cds.	-1.51	0.010442
Serpine1	NM_012620	Rattus norvegicus serine (or cysteine) peptidase inhibitor, clade E, member 1 (Serpine1), mRNA	-2.65	0.012296
Spint2	NM_199087	Rattus norvegicus serine peptidase inhibitor, Kunitz type, 2 (Spint2), transcript variant 2, mRNA	2.00	0.016166
Serpina5	NM_022957	Rattus norvegicus serine (or cysteine) peptidase inhibitor, clade A, member 5 (Serpina5), mRNA	1.63	0.025628

Figure 2-6. Analysis of proteases gene expression after induction of inflammation. **6a:** matrix metalloproteinase 9 (MMP9) was significantly up-regulated in the spinal cord dorsal horn during persistent inflammation (1.84 folds, Student's *t* test, t=2.647, df=6, p=0.038). **6b and 6c:** MMP2 and metallopeptidase inhibitor 1 (TIMP1) were not regulated during persistent inflammation. *p<0.05. Error bars indicate standard error of means.

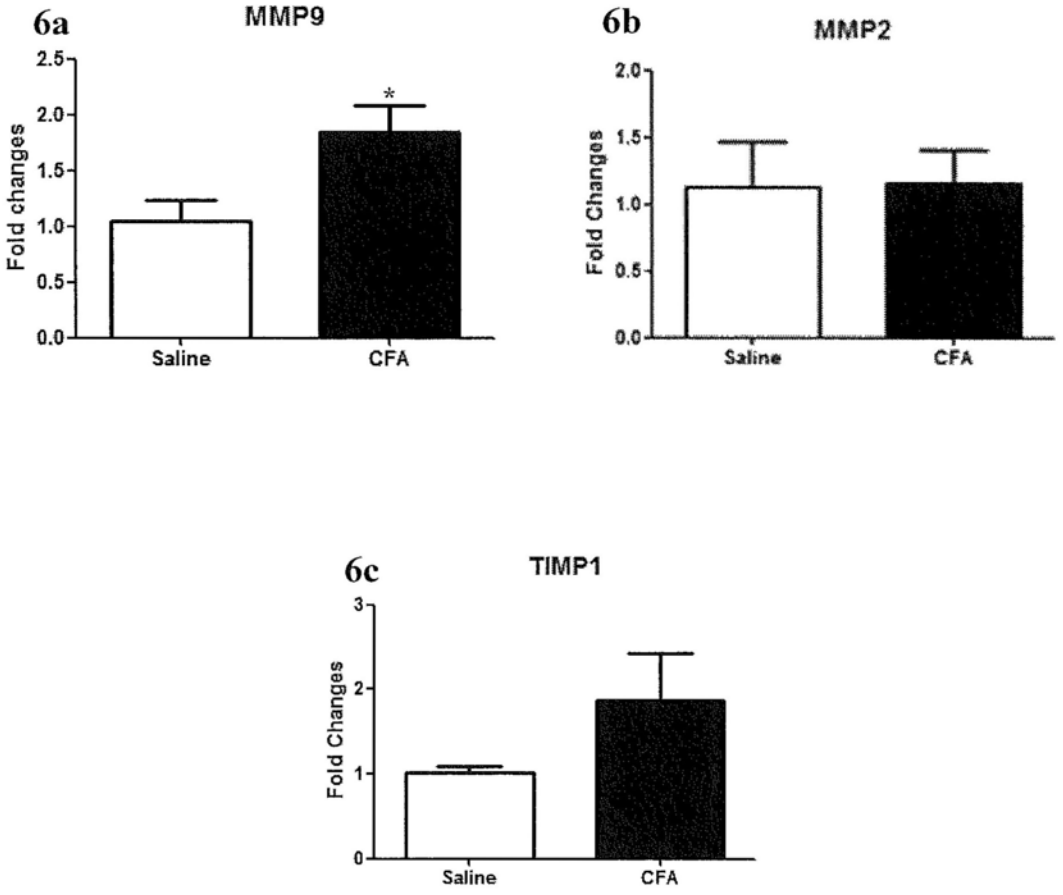

Chapter 2-4 Discussion

2.4.1 A large number of genes were regulated in response to CFA induced chronic pain in the lumbar dorsal horn.

In response to CFA induced inflammation, mediators may exert immediate actions on both nociceptors and other neurons in the spinal cord. This will lead to an increase in the firing rate of action potential that lasts for minutes or hours. On the other hand, the release of neurotransmitters and neuromodulators from nociceptors and local cells in the spinal cord dorsal horn may also exert long term modification, primarily by activating the receptors and related signaling transduction (Woolf and Costigan, 1999; Kuner, 2010). For example, an increase in glutamate from nociceptors is able to activate metabotrophic glutamate receptors causing the activation of G protein-coupled receptor (GPCR) dependent signaling transduction and subsequent transcription factor activation, such as cAMP response element-binding (CREB) (Kawasaki et al., 2004). The activation of these transcription factors contributes to synapse plasticity in chronic pain. The inflammatory mediators from glial cells are thought to activate receptors dependent signal transduction and transcriptional change in neurons (Ji et al., 2003). On the other hand, a large number of receptors are also found in the glial cells, which mediate transcriptional change and activation of the glial cells (Suter et al., 2007). In this regard, IL1β receptor was found

in both neurons and astrocytes (Zhang et al., 2007). Increased IL1β up-regulates the gene expression in both cells, based on nuclear factor kappa light chain enhancer of activated B cells (NFκB) dependent mechanism (Lee et al., 2004; Xia and Zhai, 2009). Therefore, genome wide profiling of spinal cord dorsal horn after periphery inflammation may reveal spinal cord dependent mechanism of central sensitization and nociceptive transmission. We established a chronic pain model due to peripheral inflammation by intraplantar injection of CFA. The development of heat hyperalgesia in the rats suggested the establishment of peripheral and central sensitization. To focus on the central sensitization mechanism of chronic pain, we used ipsilateral dorsal horn of spinal cord for the genome wide gene profiling. HCL analysis of the whole genome expression profiles suggested that different gene expression pattern compared with control. This result indicated the presence of specific transcriptional response in the spinal cord dorsal horn after induction of peripheral inflammation. A total of 391 differential genes were identified (188/391, 48% up-regulated; 203/391, 52% down-regulated) with at least 1.5 folds of change in our study and 169 genes (43%) are belonged to the known genes according to the NCBI gene database. Consistent with this, quantitative RT PCR also confirmed that the up-regulation of selected genes in this list. These results are consistent with the concept that multiple cells from spinal cord dorsal horn can be transcriptionally activated in response to peripheral

inflammation.

Perfusion has been used in previous studies which focus on the mRNA and protein changes from samples in the nervous system. Perfusion with saline and 4% paraformaldehyde (PFA) were thought to preserve (and fix) tissue samples. However, it was reported that perfusion actually changed the expression profiles of specific genes, especially for those introduced by immune cells migration. After perfusion, the expression level of S100 calcium binding protein A8 (S100A8) and S100A9, which are specific markers of a subpopulation of neutrophils, was significantly reduced in the CFA treated rats (Mitchell et al., 2008). This finding suggests that perfusion reduces the number of migrated cells and is responsible for data loss. Therefore, we harvested tissue samples without perfusion to preserve the change of gene expression. Our RNA integration analysis showed good quality of RNA samples (Table 2-2), suggesting that perfusion may not be necessary. Our data are helpful to reveal the regulation of blood borne immune cells during central sensitization after inflammation induction.

Generally, regulation of transcription factors depends on post-translational modification. CREB can be activated after phosphorylation at Serine-133 by p38 mitogen-activated protein kinase (p38MAKP) (Xing et al., 1998). In other cases, the subcellular location of DREAM was reported to be regulated in the spinal cord by

unknown mechanism after induction of inflammation on hind paw (Zhang et al., 2007). We identified PDYN as a differential gene with both microarray and quantitative RT PCR studies. Expression of PDYN was proved to be regulated by both CREB and DREAM (Schwarzer 2009). The up-regulation of PDYN indicated the presence of the post-translational modification of CREB and DREAM in our study. In keeping with this finding, an increase in phosphorylation of CREB has been reported in the spinal cord during chronic pain (Miletic et al., 2002; Song et al., 2005). Moreover, the transcription repressor of PDYN, DREAM was found to be excluded from nucleus, 4 days after induction of CFA mediated inflammation (Zhang et al., 2007). Taken together, these results suggested that post-translational modification contributes to the activation of transcription factors and subsequent differential gene expression in our study.

In addition, modulation of transcription factors may also contribute to the genome wide change of gene expression. FBJ osteosarcoma oncogene (c-fos) was rapidly up-regulated after peripheral nerve injury and inflammation (Gao and Ji, 2009). The subsequent transcriptional events by c-fos contribute to the maintenance of chronic pain (Hou et al., 1997; Wu et al., 2002). Molecular function clustering result showed that 14 transcription factors were involved in the list of 169 known genes (Table 2-3). In addition, according to the biological process clustering result, 25 genes

in our list are suggested to have a role in the regulation of gene expression. This result indicated further transcriptional regulation is an important event in later stage of chronic pain. Interferon regulatory factor 4 (IRF4) has been involved in the regulation of IL4 expression (Rengarajan et al., 2002; Honma et al., 2008), an anti-inflammatory gene that has analgesic effect (Hao et al., 2006). The change of IRF4 level suggested the body may activate local pain inhibitory signal by up-regulate the anti-nociceptive genes. Therefore, identification of target genes regulated by the transcription factors in our differential gene list may offer further insight on the control of chronic pain.

2.4.2 Inflammatory mediators were enriched in the lumbar dorsal horn during CFA induced chronic pain.

Clustering analysis of differentially regulated genes revealed the genes involved in cytokine production, immune effector process and adaptive immune response (Table 2-4). This result indicates that inflammation in the nervous system is important in the regulation of chronic pain. Increasing number of studies has revealed that inflammatory mediators including cytokines show either pro-nociceptive or anti-nociceptive effect on neurons or glial cells. Our results showed that the regulation of cytokines in the spinal cord can be mediated by both transcriptional and post-translational regulation. GATA binding protein 3 (GATA3) and IRF4 in this list

may contribute to the gene expression of IL4 (Ranganath et al., 1998; Rengarajan et al., 2002; Honma et al., 2008). On the other hand, cathepsin G has been shown to process inactive membrane-bound TNFα to an active soluble TNFα (Mezyk-Kopec et al., 2005), which represents the post-translational regulation of cytokine production. Glial cells including microglial cells and astrocytes regulate synaptic strength in the innate immune mechanism. However, our microarray analysis identified a cluster of genes that belongs to the adaptive immune response cluster. This agrees with the hypothesis that adaptive immune regulation mediated either by glial cells or migrated blood borne immune cells, may be involved in chronic pain (Milligan and Watkins, 2009). The involvement of IRF7, protein tyrosine phosphatase receptor type C (Ptprc) and GATA3 in our list suggest that T cells may participate in CFA induced chronic pain. These genes are found in the T cells and are key regulators of T cells function.

2.4.3 Genes on descending pathway were involved in the CFA induced chronic pain

Another important cluster in biological processes that may be related to chronic pain is the cellular biogenic amine metabolic process. Four genes in the differential gene list have been clustered, including catechol-*O*-methyltransferase (COMT) (Table 2-4). COMT is an enzyme that inactivates neurotransmitters, such as dopamine,

noradrenaline and adrenaline (Kambur and Mannisto, 2010). Knockout mice study showed that COMT deficiency caused increased pain (Walsh et al., 2010). Moreover, our previous SNP study also suggested that COMT is associated with chronic postoperative pain (Meng, 2010). The contribution of COMT in the nociception was thought to depend on its role in the adrenergic system (Kambur and Mannisto, 2010), which belongs to the descending pain modulatory pathway (Ossipov et al., 2010). The down-regulation of COMT in spinal cord may therefore represent a change of descending modulatory pathway after periphery inflammation induction. Moreover, solute carrier family 18 (vesicular monoamine) member 2 (slc18a2) was also identified in our study. Slc18a2 is a transporter protein that contributes to the secretion of monoamine neurotransmitters, including dopamine, norepinephrine and serotonin (Gopalakrishnan et al., 2007). Norepinephrine and serotonin are nociception regulators derived from descending neurons in the spinal cord (Ossipov et al., 2010). The down-regulation of slc18a2 in our microarray analysis further indicated the involvement of descending modulatory pathway during CFA induced chronic pain.

2.4.4 Anti-nociception regulation was evolved in the maintenance phase of CFA induced chronic pain.

Another interesting finding from the bioinformatics analysis refers to the

development of inhibitory signals in spinal cord. In addition to the regulation of IL4 production, two secretory proteins, including PDYN and CRH were found up-regulated and may contribute to the anti-nociceptive transmission effect. PDYN is endogenous opioid which show strong analgesia effect in spinal cord. Knockout of DREAM, which is transcription repressor for PDYN, increased the expression of PDYN in the substantia gelatinosa of the spinal cord dorsal horn. The opioid receptor delta dependent analgesia is present in almost all pain models (Cheng et al., 2002). The up-regulation of PDYN in our study confirms a "self-control" mechanism through the transcriptional regulation of PDYN expression.

Signal transduction pathway associations have highlighted glucocorticoid receptor related signaling in our study (Table 2-6). Glucocorticoid receptor is thought to play an important role in the anti-inflammatory regulation in the nervous system (Dinkel et al., 2002). Recently, administration of glucocorticoid receptor activator conferred anti-nociception effect in an animal model of neuropathic pain (Gu et al., 2011). This finding indicates that activation of glucocorticoid receptors is another self-control mechanism. In this cluster, genes such as DUSP1, CRH and PTPRC are known target genes of glucocorticoid receptors. Changes of expression in these genes suggested the activation of glucocorticoid receptors can be observed during the persistent inflammation. For example, glucocorticoid receptor as a transcription

activator is able to up-regulate the expression of CRH (King and Nicholson, 2007). Our microarray study and quantitative RT PCR both showed the up-regulation of CRH in the spinal cord, suggesting the activation of glucocorticoid receptors. Glucocorticoid receptor can also act as transcription repressor and reduce the expression of protein tyrosine phosphatase receptor type C (PTPRC, also known as CD45) (Beck et al., 2009), a pro-inflammation marker that play an essential role in T and B cell mediated inflammation. The down-regulation of PTPRC in our study further reflects the activation of glucocorticoid receptor.

2.4.5 The protease and protease inhibitors are enriched during CFA induced chronic pain in the lumbar dorsal horn.

Recently, proteases as a nociception regulating protein have attracted much attention. The subset of genes in the study suggested a role of proteolytic activity and its regulation (protease inhibitor) in the mechanism of chronic pain. The proteolytic activity of the proteases is responsible for the process of target proteins, leading to degradation of membrane bound proteins or secretory proteins in the extracellular matrix. MMP9 is able to cleave pro-IL1β into an active form in the spinal cord and is important during the development of neuropathic pain (Kawasaki et al., 2008). Our quantitative RT PCR results showed that MMP9 gene expression was induced in the

spinal cord after CFA induced inflammation. Considered that IL1β is required for the NMDAR independent pain hypersensitivity during chronic pain (Weyerbacher et al., 2009), our results confirm that regulation of IL1β cleavage by increased MMP9 is required for the maintenance of hyperalgesia. In addition to MMP9, other proteases and proteases inhibitor in our differential gene list may also be involved in the pain control. Angiotensin I converting enzyme (peptidyl-dipeptidase A) 2 (Ace2) is a homolog of anginxin converse enzyme I. It has been shown that Ace2 is able to process dynorphin A, a variant of PDYN (Warner et al., 2004). Interestingly, we have also identified the up-regulation of dynorphin gene (PDYN) in our pain model. The up-regulation of both PDYN and potential PDYN regulating protein (i.e. Ace2) indicated that PDYN is strictly managed in the nervous system. Cathepsin G (CTSG) exerts pro-inflammation potential in the peripheral tissue. The up-regulation of cathepsin G expression was shown by both microarray and quantitative RT PCR, indicating the involvement of cathepsin G during CFA induced chronic pain. Interestingly, the potential endogenous inhibitor of cathepsin G, Serpin peptidase inhibitor clade E (nexin, plasminogen activator inhibitor type 1) member 1 (SERPINE1) was found down-regulated in our study. These findings confirm the regulation of cathepsin G in the spinal cord, and may be responsible for central sensitization of chronic pain. The subset of protease or protease inhibitors that was

identified in this study offers a new prospective for further study on chronic pain control.

2.4.6. Limitations of the study

In this study, gene expression profiles were compared between rats with and without CFA induced chronic pain. As suggested in the bioinformatic analysis, up to 12.4% (21 of 169) of known pain genes participated in the transcriptional regulation and were differentially regulated on day 4. This result suggested that further alterations of gene expression might be observed after day 4 of CFA injection. Therefore, it will be important to compare the gene expression profiles at other time points. This will not only highlight further mechanism for the maintenance of chronic pain but also confirm the transcriptional regulation in our data on day 4.

Although the differential regulation of several genes was validated by quantitative RT PCR, the change of protein level of these genes was not performed. We believe further experiements using either Western blot or immunofluorescence might strengthen our observations in the alteration of molecular function of these differential genes.

2.4.7 Conclusion

In this study, we have established a CFA induced chronic pain model and

performed the genome wide gene expression profiling in the lumbar dorsal horn. A total of 391 differential genes (188/391, 48% up-regulated; 203/391, 52% down-regulated) were identified with at least 1.5 folds of change. Quantitative RT PCR confirmed the up-regulation of PDYN, CRH, AIF1L and cathepsin G in lumbar from inflamed rats versus control rats. We performed bioinformatics analysis on 169 (43%) known genes in our differential gene list. The clustering analysis suggested: (a) inflammatory regulation is an important even in the spinal cord after peripheral CFA injection; (b) regulation on the descending pain pathway and activation of self-control system are involved in CFA induced chronic pain; (c) proteases or proteases inhibitors represent a new subset of nociceptive proteins.

A total of 391 differential genes were identified in my study, however, the transcription regulators which contribute to these changes were not clear. Therefore, it is better to search the common transcription binding sites within promoter area of these genes during the bioinformatics analysis. This work will identify the common transcription regulators which could be the key factors of chronic pain maintenance.

Part 3 Pro-nociceptive function of cathepsin G: *in vitro* and *in vivo* studies

Chapter 3-1 Introduction

Extracellular proteases exert their biological effects through protein degradation and activation. Proteases play important roles in cell migration, cytokine/chemokine production and tissue remodeling. Despite multiple roles in inflammation, the functions of proteases in nociception, inflammation and pathologic pain are largely unknown. Recently, cathepsin S, originally found in the macrophage, was found to be expressed in microglial cells, the resident tissue macrophages, in the nervous system. Up-regulation of cathepsin S activity in microglial cells causes central sensitization and pain hypersensitivity through the process of chemokines after peripheral nerve injury (Clark et al., 2007). In addition, two MMPs including MMP2 and MMP9 were found to be important in the development and maintenance of neuropathic pain, respectively (Kawasaki et al., 2008). Furthermore, intrathecal injection of MMPs inhibitors reverses neuropathic pain. These findings indicate that protease is a target for the control of chronic pain primarily related to the regulation of inflammatory molecules in the spinal cord.

Cathepsin G is a serine protease that is mainly found in the neutrophils azurophilic granules. In peripheral tissue, cathepsin G exerts multiple pro-inflammation properties owing to its proteolytic activity. As a chemotactic factor, cathepsin G is responsible for the migration of monocytes/macrophages and even the

neutrophils. The chemotactic activity of cathespin G is mediated by proteolytic activation of GPCRs. Pre-treatment with Gi protein signal transduction inhibitor markedly attenuated the chemotactic activity of cathepsin G (Moriuchi et al., 2000). Interestingly, the activation of GPCRs signaling by cathepsin G also induces the production of pro-inflammatory cytokines, including IL1β and TNFα, on macrophages directly (Hazuda et al., 1990; Mezyk-Kopec et al., 2005). The receptors that may be regulated by cathepsin G are members in the protease-activated receptors (PARs) family. In this case, cathepsin G is not always exerting an activating effect. For example, cathepsin G has been shown to inactivate PAR1 and PAR2 (disarmed mechanism) depends on the cell types (Ossovskaya and Bunnett 2004; Vergnolle 2009). On the other hand, cathepsin G always activates PAR4 (Ossovskaya and Bunnett 2004;Vergnolle 2009). PAR4 is a mediator of inflammation. The activation of PAR4, not only contributes to granulocyte recruitment (Vergnolle et al., 2002; Mao et al., 2010), but also induces edema and an increase in vascular permeability (Houle et al., 2005). This phenomenon may therefore explain the mechanism of cathepisn G induced cell recruitment and pro-inflammation effect.

In addition to receptors, cathepsin G produces pro-inflammatory effect by the release of chemokines and cytokines. Cathepsin G has been shown to remove the N-terminal domain of four β chemokines, which then becomes a more potent ligands

for chemokine C-C motif receptor1 (CCR1) (Berahovich et al., 2005). Activation of CCR1 is pro-informatory and is able to sensitize the TRPV1 in the nociceptors (i.e. peripheral sensitization) (Zhang et al., 2005). There are also pro-nociceptive effects of CCR1 in the spinal cord of the partial sciatic nerve ligation induced neuropathic pain model (Kiguchi et al., 2010). Another example is that cathepsin G cleaves membrane bounded TNFα and turns this to a soluble active form, which is responsible for inflammation and nociception (Mezyk-Kopec et al., 2005).

After induction of peripheral inflammation, the recruitment of immune cells and subsequent production of pro-inflammatory mediators may sensitize nociceptors and cause hypersensitivity. The role of cathepsin G in chemotaxis and cytokine regulation not only highlights its pro-inflammatory effects, but also suggests that it is involved in the control of peripheral sensitization after inflammation. Our microarray study has identified cathepsin G as a differential gene in the spinal cord dorsal horn after induction of peripheral inflammation by CFA injection. Maintenance of pro-inflammatory milieu in the spinal cord dorsal horn is a key event in the maintenance of chronic pain. The increased expression in spinal cord suggests that cathepsin G might exert its pro-inflammatory potential in the nervous system and involved in the central sensitization during chronic pain.

In this study, we sought to determine whether cathepsin G could exert its

pro-inflammatory potentials on the astrocytes and whether cathepsin G is involved in the development of chronic pain due to inflammation. To do this, we performed the following experiments:

(1) The gene expression level of cathepsin G between control rats and rats with inflammation induced chronic pain was examined in the lumbar dorsal horn and DRGs.

(2) We determined whether cathepsin G responds specifically to inflammation induced chronic pain. In this regard, the expression of cathepsin G was also tested in another chronic pain model using nerve ligation (chronic constriction injury model) in rats.

(3) The cathepsin G mediated pro-inflammatory effects on astrocytes were evaluated by analyzing the changes of signaling pathways and pro-inflammatory genes expression.

(4) Finally, systemic administration of cathepsin G inhibitor was used to examine the pro-nociceptive potentials of cathepsin G in animals with CFA induced chronic pain.

Chapter 3-2 Materials and Methods

3.2.1 CFA induced chronic pain model

All animal experiments were performed in accordance with the Hong Kong Animals Act [no. (10-3) in DH/HA&P/8/2/1 Pt.10] and were approved by the Animal Experimentation Ethics Committee of the Chinese University of Hong Kong. Adult male Sprague Dawley rats, weighing 200 g, were used in this chronic pain model. The details of pain model are described in section 2.2.1.

3.2.2 Chronic constriction injury (CCI) pain model

In addition, male adult Sprague Dawley rats, weighing 250 g, were used for another pain model using chronic constriction injury. Surgeries were performed during isoflurane anesthesia. Chronic constriction injury was induced in rats (n = 4) by ligating the left sciatic nerve loosely according to the method by Bennett and Xie (Bennett and Xie, 1988). Briefly, the left sciatic nerve was exposed in the mid-thigh, and three loose ligatures of 4-0 chromic cat gut were placed around the dissected nerve 1.0 mm apart (Figure 3-1). Following injury, skin wound was closed with 4-0 nylon sutures. Sham experiments were done in rats following the same procedure with the sciatic nerve exposed but nerve ligation was not attempted (n = 4).

Figure 3-1. Chronic constriction injury pain model. a: Exposure of left sciatic nerve in the mid-thigh. Blue triangle points at the sciatic nerve. **b:** Constriction injury induction. Three loose ligatures of 4-0 chromic cat gut were placed around the exposed sciatic nerve, 1 mm apart. This procedure produced chronic constriction injury to the sciatic nerve. Black arrow shows the chromic cat gut ligature.

3-1a

3-2b

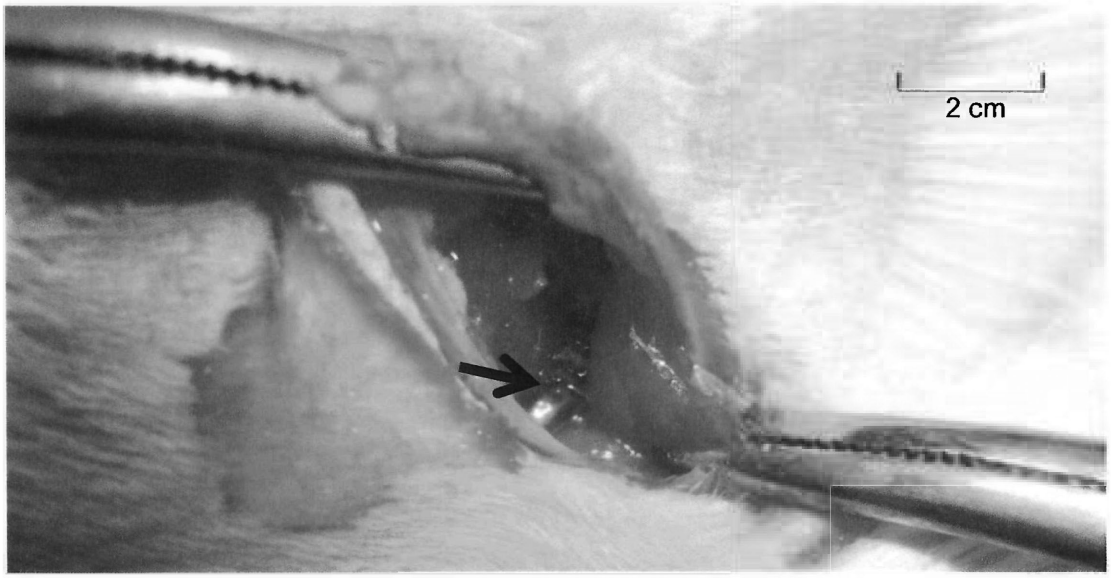

3.2.3 Behavioral test

Rats were habituated to the test environment for at least 2 days before baseline testing. All animals were allowed to recover from anesthesia before behavioral testing. Rats for CFA induced chronic pain were tested for thermal hyeralgesia. Rats for CCI pain study were tested for mechanical allodynia.

The method for measuring thermal hyperalgesia was described above in section 2.2.2. Mechanical nociceptive response and mechanical allodynia after CCI were tested with the electronic von Frey anesthesiometer (IITC Life Science, Woodland Hills, CA). The rats were placed in a Plexiglas chamber on the mesh stand. The rigid filament (for normal nociception) or number 8-15 filament (for mechanical allodynia) was applied to the middle plantar surface of each hind paw. The nociception or allodynia like reaction was determined using Dixon's up-down method and the forces applied to the hind paw were recorded as paw withdrawal threshold (PWT). The PWT for each rat before or after surgery was calculated as the mean of at least three measurements recorded 5 min apart.

3.2.4 Tissue preparation, RNA extraction for gene expression study

Ipsilateral spinal cord and DRG tissue were harvested and total RNA was extracted using TRIzol (Life Technologies, Carlsbad, CA) as described above

(sections 2.2.3 to 2.2.6). Spinal cord tissue from the CFA induced chronic pain model was harvested on day 4 after injection, whereas tissue from the CCI chronic pain model was taken on day 7 after surgery.

The primer pairs for quantitative RT PCR were designed with Primer express software (Life Technologies, Carlsbad, CA) and the primers sequences are shown in Table 3-1. All the primers were obtained from Invitrogen (Life Technologies, Carlsbad, CA).

Table 3-1. Primer sequences for quantitative RT PCR.

Gene symbol	Accession	Primer sequences
IL1β	NM_031512	For[1]: 5'-GACCTGTTCTTTGAGGCTGACA-3'
		Rev[2]: 5'-CTCATCTGGACAGCCCAAGTC-3'
TNFα	NM_012675	For: 5'-GACCCTCACACTCAGATCATCTTCT-3'
		Rev: 5'-TGCTACGACGTGGGCTACG-3'
IL6	NM_012589	For: 5'-TCCTACCCCAACTTCCAATGCTC-3'
		Rev: 5'-TTGGATGGTCTTGGTCCTTAGCC-3'
MMP9	NM_031055	For: 5'-GTGCCCTGGAACTCACACAAC-3'
		Rev: 5'-CCAGAAGTATTTGTCATGGCAGAA-3'
MMP2	NM_031054	For: 5'-TCAAGTTCCCCGGCGATGTC-3'
		Rev: 5'-TTGCGGGGAAAGAAGTTGTAGT-3'
ACTB	NM_031144	For: 5'-GGGAAATCGTGCGTGACATT-3'
		Rev: 5'-GCGGCAGTGGCCATCTC-3'

For = Forward primer sequence; Rev = Reverse primer sequence.

3.2.5 Cell culture

Cell line

C6 cells were cultured in high glucose Dulbecco's modified Eagle medium (DMEM) (Life Technologies, Carlsbad, CA) supplemented with 10% fetal bovine serum (Life Technologies, Carlsbad, CA), 100 units/ml penicillin and 100 μg/ml streptomycin (i.e. complete DMEM). The cells were maintained at 37°C in a humidified atmosphere with 5% carbon dioxide in air. The medium was changed every second day.

Primary cell culture

Cervical to sacrum spine were removed from 18 to 21 day-old Sprague Dawley rat embryos. All meninges were carefully removed under the dissecting microscope. A total of 6-8 spines were pooled together in the Hank's balanced salt solution (Life Technologies, Carlsbad, CA) to wash the residual blood. All the spines were transferred to a 30 mm petri dish containing 3 ml of Trypsin solution [0.05%, ethylenediaminetetraacetic acid free] (Life Technologies, Carlsbad, CA). The spines were cut into pieces in the dish and then incubated at 37°C with 5% carbon dioxide for 30 min. After incubation, complete DMEM 3 ml was added into the dish in order to stop the trypsinization procedure. Single cell suspension was prepared by pipetting

up and down several times. The cell suspension was transferred to a new 15 ml tube and centrifuged at 1,500 rpm for 10 min. All the suspension was removed and the cell pellets were re-suspended with complete DMEM. Cells were plated in 75 cm^2 flask and maintained at 37°C in a humidified atmosphere with 5% carbon dioxide in air. The medium was changed every 2 days until cells grew to confluency. Cells were then placed on the orbital shaker and were shook at 250 rpm at 37°C for 6-8 hours to remove the microglial cells and oligodendrocytes. Afterwards, cells were subcultured and maintained as previously described. The medium was then changed every 3 days and subcultured for 7-10 days.

3.2.6 Immunofluorescence

Primary spinal astrocytes of 18 to 20 days cultures were seeded on the glass coverslips. After 24 hours in culture, cells were washed with cold phosphate buffered saline (PBS) three times and then fixed with PFA 4%, in PBS for 15 min. Cells were then washed with cold PBS three times (5 min for each treatment) and permeabilized with Triton X-100 (1%) in PBS for 10 min. This is followed by another three washes with PBS (5 min each time). Cells were blocked with bovine serum albumin (1%)/Tween-20 (0.05%)/glycine (3M) in PBS for 30 min. The cells were incubated with a polyclonal antibody specific to glial fibrillary acidic protein (GFAP) (1:200)

(Santa Cruz Biotechnology, Santa Cruz, CA) overnight. After primary antibody incubation, cells were washed three times with cold PBS (5 min for each treatment). Anti-goat antibodies conjugated to Alexa Fluor® 488 (1:1,000) (Life Technologies, Carlsbad, CA) were used as secondary antibody. The cells were washed three times with PBS and then stained with 4',6-diamidino-2-phenylindole (DAPI) (1 μg/ml) in PSB for 1 min. Immunofluorescence images were obtained from a Axioplan 2 imaging fluorescence microscope (Carl Zeiss MicroImaging, Thornwood, NY). The total cell number was counted as DAPI staining nuclear and the primary spinal astrocytes were counted as GFAP positive cells.

3.2.7 Western Blot

After treatment with purified cathepsin G (human neutrophil) (Merck KGaA, Darmstadt, DE), cells were washed with cold PBS twice and lysed in radio-immunoprecipitation assay (RIPA) buffer [50 mM Tris-HCl, 150 mM NaCl, 1 mM EDTA, 1% (v/v) NP40, pH7.6] containing protease and phosphatase inhibitors cocktails (1X, in RIPA buffer) (Roche, Basel, Switzerland). The lysate was then incubated on ice for 30 min and stored at -80°C overnight. The samples were thawed on ice and centrifuged at 12,000×g for 10 min at 4°C. The supernatant was collected and protein concentration was determined using protein assay kit (Bio-Rad, Hercules,

CA). Samples were then mixed with 4×protein loading buffer [5mM Tris-HCl, pH 6.8, 2% (w/v) SDS, 10% (v/v) glycerol, 1% (v/v) β-mercaptoethanol, 12.5 mM EDTA, 0.02% (w/v) bromophenol blue] and heated at 99°C for 10 min. For each sample, 25 μg of protein in 25 μl of loading buffer was loaded onto a 12% SDS-polyacrylamide gel. The protein samples were separated in the presence of a running buffer (15 mM Tris base, 115 mM glycine and 0.06% (w/v) SDS, pH 8.0) at room temperature for 120 min at 100 V. The separated protein samples were then transferred onto a hybridization nitrocellulose membrane (0.45 μm) (Millipore). Protein transfer was performed using the Bio-Rad Mini Trans Blot system in the presence of cold transfer buffer [25 mM Tris base, 192 mM glycine and 20% (v/v) methanol, pH 8.0] for 60-120 min at 100 V. The membrane was blocked by incubation solution [5% (w/v) skim milk powder in Tris-buffered saline containing Tween-20 (TBST) (50 mM Tris-HCl, 400 mM NaCl, 0.05% (v/v) Tween-20, pH 8.0)] for 1.5 hour at room temperature. After blocking, the membrane was incubated with antibodies against p-p38MAPK (mouse monoclonal antibody, 1:1,000), p38MAPK (mouse monoclonal antibody, 1:1,000), p-extracellular signal regulated kinases 1/2 (Erk1/2) (rabbit polyclonal antibody, 1:1,000), Erk1/2 (mouse monoclonal antibody,1:1,000), p-c-Jun N-terminal Kinase (JNK) (mouse monoclonal antibody, 1:1,000), JNK (rabbit polyclonal antibody, 1:1,000), p-IκB (mouse monoclonal antibody, 1:1,000), p-STAT3

(rabbit polyclonal antibody, 1:1,000), STAT3 (rabbit polyclonal antibody, 1:2,000), p-CREB (goat polyclonal antibody, 1:500), CREB (rabbit polyclonal antibody, 1:500), p-activating transcription factor 2 (ATF2) (mouse monoclonal antibody, 1:500), ATF2 (rabbit polyclonal antibody, 1:500), cathepsin G (goat polyclonal antibody, 1:200) and β-actin (goat polyclonal antibody, 1:2,000) in incubation solution overnight at 4°C. The antibodies against p-p38MAPK, p38MAPK, p-Erk1/2, Erk1/2, p-JNK, p-STAT3 were obtained from Cell signaling technology (Cell signaling technology, Beverly, CA). The remaining antibodies were obtained from Santa Cruz Company (Santa Cruz Biotechnology, Santa Cruz, CA). After primary antibodies incubation, the membrane was washed with TBST three times (10 min each time at orbital shaker) and then incubated with a 1:2,000 dilution in incubation solution of goat anti-rabbit IgG, goat anti-mouse IgG, or rabbit anti-goat IgG secondary antibodies for 1 hour at room temperature. The membrane was washed with TBST for another three times (10 min for each treatment) and developed using the enhanced chemiluminescence detection system and Hyperperformance chemiluminescence film (GE Healthcare, Little Chalfont, UK).

3.2.8 Gelatin Zymography

Conditioned medium from cathepsin G treated C6 cells were collected and

centrifuged at 200×g for 10 min at room temperature. 100 µl of supernatant was transferred to a new 1.5 ml tube and lyophilized overnight. The powder was dissolved in 30 µl of water. The protein concentration was determined as before. One part of sample was mixed with one part of sample buffer [125 mM Tris-HCl, 20% (v/v) glycerol, 4% (w/v) SDS and 0.005% bromophenol blue, pH 6.8] and incubated at room temperature for 10 min. 30 µl of mixed samples were applied and separated in the gelatin gel (12% PAGE gel with 1mg/ml gelatin) with running buffer (see above) at 125 V for 120 min. After running, the gel was incubated in the 100 ml of renaturing buffer (2.5% (v/v) Triton X-100 in water) with gentle agitation for 30 min at room temperature. The renaturing buffer was decanted and replaced with 100 ml of Zymogram developing buffer (50 mM Tris-HCl, 200 mM NaCl, 5 mM $CaCl_2$, 0.02% (w/v) Brij 35). The gel was equilibrated for 30 min at room temperature with gentle agitation and then replaced with fresh Zymogram developing buffer 100 ml and was incubated at 37°C overnight. The gel was stained with Coomassie Blue R-250 solution (0.5% (w/v) in water) for 30 min at room temperature and then destained with destaining solution (Methanol: Acetic acid: Water (50: 10: 40)) until clear bands appeared.

3.2.9 Cell transfection and luciferase assay

C6 cells (3,000 cells/ml) were re-plated in the 24-well plate and maintained in DMEM under the standard cell culture condition. After 24 hours, cultural medium was changed (450 μl). Luciferase reporter plasmid containing 5×NFκB DNA binding sites (200 ng) and β-galactosidase reporter receptor (10 ng) were diluted in 50 μl of serum free Opti-Eagle's minimum essential media. This was then mixed with 0.8 μl of Fugene HD transfection reagent (Roche, Basel, Switzerland). The mixture was immediately vortexed for 10 sec and incubated at room temperature for 20 min. After incubation, the mixture was transferred to the cell plate containing 450 μl of DMEM, and distributed by gently shaking the plate several times. The cells were cultured under the standard condition for 24 hours. The cells were then treated with cathepsin G (1 μg/ml or 2 μg/ml) for another 24 hours. After treatment, the medium was removed and the cells were lysed with 100 μl of lysis buffer (Promega, Madison, WI) by vortexing for 15 min. The lysate was collected and centrifuged at 200×g for 5 min. The supernatant was applied to the measurement of luciferase (A_{luc}) and β-galactosidase (A_{gal}) activity. The activity of NFκB was determined by A_{luc}/A_{gal}. All treatments were performed in triplicates.

Chapter 3-3 Results

3.3.1 Differential regulation of cathepsin G in the DRGs and lumbar dorsal horn after peripheral inflammation

The microarray analysis showed a maximum change of cathepsin G expression among all differential proteases and protease inhibitors (6.17 folds, p=0.036) (Table 2-7). Quantitative RT PCR also confirmed the up-regulation of cathepsin G (4.0 folds, Student's t test, t=3.115, df=6, p=0.027) at the lumbar dorsal horn after CFA induced peripheral inflammation (n = 4) (Figure 3-2a). Since both peripheral (e.g. DRG) and central parts of the pain pathway contribute to pain hypersensitivity after CFA induced inflammation, we examined whether cathepsin G expression is also regulated in DRGs by quantitative RT PCR. Surprisingly, in contrast to lumbar spinal cord, the gene expression of cathepsin G is significantly down-regulated in DRGs (2.19 folds, Student's t test, t=2.565, df=6, p=0.043) (figure 3-2b). These results suggested that cathepsin G expression in response to CFA induced inflammation is different in different parts of pain pathway.

To investigate whether cathepsin G only responds to CFA induced chronic pain, we examined the expression of cathepsin G during chronic neuropathic pain model using CCI surgery. Seven days after surgery, paw withdrawal threshold (PWT) to mechanical pinch was significantly decreased in CCI animals (PWT = 22.1 g, n = 4)

compared with sham group (PWT = 41.9 g, n = 4) (Student's t test, t=6.522, df=6, p=0.0006) (Figure 3-2c). This finding confirmed mechanical allodynia was developed after peripheral nerve injury.

After behavioral testing, ipsilateral lumbar dorsal horn and DRGs were harvested from CCI rats (n = 4) and sham rats (n = 4). Total RNA was extracted as described above (sections 2.2.3 to 2.2.6 and 3.2.4). Cathepsin G level was then analyzed by quantitative RT PCR (Figure 3-2d and 3-2e). In contrast to CFA induced chronic pain, cathepsin G expression was not changed in lumbar dorsal horn or DRGs after peripheral nerve injury in CCI rats. We therefore conclude that the response of cathepsin G is specific to CFA induced chronic pain.

Considering that cathepsin G was only regulated in the CFA induced chronic pain (e.g. Day 4) and that astrocytes is important in CFA induced chronic pain, we examined whether cathepsin G could be regulated in glial cells by using C6 cells. Since cytokines, ATP and toll-like receptors (TLRs) are important mediators during chronic pain and inflammation in the nervous system, we treated the C6 cells with IL1β (50 ng/ml), TNFα (50 ng/ml), ATP (500 μM), E. coli lipopolysaccharide (LPS) (1 μg/μL, TLRs ligand) for 12 hours and examined the mRNA expression level of cathepsin G by using quantitative RT-PCR. None of these treatments changed the mRNA level of cathepsin G (Figure 3-3a). However, IL1β (50 ng/ml), TNFα (50

ng/ml) and LPS (1 μg/μL), but not ATP (500 μM) treatment for 24 hours slightly up-regulate cathepsin G protein in C6 cells as shown by Western blot study (Figure 3-3b).

Figure 3-2. Regulation of cathepsin G mRNA in pain pathway in CFA induced inflammatory pain model. 2a and 2b: cathepsin G mRNA expression level in lumbar spinal cord and dorsal root ganglions (DRGs) after complete Freud's adjuvant (CFA) injection. Cathepsin G gene expression is significantly up-regulated in lumbar (2a) (4.0 folds, Student's *t* test, t=3.115, df=6, p=0.027), but down-regulated in DRGs (2b) (2.19 folds, Student's *t* test, t=2.565, df=6, p=0.043) on 4 days after CFA injection. Error bars indicate SEM.

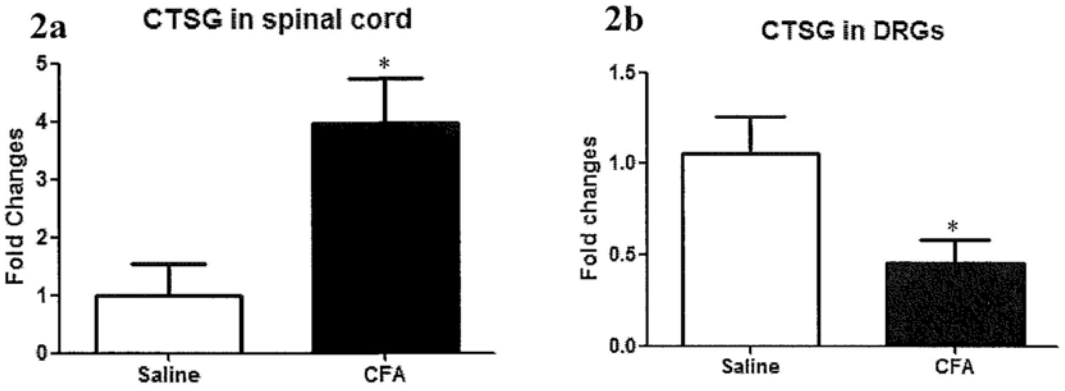

Figure 3-3. Regulation of cathepsin G mRNA in pain pathway in the CCI neuropathic pain model. 3a: Mechanical allodynia measurement. Sham surgery did not cause behavioral change on animals on day 7 as compared with baseline (n=4, Student's paired t test, t=2.292, df=3, p=0.106). In the contrast, CCI surgery successfully decreased the response threshold of mechanical stimulius on animals on day 7 as compared with baseline (n=4, Student's paired t test, t=7.145, df=3, p=0.0056). Behavioral tests showed the development of mechanical allodynia in rats after CCI surgery (Student's t test, t=6.522, df=6, p=0.0006) as compared with sham surgery. BL: baseline of paw withdrawal threshold; 7D: 7 days after surgery; **3b and 3c:** cathepsin G mRNA expression level in lumbar spinal cord and DRGs after peripherial nerve injury (CCI). Cathepsin G gene expression did not response to peripherial nerve injury in lumbar (2d) and DRGs (2e). Error bars indicate SEM.

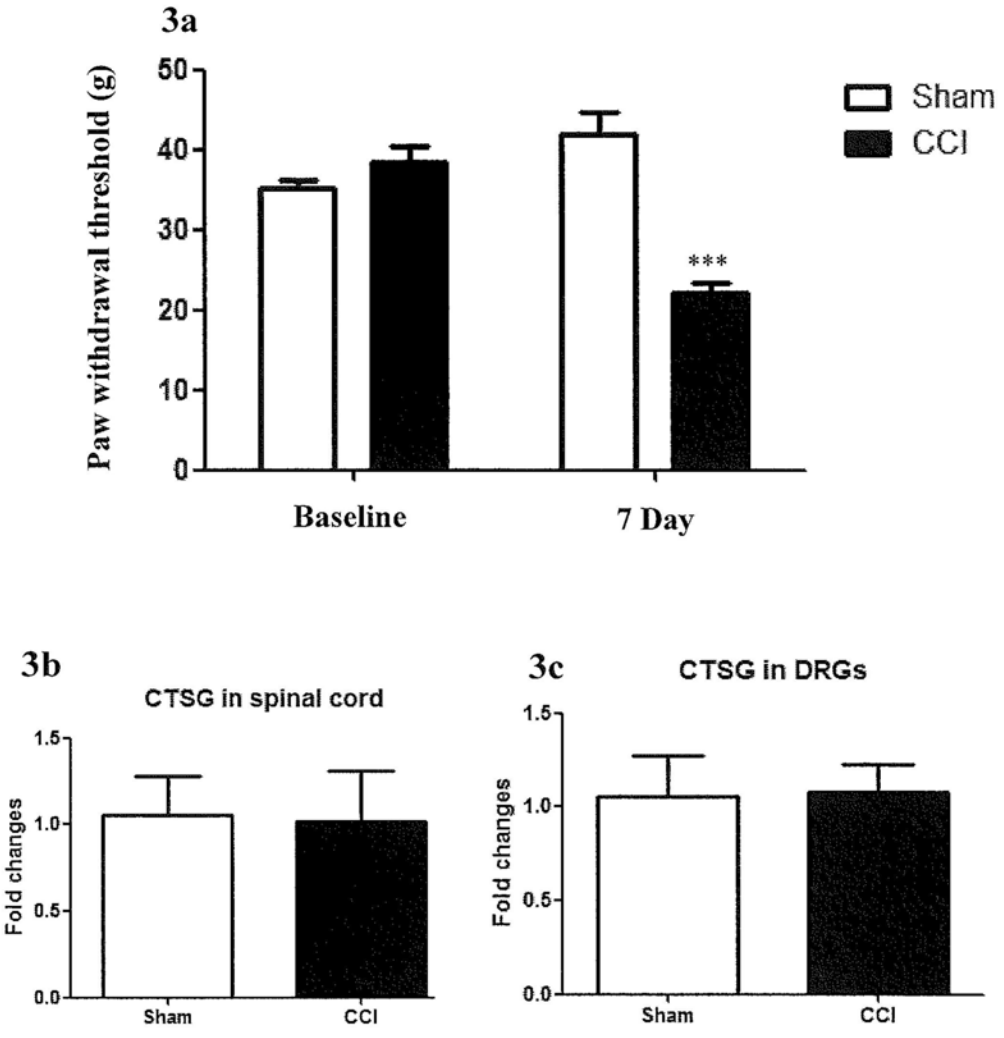

Figure 3-4. Regulation of cathepsin G mRNA and protein in C6 cells. 3a and 3b: cathepsin G mRNA and protein level in C6 cells after treatment with inflammatory mediators. Gene expression was not changed with cathepsin G treatment (2f), but slightly up-regulate the cathepsin G protein in C6 cell (2g). Error bars indicate SEM.

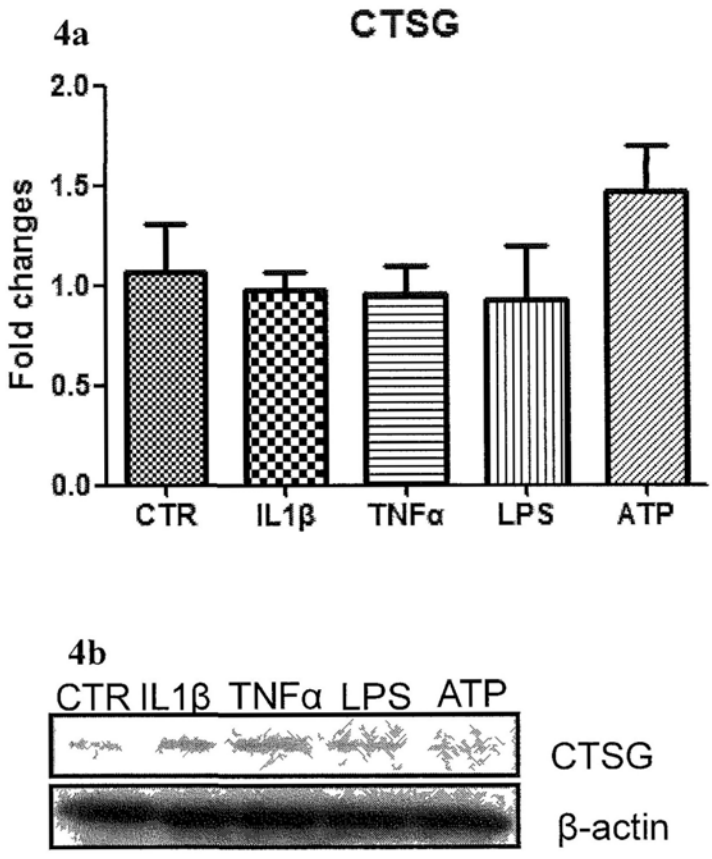

3.3.2 Cathepsin G activates signaling proteins in C6 cells and primary spinal astrocytes

As the up-regulation of cathepsin G mRNA expression was correlated with CFA induced chronic pain, the potential function of cathepsin G was examined. C6 cells and primary spinal astrocytes were used to test the signal transduction pathways involved in cathepsin G treatment. Firstly, C6 cells were treated with cathepsin G at different time points (0.5 and 1 hour) and doses (1 and 2 μg/ml). Samples were then analyzed by using Western blot and stained with p-p38MAPK, p38MAPK, c-Jun N-terminal kinase (JNK), phosphorylated-JNK (p-JNK), extracellular signal regulated kinases 1/2 (Erk1/2), p-Erk1/2, p-IκB and β-actin antibodies (figure 3-5a). As a control, LPS (1 μg/ml, 0.5 hour) was also used in this experiment. LPS treatment strongly induced the phosphorylation of p38MAPK, IκB, JNK, but not the Erk1/2 (Figure 3-5a). Treatment with cathepsin G phosphorylated IκB at all the time points and in all doses, as suggested by an increase in p-IκB staining, but not JNK and Erk1/2. In addition, p38MAPK was also activated by cathepsin G treatment in higher concentration (2 μg/ml) at both 0.5 hour and 1 hour. To further confirm the activation of signal transduction pathway, related downstream transcription factors were also analyzed. C6 cells were treated with cathepsin G (2 μg/ml) for 4 hours. Proteins were then harvested and analyzed by Western blot using p-CREB, CREB, p-ATF2 and

ATF2 antibodies. The results showed that CREB but not ATF2 was activated in response to cathepsin G treatment (Figure 3-5b). As one of the downstream transcription factors, increased CREB phosphorylation by cathepsin G treatment confirmed the activation of p38MAPK signaling pathway in C6 cells. NFκB activity was also monitored by luciferase assay. C6 cells were transfected with pNFκB-luc plasmids which containing 6×NFκB binding sites and luciferase reporter. After 24 hours, transfected cells were treated with cathepsin G (1 and 2 μg/ml, n = 3) for another 24 hours and luciferase assay was performed. The result showed that high concentration of cathepsin G treatment (2 μg/ml) up-regulated NFκB activity (1.72 folds, Student's t test, t=3.658, df=4, p=0.021) and therefore confirmed the activation of IκB-NFκB signaling pathway in C6 cells (Figure 3-5c).

We explored whether cathepsin G treatment could exert similar effects on primary spinal astrocytes. Primary culture of astrocytes was isolated and purified from spinal cord of 18 to 21-day Sprague Dawley rat embryos (Figure 3-6a-b). After purification (purity > 98%), the primary cells were treated with cathepsin G for Western blot studies. Similarly, cathepsin G (2 μg/ml) treatment was also able to induce the phosphorylation of p38MAPK and IκB in primary spinal astrocytes (Figure 6c). Furthermore, another important transcription factor, STAT3 was phosphorylated after cathepsin G treatment in primary astrocytes (Figure 3-6c).

Figure 3-5. Activation of signal transduction after cathepsin G treatment in C6 cells. 5a: Increased phosphorylation of inhibitor of kappa B (IκB) and p38 mitogen-activated protein kinase (p38MAPK) after cathepsin G treatment in C6 cells, but not for extracellular signal regulated kinases 1/2 (Erk1/2) and c-Jun N-terminal kinase (JNK). **5b:** Cathepsin G treatment induced phosphorylation of cAMP response element-binding (CREB), but not activating transcription factor 2 (ATF2). **5c:** Cathespin G significantly induced the NFκB activity at 2 μg/ml (1.72 folds, Student's *t* test, t=3.658, df=4, p=0.0216). Artificial unit was calculated by Luciferase activity readout divided by β-galactosidase activity readout. Error bars indicate standard error of the means.

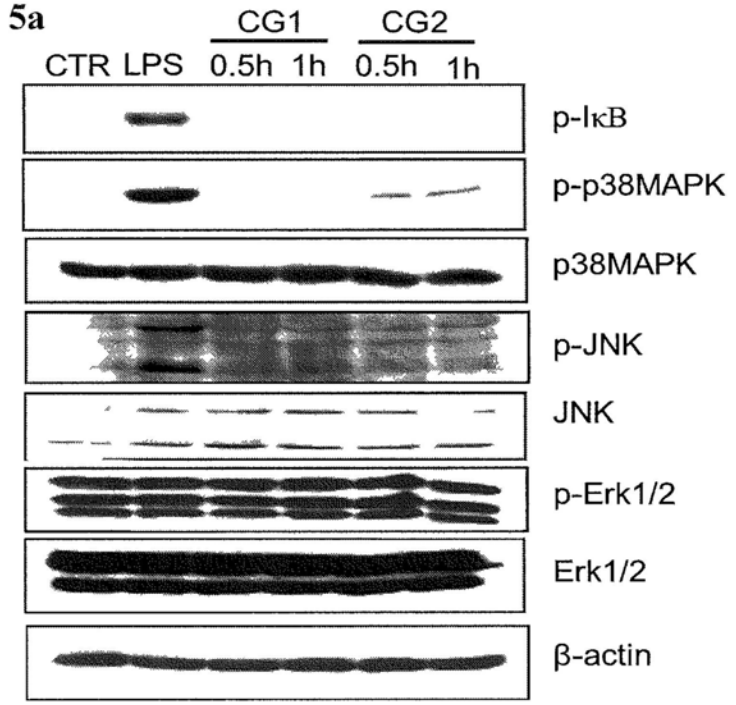

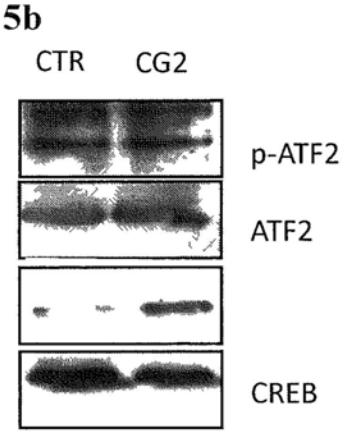

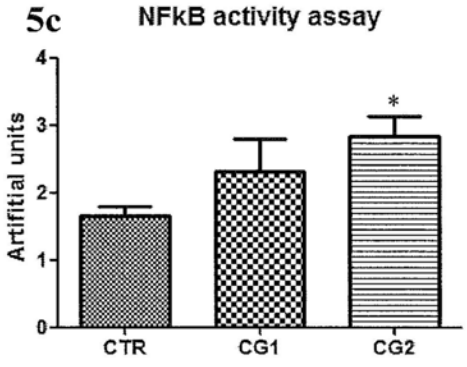

Figure 3-6. Activation of signal transduction after cathepsin G treatment in primary astrocytes. 6a (10×) and **6b** (20×), Immunofluorescence staining for GFAP on primary cells. Green, GFAP staining; blue, DAPI staining. **6c:** cathepsin G (2 μg/ml) induced the phosphorylation of p38MAPK, IκB and STAT3 in primary astrocytes. CG, cathepsin G; CG1, cathepsin G at 1 μg/ml; CG2, cathepsin G at 2 μg/ml; CTR, control. *p<0.05, student's t test. Error bars indicate standard error of the means.

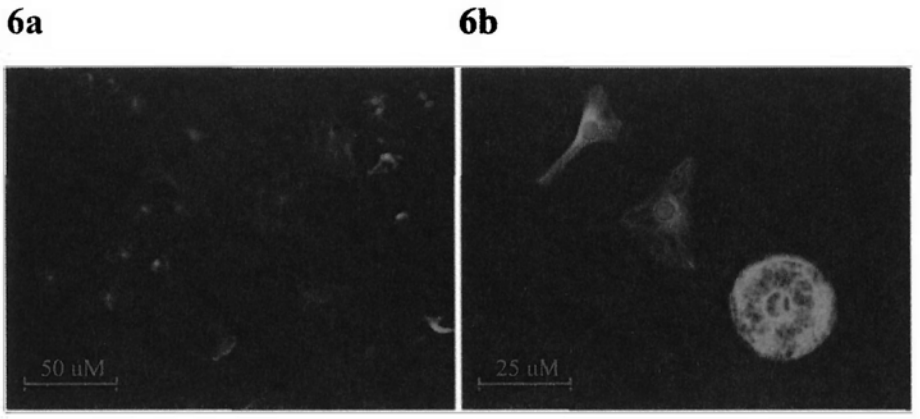

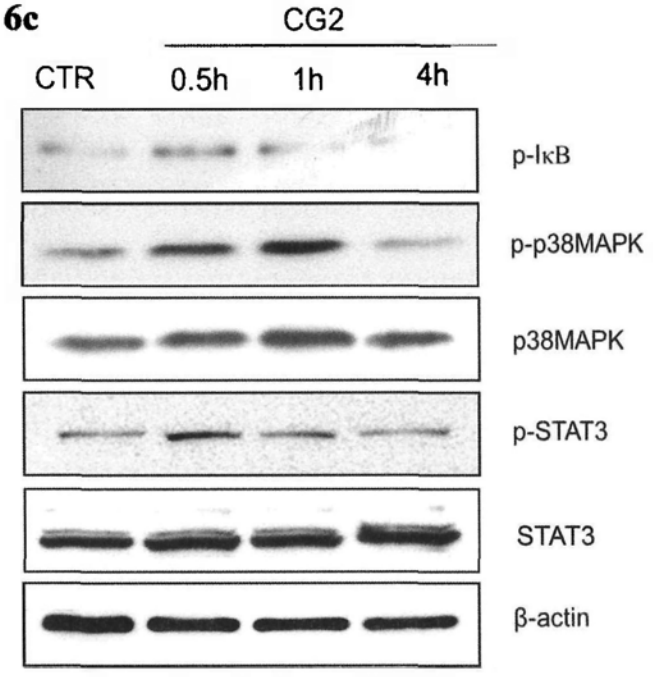

3.3.3 Cathepsin G induced pro-inflammatory genes expression in C6 cells and primary spinal astrocytes

Due to its role in the p38MAPK and IκB signaling pathway, we examined whether cathepsin G treatment could induce the expression of pro-inflammatory genes. We quantified IL1β, TNFα, IL6, MMP9 and MMP2 gene expression in C6 cells after cathepsin G treatment by using quantitative RT PCR (Figure 3-7a-e). The results showed that cathepsin G treatment up-regulated gene expression of IL6 (1.6 folds, Student's *t* test, t=5.027, df=4, p=0.007) and MMP9 (1.8 folds, Student's *t* test, t=15.29, df=4, p=0.0001), but not IL1β, TNFα and MMP2. Interestingly, consistent with the effects on MMP9 expression, MMP9 but not MMP2 activity was also increased by gelatin zymography study under the conditioned medium of cathepsin G treated C6 cells (Figure 3-7f). Similarly, cathepsin G also up-regulated the mRNA expression of IL6 (1.60 folds at 1 μg/ml, Student's *t* test, t=5.027, df=4, p=0.007; 1.83 folds at 2 μg/ml, Student's *t* test, t=5.416, df=4, p=0.006) and MMP9 (1.57 folds at 1 μg/ml, Student's *t* test, t=10.26, df=4, p=0.0005; 1.73 folds at 2 μg/ml, Student's *t* test, t=8.941, df=4, p=0.0009) in primary astrocytes, except for IL1β, TNFα and MMP2 (Figure 3-8a-e). Furthermore, pre-treatment of p38MAPK inhibitor (SB203580) completely reversed the effect of cathepsin G on IL6 and MMP9 mRNA expression (Figure 3-8a-e).

Figure 3-7. Pro-inflammatory genes expression after cathespsin G treatment in C6 cells. 7a-7e: Pro-inflammatory genes in C6 cells. After treatment with cathepsin G at 2 μg/ml for 12 hours, interleukin 6 (IL6, 1.6 folds, Student's *t* test, t=5.027, df=4, p=0.0073) and Matrix metalloproteinases 9 (MMP9, 1.8 folds, Student's *t* test, t=15.29, df=4, p=0.0001), but not IL1β, tumor necrosis factor α (TNFα) and MMP2 were significantly up-regulated in C6 cells. 4f, gelatin zymography of C6 conditioned medium. In keeping with the quantitative RT PCR results, cathepsin G significantly increased the MMP9 activity but not MMP2. Error bars indicate standard error of the means. $^{**}p<0.01$, $^{***}p<0.0001$, compared with control group, n=3 for each group, Student's *t* test. CG1, cathepsin G at 1 μg/ml; CG2, cathepsin G at 2 μg/ml; CTR, control.

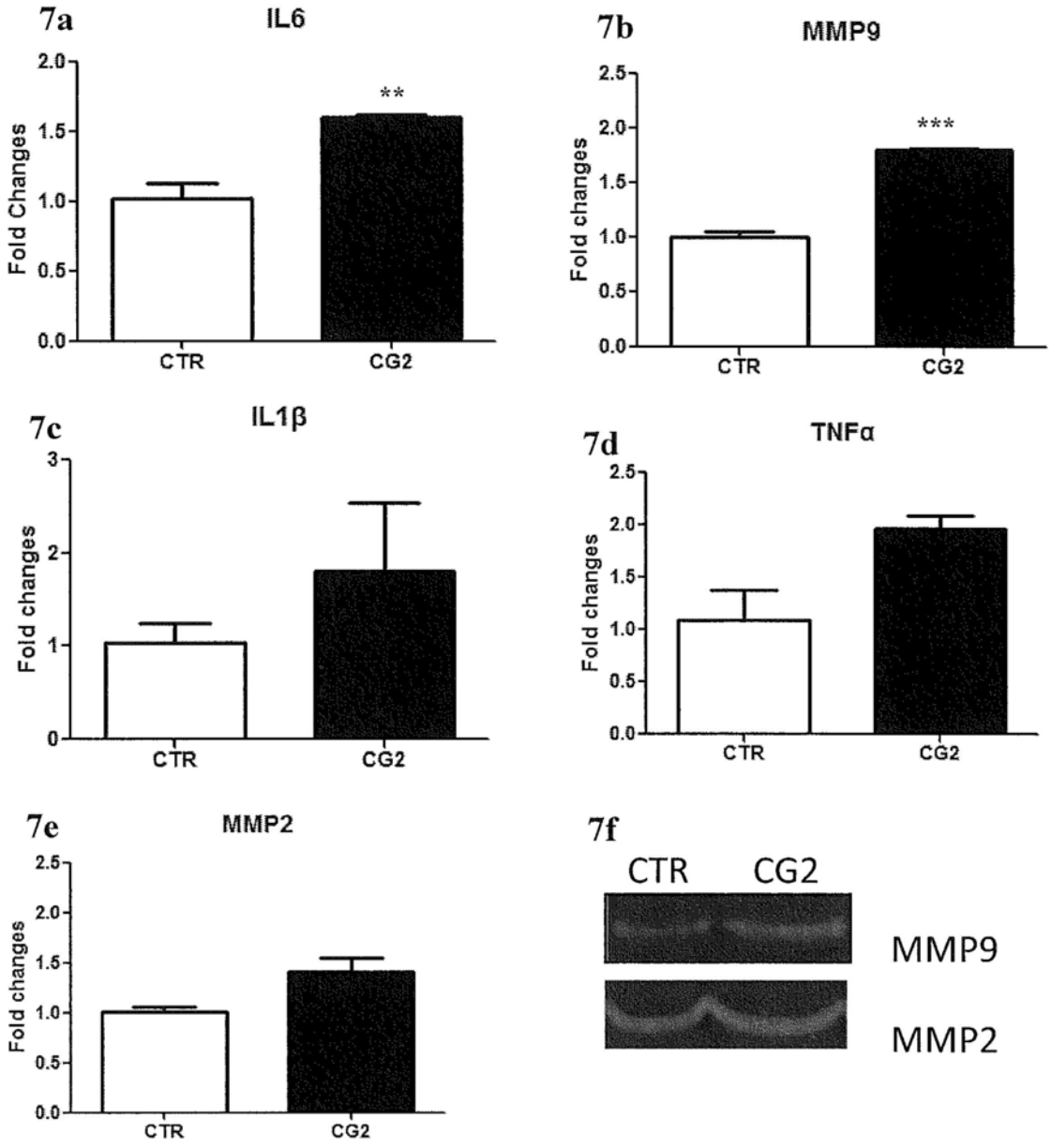

Figure 3-8. Pro-inflammatory genes expression after cathespsin G treatment primary spinal astrocytes. 8a-8e: Pro-inflammatory genes in primary spinal astrocytes. Cathepsin G treatment at 1 and 2 μg/ml both increase the expression of IL6 (1.60 folds at 1 μg/ml, Student's *t* test, t=5.027, df=4, p=0.0073; 1.83 folds at 2 μg/ml, Student's *t* test, t=5.416, df=4, p=0.0056) and MMP9 (1.57 folds at 1 μg/ml, Student's *t* test, t=10.26, df=4, p=0.0005; 1.73 folds at 2 μg/ml, Student's *t* test, t=8.941, df=4, p=0.0009), but not IL1β, TNFα and MMP2. Pre-treatment with p38MAPK inhibitor (SB203580) completely reversed the effects of cathepsin G on the gene expression. $^{**}p<0.01$, $^{***}p<0.0001$, compared with control group, n=3 for each group, Student's *t* test. CG1, cathepsin G at 1 μg/ml; CG2, cathepsin G at 2 μg/ml; CTR, control. Error bars indicate standard error of the means.

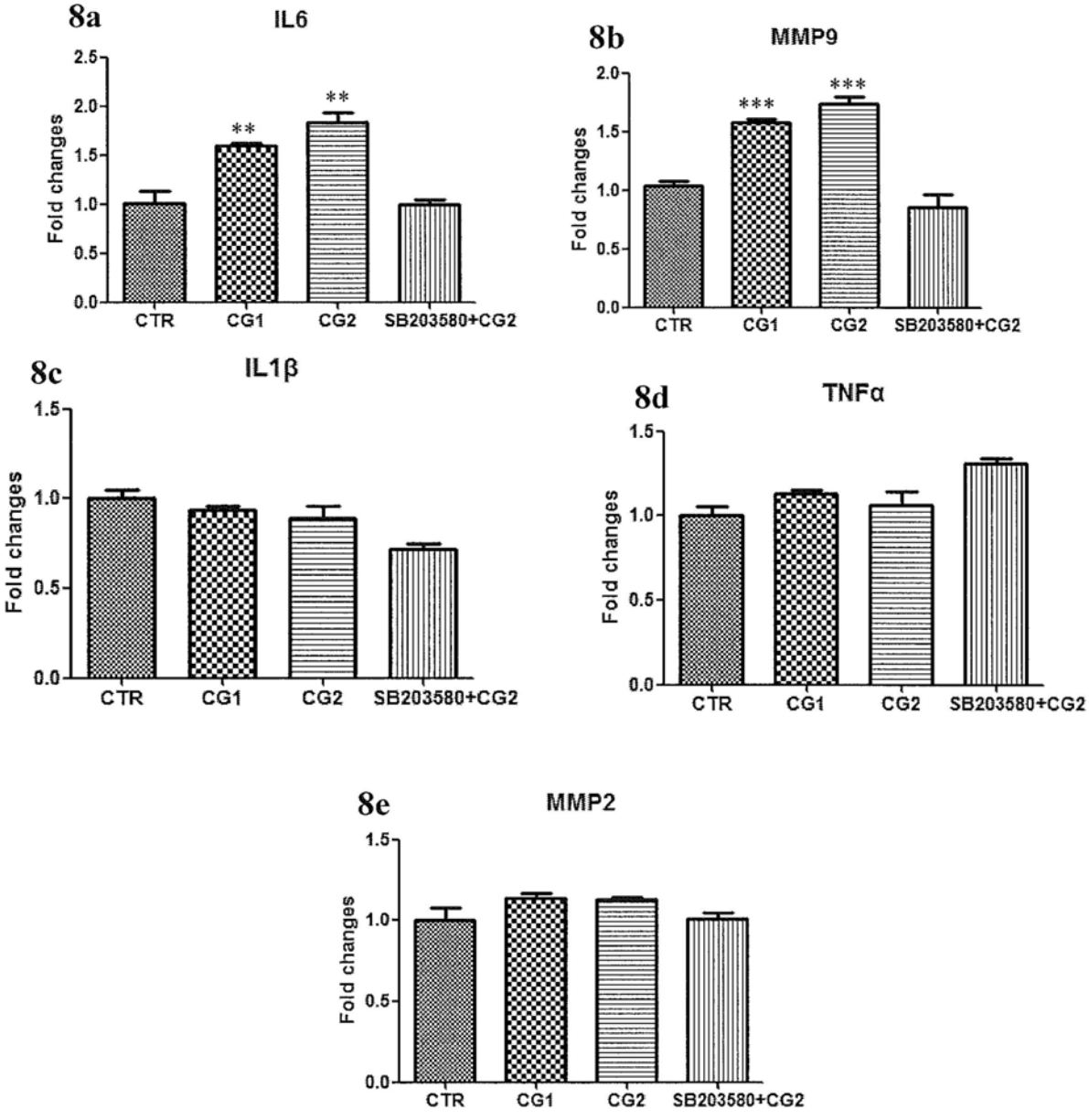

3.3.4 Inhibition of cathepsin G attenuated CFA induced inflammatory pain

We have shown that cathepsin G gene expression was regulated in both peripheral tissue and the nervous system after CFA induced chronic pain, there are also *in vitro* functional studies to suggest the role of cathepsin G in the regulation nervous system inflammation, it is reasonable to consider cathepsin G may be a new nociceptive protein in CFA induced chronic pain. We therefore used a cathepsin G inhibitor to animals to investigate the function of cathepsin G *in vivo*.

We first investigated the role in the inflammation induction by pre-administration with cathepsin G inhibitor before CFA injection. Baseline behavioral testing was recorded. One day before CFA injection, dimethyl sulfoxide (DMSO, 100 μl/rat, vehicle control) or cathepsin G inhibitor (Tosyl phenylalanyl chloromethyl ketone, TPCK, dissolved in DMSO, 1 mg/100 μl per rat) was administrated subcutaneously. On the day of CFA injection, heat hyperalgesia was used to examine the *de novo* effects of TPCK or DMSO on nociception. After behavioral testing, TPCK or DMSO was given again subcutaneously. One hour after TPCK or DMSO administration, inflammation was induced by intraplantar injection of 100 μl CFA (25% (v/v) in inCFA) in the left hind paw. The heat hyperalgesia was tested at 0.5 hour, 1 hour, 3 hour, 5 hour, 1 day, 2 day, 3 day, 4 day and 5 day after CFA injection.

Repeated measures showed that CFA injection caused heat hyperalgesia on

animals in a time dependent manner (Figure 3-9a, n = 8, ANOVA with repeated measures, F=17.874, p<0.001) and there was significant difference between TPCK and DMSO groups (Figure 3-9a, n = 8, factorial ANOVA with repeated measures, F=12.814, p=0.006). Neither TPCK (n = 6, Student's t test, t=1.230, df=10, p=0.2468) nor DMSO (n = 6, Student's t test, t=0.2888, df=10, p=0.7787) treated animals had changes in the thermal nociception compared with baseline (Figure 3-9a). Also, there was no difference in nociception between TPCK and DMSO administration (n = 6, Student's t test, t=1.185, df=10, p=0.2635) (Figure 3-9a). CFA injection induced heat hyperalgesia on all the rats soon after 0.5 hour and this effect lasted for at least 5 days. However, TPCK administration significantly increased the PWL compared with DMSO (vehicle control) at time points of 0.5 hour (n = 6, Student's t test, t=3.012, df=10, p=0.0131, pain recovery compared to DMSO, 40.4%), 1 hour (n = 6, Student's t test, t=3.514, df=10, p=0.006,) and 3 hour (n = 6, Student's t test, t=3.050, df=10, p=0.012). After 5 hours (n = 6, Student's t test, t=1.890, df=10, p=0.09) and until 4 days (n = 6, Student's t test, t=1.276, df=10, p=0.2307), although there was no significant difference between TPCK and DMSO treated rats, there was a trend of increased PWL in TPCK treated rats (Figure 3-8a). As a hallmark of inflammation, the paw edema was also determined by measuring the thickness and width of paws. The results were consistent with the behavioral test, TPCK administration also

significantly reduced the edema in the paws at 3 hours (n = 6, Student's t test, t=2.282, df=10, p=0.0456), but not on day 4 (n = 6, Student's t test, t=1.289, df=10, p=0.2265) after CFA injection (Figure 3-9b).

The role of cathepsin G was examined on heat hyperalgesia during chronic phase via inhibitor administration on day 4 and day 5 after induction of inflammation. 4 days after CFA injection, all rats developed heat hyperalgesia (Figure 3-10a). TPCK or DMSO was then administrated subcutaneously as above. One day after administration (on day 5), heat hyperalgesia was tested following another delivery of TPCK or DMSO (vehicle control). On day 6, heat hyperalgesia was measured again and the paw edema was measured as previous. Repeated measures showed that CFA injection caused heat hyperalgesia on animals in a time dependent manner (Figure 3-10a, n = 8, ANOVA with repeated measures, F=52.467, p<0.001) and there was significant difference between TPCK and DMSO groups (Figure 3-10a, n = 8, factorial ANOVA with repeated measures, F=7.149, p=0.018). Moreover, the result showed that TPCK treatment significantly increased PWL compared with DMSO treatment on both day 5 (n = 8, Student's t test, t=2.472, df=14, p=0.0269) and day 6 (n = 8, Student's t test, t=4.333, df=14, p=0.0007). However, this therapeutic effect disappeared after 48 hours of TPCK injection on day 7 (n = 8, Student's t test, t=0.7050, df=14, p=0.4923). Interestingly, it seems that post-administration of TPCK

did not reduce the paw edema as in the previous study. The paw edema in the TPCK group was actually worse than in the DMSO group (n = 8, Student's t test, t=2.607, df=14, p=0.021) (Figure 3-10b).

Figure 3-9. The preventive effects of TPCK on heat hyperalgesia and paw edema after CFA injection. 9a: heat hyperalgesia measurement. Pre-administration of Tosyl phenylalanyl chloromethyl ketone (TPCK) or dimethyl sulfoxide (DMSO) before inflammation induction significantly increased the paw withdrawal time (PWL) of rats during acute inflammation. However, TPCK did not affect normal nociception. **9b**: paw edema after inflammation induction. Pre-administration of TPCK reduced paw edema in the acute inflammation phase. *p<0.05, **p<0.01, ***p<0.001, Student's t test, n=6 in each group for post-administration experiments. Error bars are SEM.

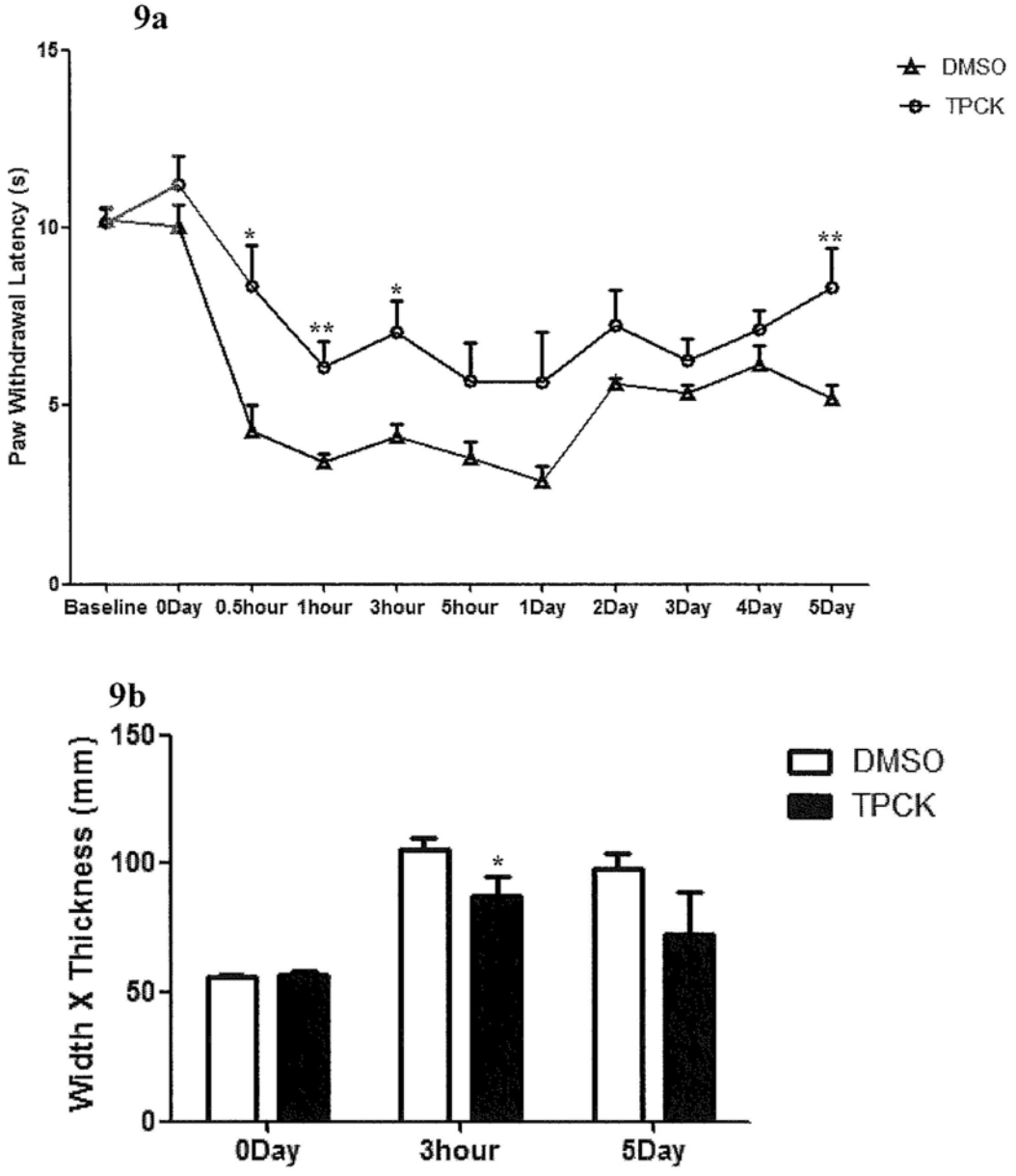

Figure 3-10. The therapeutic effects of TPCK on heat hyperalgesia and paw edema after CFA injection. 10a: Heat hyperalgesia measurement. TPCK or DMSO was given on day 4 and day 5 after inflammation induction (blue shadow). Post-administration of TPCK after inflammation also exerted analgesia effect on rats. But this effect disappeared 48 hours after administration (day 7, 48 hours after TPCK injection on day 5). **10b**: Paw edema measurement. Post-administration of TPCK did not show anti-inflammatory potential. The blue shadow indicates time when TPCK or DMSO administration subcutaneously. *p<0.05, **p<0.01, ***p<0.001, Student's t test, n=8 in each group for post-administration experiments. Error bars are SEM.

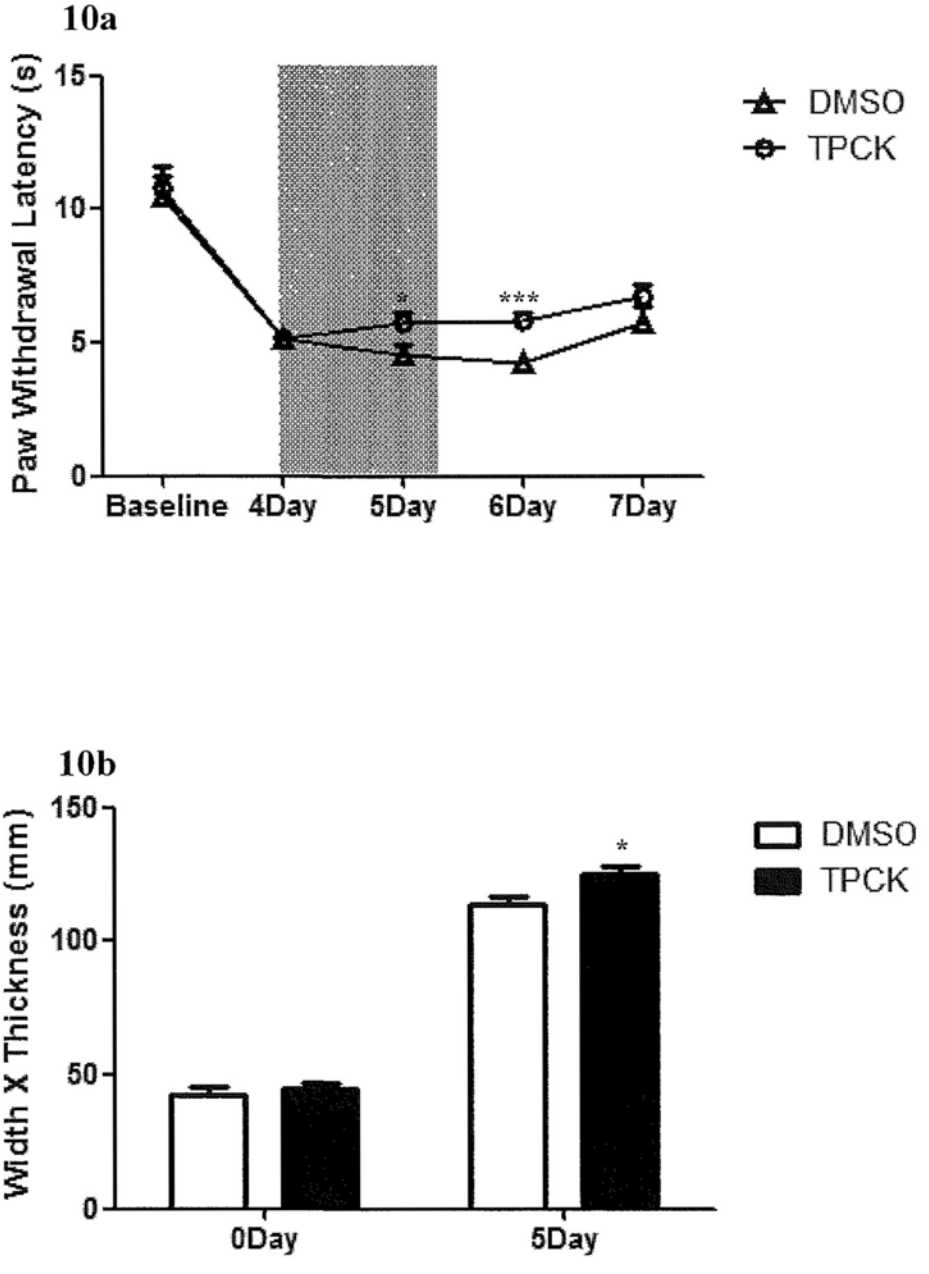

Chapter 3-4 Discussion

3.4.1 Cathepsin G expression in lumbar dorsal horn responded to peripheral inflammation but not peripheral nerve injury

Our results by quantitative RT PCR showed that cathepsin G mRNA expression was increased in the spinal cord, but decreased in the DRGs after CFA induced chronic pain. In contrast, neither spinal cord nor DRG changes the level of cathepsin G in the model of neuropathic pain (CCI model). This result strongly suggested that cathepsin G is specific for inflammatory pain such as those induced by CFA.

Recently, it was reported that after peripheral inflammation, the intercellular adhesion molecule (ICAM) which mediates neutrophils adhesion was significantly up-regulated in the endothelium of spinal cord. A subset of S100A8 and S100A9 expressing neutrophils were also found increased in this area (Mitchell et al., 2008). Since cathepsin G is mainly found in the neutrophils, the up-regulation of cathepsin G mRNA in the spinal cord may be induced by neutrophils migration after inflammation. Neutrophils migration was also reported in spinal cord after peripheral nerve injury. However, our results did not show an increase of cathepsin G mRNA expression after CCI. After peripheral inflammation, the expression of MCP-1, S100A8 and S100A9 was increased in the blood borne neutrophils. However, only S100A8 and S100A9 were found increased in the spinal cord, in contrast to MCP-1 (Mitchell et al., 2008).

This finding suggested a selective recruitment of the subpopulation of S100A8 and S100A9 expressing neutrophils to the spinal cord, other than the whole population of neutrophils. Therefore, the differential regulation of cathepsin G in CFA induced (inflammatory) versus CCI induced (neuropathic) chronic pain in our study may be due to the selective recruitment of neutrophils (i.e. cathepsin G expressing neutrophils). Similarly, the differential regulation in spinal cord versus DRGs after inflammation may also be due to the different recruitment of neutrophils. Further study on the definition of neutrophils subpopulation may reveal the function of neutrophil infiltration in the spinal cord.

Quantitative RT PCR results suggested that astrocyte is another source of cathepsin G. IL1β, TNFα, LPS and ATP are well known pro-nociceptive molecules in the spinal cord dorsal horn. We sought to determine whether cathepsin G is regulated in response to these molecules. Quantitative RT PCR showed that mRNA of cathepsin G did not change with IL1β, TNFα, LPS and ATP treatment in C6 cells. This result suggested that there may be other mediators contributing to the up-regulation of cathepsin G mRNA expression. On the other hand, this finding implied that neutrophils migration induced cathepsin G expression is important after peripheral inflammation. Nonetheless, the cathepsin G protein was increased in C6 cells after IL1β, TNFα and LPS treatment, further supports the presence of translational

regulation of cathepsin G. Moreover, up-regulation of cathepsin G protein level may contribute to the pro-nociceptive effect of these molecules.

3.4.2 Cathepsin G regulated pro-inflammatory potentials in glial cells via activation of signal pathways.

Cathepsin G shows a strong pro-inflammation potential in the peripheral tissue owing to its proteolytic activity. Astrocytes are important in the maintenance of inflammatory milieu during chronic phase of pain models. We therefore examined the function of cathepsin G in spinal cord by investigating its role in the astrocytes. Cathepsin G is able to activate GPCRs and EGFR (transactivation) by proteolysis (Sharony et al., 2010), suggesting that it can induce signal transduction in cardiomyocytes. Indeed, our study found that treatment with cathepsin G increased phosphorylation of p38MAPK and IκB in C6 cells. p38MAPK and IκB are important upstream components of signal transduction that are required for a large number of cytokine expression in the immune system. Activation of p38MAPK may further activate different transcription factors, including CREB and ATF2, which then bind to the promoter regions of pro-inflammatory genes and increase their gene expression (Bhat et al., 2002). Our results further showed that prolonged cathepsin G treatment (4 hour) induced the phosphorylation of CREB at Serine-133, but not ATF2. The

phosphorylation at CREB serine-133 by p38MAPK has been reported by other studies (Xing et al., 1998; Arthur et al., 2004). Our results therefore suggest that cathepsin G induce p38MAPK following by CREB activation and CREB dependent gene expression. IκB inhibits the NFκB complex by trapping it in the cytoplasm. Phosphorylation on the IκB by kinases marks them for degradation in the ubiquitination pathway, in turns p-IκB releases and activates the NFκB complex. Activated NFκB translocates into the nucleus and binds to the promoter regions of cytokine genes (Karin, 1999; Tak and Firestein, 2001). In consistent with the result of IκB phosphorylation, the luciferase assay revealed that cathepsin G treatment also increased the NFκB activity, suggesting the activation of IκB-NFκB signaling pathway by cathepsin G treatment in C6 cells. Similarly, cathepsin G also induced the phosphorylation of p38MAPK and IκB in primary spinal astrocytes, indicating the presence of similar upstream receptors processed by cathepinsn G. It has been reported that cathepsin G treatment can generate soluble receptor activator of nuclear factor-κB ligand (RANKL) and contributed to mammary tumor induced osteolysis (Wilson et al., 2008). In addition, membrane shedding of epidermal growth factor (EGF) by cathepsin G lead to transactivation of EGFR and induced p38MAPK and Erk1/2 activation in cardiomyocytes (Rafig et al., 2008). Therefore, it is interesting to see a similar receptor ligand processing mechanism attribute to the cathepsin G

induced signal transduction in C6 cells and astrocytes. PAR4 is a direct target of cathepsin G. Activation of PAR4 could induce p38MAPK phosphorylation in cells from several sources (Sabri et al., 2003; Fujiwara et al., 2005). We observed PAR4 expression in primary astrocytes. Therefore, the induction of signal transduction by cathepsin G might be also mediated by its proteolytic activation of PAR4.

STAT3 is a member of the signal transducer and activator of transcription (STAT). In response to cytokines and growth factors, STAT3 is phosphorylated and its dimer form is translocated to the nuclear where it acts as a transcription activator (Reich and Liu, 2006). STAT3 activation has been reported in the spinal cord astrocytes after spinal cord injury or peripheral nerve injury. Blockade of JAKs, which are upstream activators of STAT3, reduces STAT3 phosphorylation and nuclear translocation, and reverses pain hypersensitivity (Tsuda et al., 2011). Our data showed that STAT3 phosphorylation at Tyr 705 was induced by cathepsin G treatment in primary astrocytes. This finding thus indicated that cathepsin G is an inducer of STAT3 during the development of chronic pain. Blockade of cathepsin G may reverse STAT3 dependent central sensitization.

To further investigate the effects of signal transduction after cathepsin G treatment, the expression of several pro-nociceptive genes was examined in C6 cells and primary spinal astrocytes. Quantitative RT PCR analysis showed that cathepsin G

induced the expression of MMP9 in the C6 cells and astrocytes. Moreover, the gelatin zymography study also confirmed the increased MMP9 activity in the conditioned medium after cathepsin G treatment. Cathepsin G induced MMP9 activity has been reported in several studies (Han et al., 2007; Wilson et al., 2009). This is the first experiment, to the best of my knowledge that shows this enhancement effect can be mediated by transcriptional control of MMP9 gene. Interestingly, MMP9 mRNA up-regulation can be found in the spinal cord after peripheral inflammation (Part 2). Our study indicates cathepsin G is involved in the regulation of MMP9 gene expression. Pre-treatment with p38MAPK inhibitor completely reversed the up-regulation of MMP9 by cathepisn G. This result suggested that p38MAPK activation is required for cathepsin G induced gene expression. In keeping with our finding, activation of p38MAPK was shown to be involved in the IL1β induced MMP9 expression in smooth muscle cells (Liang et al., 2007).

MMP9 is an important mediator during peripheral inflammation. It was involved in the central sensitization of chronic pain through its ability of IL1β cleavage (Kawasaki et al., 2008). Our study showed that cathepsin G failed to induce the expression of IL1β in either C6 cells or astrocytes. However, cathepsin G may still regulate the IL1β cleavage through its activity to MMP9 activation. It has also been reported that several neutrophils derived proteases, including cathepsin G, were able

to convert pro-IL1β into a form with the same size of functional IL1β *in vitro* (Hazuda et al., 1990). This suggests that cathepsin G can be an endogenous regulator of IL1β.

Cathepsin G induced the expression of IL6 in both C6 cells and astrocytes. Similarly, pre-treatment with p38MAPK inhibitor also reverses the up-regulation of IL6 in astrocytes. It has also been shown that p38MAPK and CREB activation is required for IL17 induced IL6 expression in astrocytes (Ma et al., 2010). Our study showed an increase in phosphorylation of CREB (activation) by cathepsin G treatment. Taken together, I believe activation of p38MAPK/CREB signal transduction pathway is required for cathepsin G induced IL6 expression in astrocytes.

IL6 is the most potent inducer of STAT3 activity. On the other hand, it has also been shown that IL6 is a potential target gene of STAT3 (Yoon et al., 2010). Our Western blot study showed that cathepsin G treatment can also induce STAT3 activation. It is reasonable to consider that IL6 up-regulation by cathepsin G may partially depend on STAT3 signaling pathway. These findings suggest cathepsin G can activate multiple signal transduction pathways and regulate the expression of cytokines.

In summary, our studies on signal transduction and gene expression suggested that cathepsin G activates multiple signaling pathways and transcription factors and

directly up-regulate the gene expression. On the other hand, cathepsin G may also exert its pro-inflammatory potentials via up-regulation of effective proteins (e.g. MMP9). These results therefore strongly suggested the elevated cathepsin G levels contribute to the inflammation milieu in the spinal cord.

3.4.3 Inhibition of cathepsin G affected the pain hypersensitivity in acute and maintenance phase of CFA induced inflammatory pain.

Considering that cathepsin G might exert pro-inflammation effects in both peripheral tissues and spinal cord, we tested whether cathepsin G was involved in the persistent inflammation pain *in vivo*. We treated the animals with TPCK before the inflammation induction. TPCK is a serine protease inhibitor that has been used for cathepsin G blockade in several studies (Wilson et al., 2008; Wilson et al., 2009; Wilson et al., 2010). Our result showed that the treatment of TPCK did not change the nociceptive response on rats. However, TPCK increased the PWL of rats during acute inflammation. Although the difference can no longer be observed from 5 hour until day 4 after CFA injection, there is a trend showing that TPCK might decrease pain hypersensitivity. In consistent with these results, TPCK also reduced paw edema 3 hours after CFA injection. Cathepsin G may be responsible for edema in peripheral tissue because of its chemotactic activity. The recruitment of neutrophils and

subsequent monocytes/macrophages and mast cells may be mediated by cathepsin G (Sharony et al., 2010). These immune cells cause edema of peripheral tissue by releasing substance P and increase the vascular permeability (Cao et al., 1999). The recruited immune cells are able to release pro-inflammatory cytokines and chemokines which then sensitize nociceptors and cause peripheral sensitization. Our result showed that TPCK administration reduced paw edema after CFA injection, indicating that blockade of cathepsin G reduced the recruitment of immune cells and may be responsible for the improved analgesia.

To further investigate whether cathepsin G may actually participate in the central sensitization control of CFA induced chronic pain, we treated animals with TPCK in the maintenance phase of inflammation. After inflammation induction, all the rats developed heat hyperalgesia on day 4. Administration of TPCK on day 4 and day 5 significantly increased the PWL on day 5 and day 6, respectively. On the other hand, the post-administration of TPCK did not reduce the paw edema in contrast to the pre-treatment experiement. Rather, the paw edema was worse in the TPCK group than in the DMSO group. This result suggested that TPCK induced analgesia effect was not depending on the regulation of peripheral inflammation during this maintenance phase. Cathepsin G exerts pro-inflammation potential on astrocytes which are important in the maintenance of chronic pain. For example, cathepsin G was able to

induce the expression of IL6 in astrocytes, which can directly produce a pro-nociceptive effect in spinal cord. In addition, cathepsin G induced MMP9 up-regulation may increase the IL1β cleavage in the spinal cord. Finally, it has been reported that cathepsin G could convert membrane-bounded inactive TNFα into a soluble active form (Mezyk-Kopec et al., 2005). This proteolytic activity of cathepsin G may be important in TNFα induced central sensitization. Therefore, it is reasonable to propose that the analgesic effect by the administration of TPCK is mediated by blockade of cathepsin G function in the spinal cord and not a peripheral event. Further study using intrathecal injection will reveal the precise role of cathepsin G in central sensitization mechanism of chronic pain.

3.4.4 Weakness of the study

In this study, the pro-nociceptive roles of cathepsin G were evaluated by a series of *in vitro* and *in vivo* experiments. Although the differential regulation of cathepsin G was validated by using quantitative RT PCR, experiements on the protein level and function of cathepsin G was not performed. We plan to further our study by analyzing cathepsin G immuno-reactivity and monitoring the cathepsin G dependent protease function in the spinal dorsal horn.

In this study, I found that the administration of TPCK attenuated CFA induced heat hyperalgesia. Since TPCK may also inhibit the enzyme activity of some other

proteases, therefore specific inhibitor of cathepsin G should be used in the future studies. It should be noted that TPCK is potentially cytotoxic, we have therefore limited its dosage during the animal study. Our data and those from others suggested that cathepsin G can increase inflammatory cell recruitment in the peripheral tissue and could lead to central sensitization in the spinal dorsal horn. Given these limitations, a specific cathepsin G is required for future experiments.

3.4.5 Conclusion

The microarray analysis showed that a subset of proteases and protease inhibitors, including cathepsin G are identified in the differential gene expression list after peripheral inflammation with CFA injection. Further studies by quantitative RT PCR confirmed the regulation of cathepsin G mRNA expression in the both spinal cord and DRGs after CFA induced chronic pain, but not after peripheral nerve injury. Cellular biology study on cell line and primary astrocytes showed that cathepsin G activates p38MAPK-CREB, IkB-NFkB signaling pathways. Cathepsin G also activates the STAT3 transcription factor in primary astrocytes. More importantly, cathepsin G up-regulates the mRNA expression of IL6 and MMP9, at least through p38MAPK pathway. In addition, our animal studies showed that cathepsin G exert pro-nociceptive effect in CFA induced chronic pain. This is possibly due to a mechanism of pro-inflammation in the spinal cord. Our results strongly suggested that

cathepsin G is a new pro-nociceptive protein during the inflammation pain. Modulation of cathepsin G activity may benefit with management of both acute and chronic pain due to peripheral inflammation (such as CFA injection).

Part 4 The association of SNPs in differential genes and postoperative pain

Chapter 4-1 Introduction

Wound pain is a common complaint after surgery. Up to 80% of patients had moderate to severe pain when asked to report using a self-assessing verbal scale (Apfelbaum *et al.*, 2003). The incision (tissue damage) after surgery initiates inflammatory responses, causing the recruitment of pro-inflammatory immune cells, such as neutrophils and mast cells (Egozi et al., 2003). This may be responsible for persistent wound pain that can last for days and weeks. More seriously, it was found that some patients may experience wound pain even for months and develop chronic postoperative pain even after the wound has apparently healed. Depending on the types of surgery, 5-80% of patients developed chronic postoperative pain (Ephraim et al., 2005). Therefore, preventing postoperative pain, acute or chronic is beneficial in the management of the surgical patients.

Our animal studies have strongly indicated the role of cathepsin G in the acute and chronic pain in rats. It would be reasonable to ask whether cathepsin G can be served as predictor of acute and chronic postoperative pain by studying the single nucleotide polymorphism (SNPs) in cathepsin G. Two target SNPs from cathepsin G were selected from international Hapmap project. In this clinical study, we examined the association between SNPs for cathepsin G and acute or chronic postoperative

wound pain in a cohort of patients who had major abdominal surgery in our hospital.

Chapter 4-2 Materials and Methods

4.2.1 Patients

The study was approved by the Joint NTEC and CUHK Clinical Research Ethics Committee. Written informed consent was obtained from all patients. The patients who satisfied the following criteria were recruited to the study:

(1) Aged between 18 and 80 years,

(2) Planned for intra-abdominal surgery that required an open wound,

(3) Able to participate and comprehend education regarding the use of patient controlled analgesia and opioid therapy,

The exclusion criteria were as follows:

(1) Patients who were unable to provide informed consent;

(2) Patients with pre-existing chronic pain syndrome requiring ≥ two weeks of opioid therapy up to the time of surgery;

(3) Allergy to morphine, or paracetamol;

(4) Patients with pre-existing liver impairment as evidenced by abnormal liver function testing,

(5) Expected to require further surgery ≤ 72 hours of initial surgery,

(6) Patient requiring neuraxial or other regional techniques for postoperative pain

management.

Sevoflurane based anesthesia was provided in all patients during surgery. Patient controlled analgesia machine was used for postoperative pain relief. This is changed to oral paracetamol tablets as appropriate. Whole blood (5 ml) from recruited patients was collected during surgery. The blood was then used for genomic DNA extraction (see below). Acute pain intensity was recorded using the visual analogue scale (VAS) (Myles et al., 1999; Aun et al., 1986) at 24, 48 and 72 hours after surgery. The VAS is an 11 point scale, with 0 indicates no pain and 10 represents the worst imaginable pain. Three types of VAS pain intensity was measured, i.e. when patients were at rest, with deep breathing and with coughing were measured at all time points. Chronic pain intensity was recorded using the modified brief pain inventory (mBPI) (Wang et al., 1996) during a phone or face-to-face interview 3 months after surgery. Similarly, a scale of 0-10 points was used in the mBPI to measure pain intensity. During the study, the patients and research assistants who collect the pain data were blinded to the genotyping analysis.

4.2.2 Genomic DNA extraction

Genomic DNA extraction was done using the QIAamp DNA blood mini kit (QIAGEN, Hilden, DE). Buffy coat was purified from whole blood. To do this, 2 ml

of whole blood was diluted with 2 ml of PBS, and then carefully layered onto 3 ml of Ficoll reagents (GE Healthcare, Little Chalfont, UK) in a 15 ml tube. The tube was centrifuged at 400×g for 30 min at 18°C. The buffy coat layer in the middle was then collected and performed with genomic DNA extraction. 200 μl of buffy coat was mixed with 20 μl of QIAGEN proteinase K. 200 μl of buffer AL was then added to this mixture and pulse-vortexed for 15 sec. This is followed by incubation at 56°C for 10 min. 200 μl of ethanol (100%) was then added to the mixture and pulse-vortexed for 15 sec. After this, all the mixture was applied to the QIAamp mini spin column and centrifuged at 6,000×g for 1 min. The genomic DNA was thus attached on the column. The column was washed with 500 μl of buffer AW 1 at 6,000×g for 1 min and 500 μl of buffer AW 2 at 16,000×g for 3 min. The genomic DNA was eluted with 200 μl of water with centrifugation at 6,000×g for 1 min. The DNA concentration was measured using Nanodrop 1000 spectrophotometer (Nanodrop, Wilmington, DE).

4.2.3 Genotyping

Genotyping was done by Taqman SNP genotyping assay using the Taqman Genotyping master mix kit (Life Technologies, Carlsbad, CA). The SNPs and their flanking sequence were listed in the Table 4-1. The PCR mixture was prepared in a volume of 5 μl containing 10 ng of genomic DNA, 2.5 μl of Taqman genotyping

master mix and 0.25 μl of 20 × SNP specific probes and primers. All the mixture were added to the 384-well optical plate and analyzed at 7900HT fast real-time PCR system (Life Technologies, Carlsbad, CA). Before the PCR, a pre-read was done to record the background of each well. After that, the mixture was incubated at 50°C for 5 min and denatured at 95°C for 10 min, followed by 40 cycles of PCR (denaturation at 95°C for 15 sec; primers/probes annealing and extension at 60°C for 1 min). After PCR, post-read was performed to discriminate the genotypes in each well.

4.2.4 Data analysis

The genotype frequencies were analyzed using the Hardy-Weinberg Equilibrium (HWE) analysis. Repeated measures analysis of variance (ANOVA) was used to detect the effects of the three genotypes (homozygous wide-type, homozygous SNP and heterozygous) on the VAS pain scores recorded on the first three consecutive days after surgery. Similarly, the association between genotypes and chronic pain scores was also examined by one-way ANOVA. The development of severe acute pain was defined average VAS pain scores ≥ 5 during the first three days after surgery. The association between genotypes and severe acute postoperative pain was tested using logistic regression. All the statistical analysis was done using SPSS 15.0 (SPSS, Chicago, IL). The probability of < 0.05 was considered as the statistically significant

difference.

Table 4-1. SNPs sequences of cathepsin G and BDNF and their Taqman assays.

SNPs	ABI assay ID	Context Sequence*	Chromosome	Location on NCBI Assembly
rs2070697	C__348846_1_	TGGTTAGCTGCAGTCTTGCCCTCCCC**[G/A]**TGCTGTCTGCCTACCCTGCAGAGCT	14	24113929
rs2236742	C__15954989_10	ATAAGTGCTATAAAAACATGCTTTGT**[G/A]**TAAATAATTTGGCAGCATGTGTCAG	14	24114970
rs8019787	C__29358336_10	ATTTTCTTTCACAAGGTTTAGGACAA**[C/G]**CATGCGGGCTGGTGATGGACGCTAT	14	24111686
rs6265	C__11592758_10	CATCATTGGCTGACACTTTCGAACAC**[A/G]**TGATAGAAGAGCTGTTGGATGAGGA	11	27679916

*In context sequence, SNP alleles are in brackets, where [$Allele_1$ = VIC / $Allele_2$ = FAM].

Chapter 4-3 Results

4.3.1 Patient characteristics and genotyping

Between 2nd February, 2009 and 6th October, 2009, a total of 267 patients undergoing open intra-abdominal surgery entered the study. Table 4-2 summarizes patient characteristics and surgical details in the entire cohort. The genotyping results of rs2070697, rs2236742, rs8018792 and rs6265 were shown in Table 4-3. The genotypes distributions of these SNPs were in HWE, except for rs8018792 (Table 4-3). Therefore, the genotypes of rs8018792 were ruled out for further analysis.

4.3.2 The genotypes of rs2236742 were significantly associated with acute postoperative pain development.

ANOVA with repeated measures showed no statistical difference among the three different genotypes (rs6265, rs2070697 or rs2236742) and VAS pain scores at rest, with deep breathing or during coughing (Figure 4-1, Figure 4-2 and Figure 4-3, respectively). However, the genotypes at rs2236742 were significantly associated with the incidence of severe acute pain at 48 hours after surgery (average pain > 5), p = 0.016 (Figure 4-4a). Fewer patients carrying the homozygous SNP (AA) developed severe acute pain than those carrying homozygous wide type (GG), adjusted odds ratio 12.4, 95% confidence interval (CI): 1.4-106 or heterozygous (AG), adjusted

odds ratio 9.9, 95%CI: 1.1-88 (Figure 4-4b).

Table 4-2. Patient characteristics and surgical details.

Demographic information	Values
Female	175 (65.5%)
Age	54.4 ± 11.2
Height (cm)	157 ± 19
Weight (kg)	59.3 ± 13
BMI (kg/m^2)	22.8 ± 5.6
Education level (0/1/2/3)*	45/121/57/40
Pre-existing major medical conditions	
Liver disease	71 (37.5%)
Respiratory disease	12 (4.5%)
Kidney disease	6 (2.2%)
Diabetes mellitus	39 (14.6%)
Current smoker	19 (7.1%)
Anti-epileptic medication	3 (1.1%)
Antidepressant use	4 (1.5%)
Alcohol abuse	3 (1.1%)
Surgical wound	
Infra-umbilical	172 (64.4%)
Both infra- and supra-umbilical	86 (32.2%)
Horizontal	125 (46.8%)
Wound longer than 10 cm	204 (76.4%)
Surgical details	
Duration of surgery (min)	202 ± 118
Total intraoperative dose of morphine (mg)	14.1 ± 25.7
Use of nitrous oxide	116 (43.4%)

Table 4-3. Genotypic and allelic distribution of Chinese patients.

Gene	rs number of SNPs*	Genotypic distribution			Minor allelic frequency	*p*-value**
		Homozygous Wide-type	Heterozygous	Homozygous Minor allele		
CTSG	rs2070697[G/A]	77	105	38	0.411	0.8299
CTSG	rs2236742[G/A]	156	63	7	0.170	0.8354
CTSG	rs8018792[A/G]	120	84	51	0.365	3.9E-06
BDNF	rs6265[G/A]	64	114	50	0.469	0.95443

*In rs number for any single nucleotide polymorphism (SNP), SNP alleles are in brackets, where [Allele1=Wild-type/Allele2=variant SNP].
***p* value from HWE test.

Figure 4-1. No association of genotypes in rs6265 with VAS pain score at different time points. 1a, VAS pain score at rest. ANOVA with repeated measures showed that there was significant difference of VAS pain score at rest among three time points (F=138.559, p<0.001). However, no significant can be observed among the 3 genotypes (F=0.979, p=0.38). 1b, VAS pain score with deep breath. ANOVA with repeated measures showed that there was significant difference of VAS pain score at rest among three time points (F=72.599, p<0.001). However, no significant can be observed among the 3 genotypes (F=1.258, p=0.29). 1c VAS pain score with cough. ANOVA with repeated measures showed that there was significant difference of VAS pain score at rest among three time points (F=32.046, p<0.001). However, no significant can be observed among the 3 genotypes (F=3.032, p=0.051).

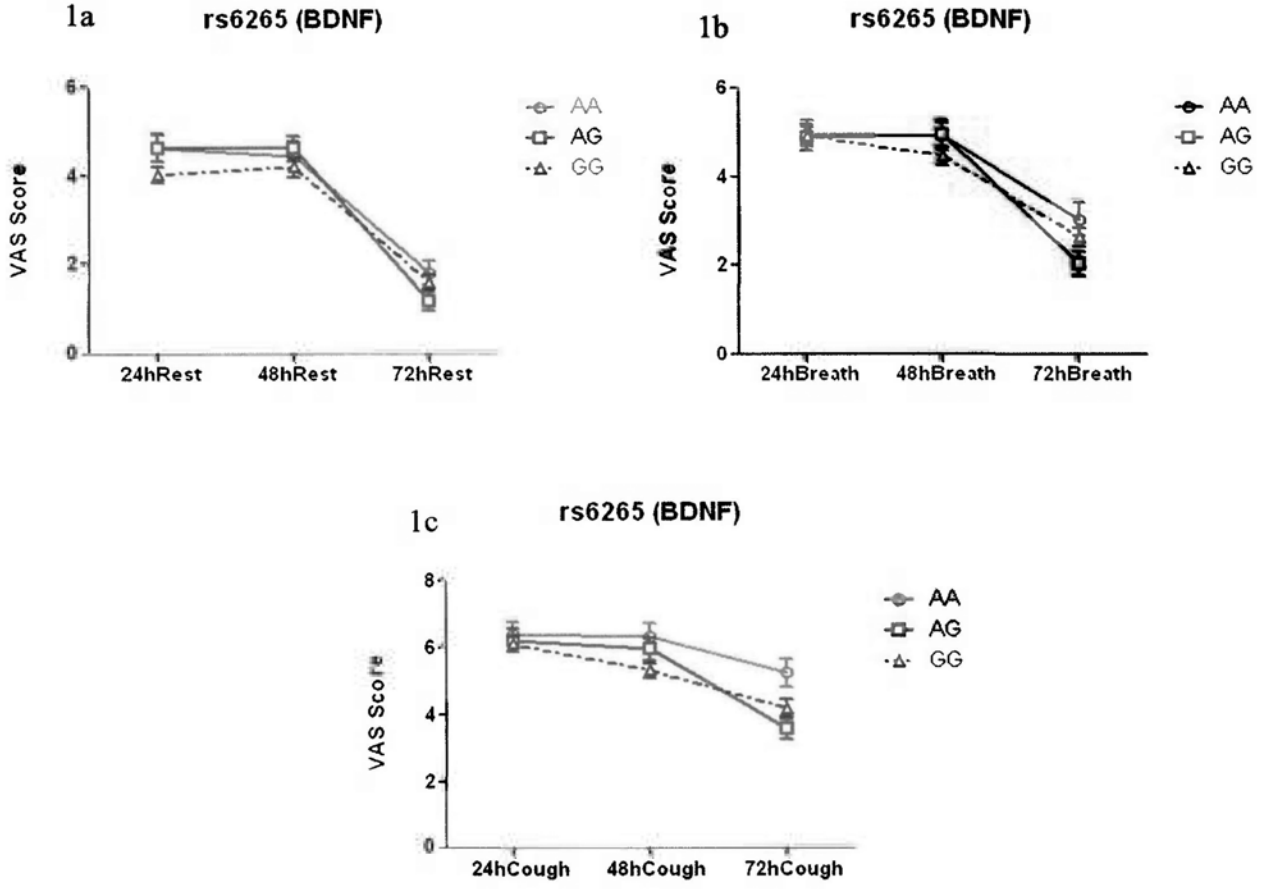

Figure 4-2. No association of genotypes in rs2070697 with VAS pain score at different time points. 2a, VAS pain score at rest. ANOVA with repeated measures showed that there was significant difference of VAS pain score at rest among three time points (F=118.439, p<0.001). However, no significant can be observed among the 3 genotypes (F=0.635, p=0.53). 2b, VAS pain score with deep breath. ANOVA with repeated measures showed that there was significant difference of VAS pain score at rest among three time points (F=59.630, p<0.001). However, no significant can be observed among the 3 genotypes (F=0.268, p=0.71). 2c VAS pain score with cough. ANOVA with repeated measures showed that there was significant difference of VAS pain score at rest among three time points (F=24.429, p<0.001). However, no significant can be observed among the 3 genotypes (F=0.754, p=0.47).

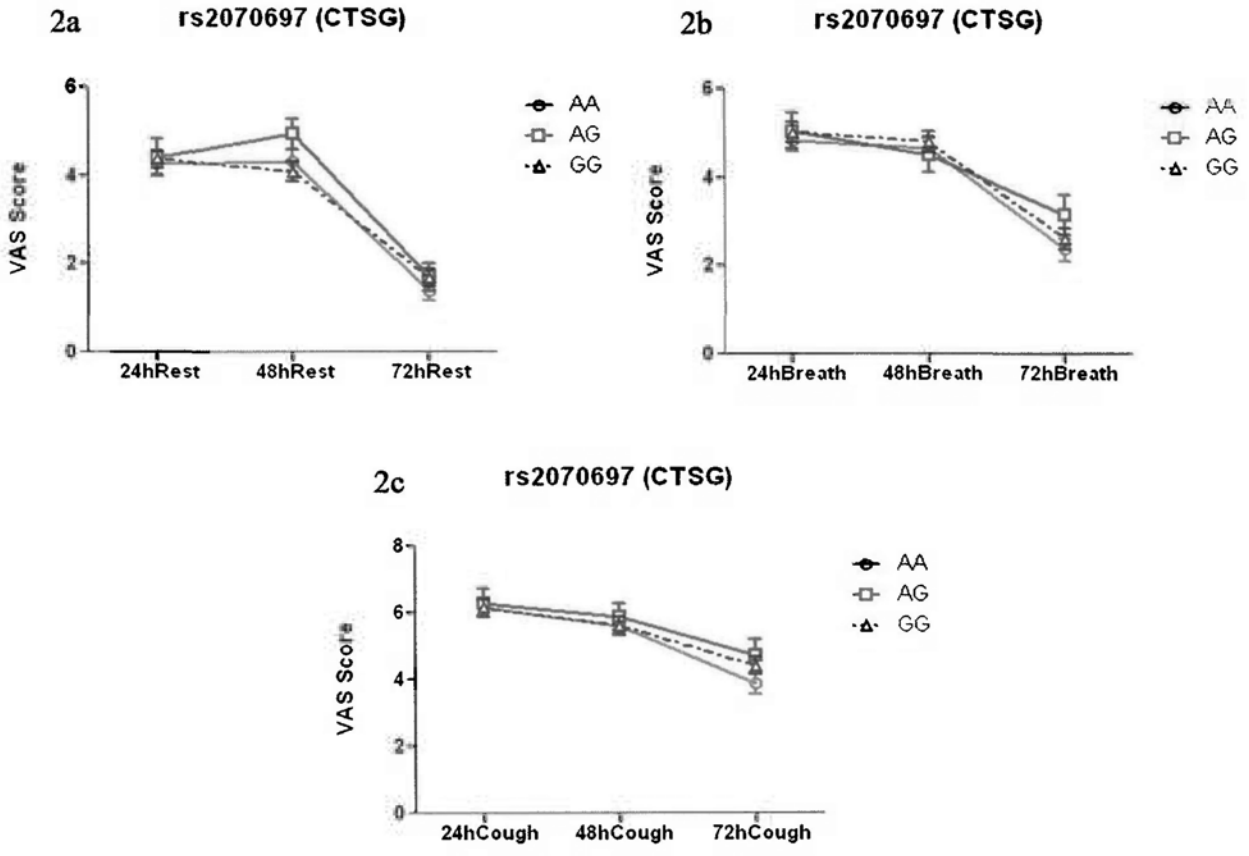

Figure 4-3. No association of genotypes in rs2236742 with VAS pain score at different time points. 3a, VAS pain score at rest. ANOVA with repeated measures showed that there was significant difference of VAS pain score at rest among three time points (F=43.688, p<0.001). However, no significant can be observed among the 3 genotypes (F=0.648, p=0.524). 3b, VAS pain score with deep breath. ANOVA with repeated measures showed that there was significant difference of VAS pain score at rest among three time points (F=18.403, p<0.001). However, no significant can be observed among the 3 genotypes (F=.637, p=0.530). 3c VAS pain score with cough. ANOVA with repeated measures showed that there was significant difference of VAS pain score at rest among three time points (F=16.761, p<0.001). However, no significant can be observed among the 3 genotypes (F=0.369, p=0.692).

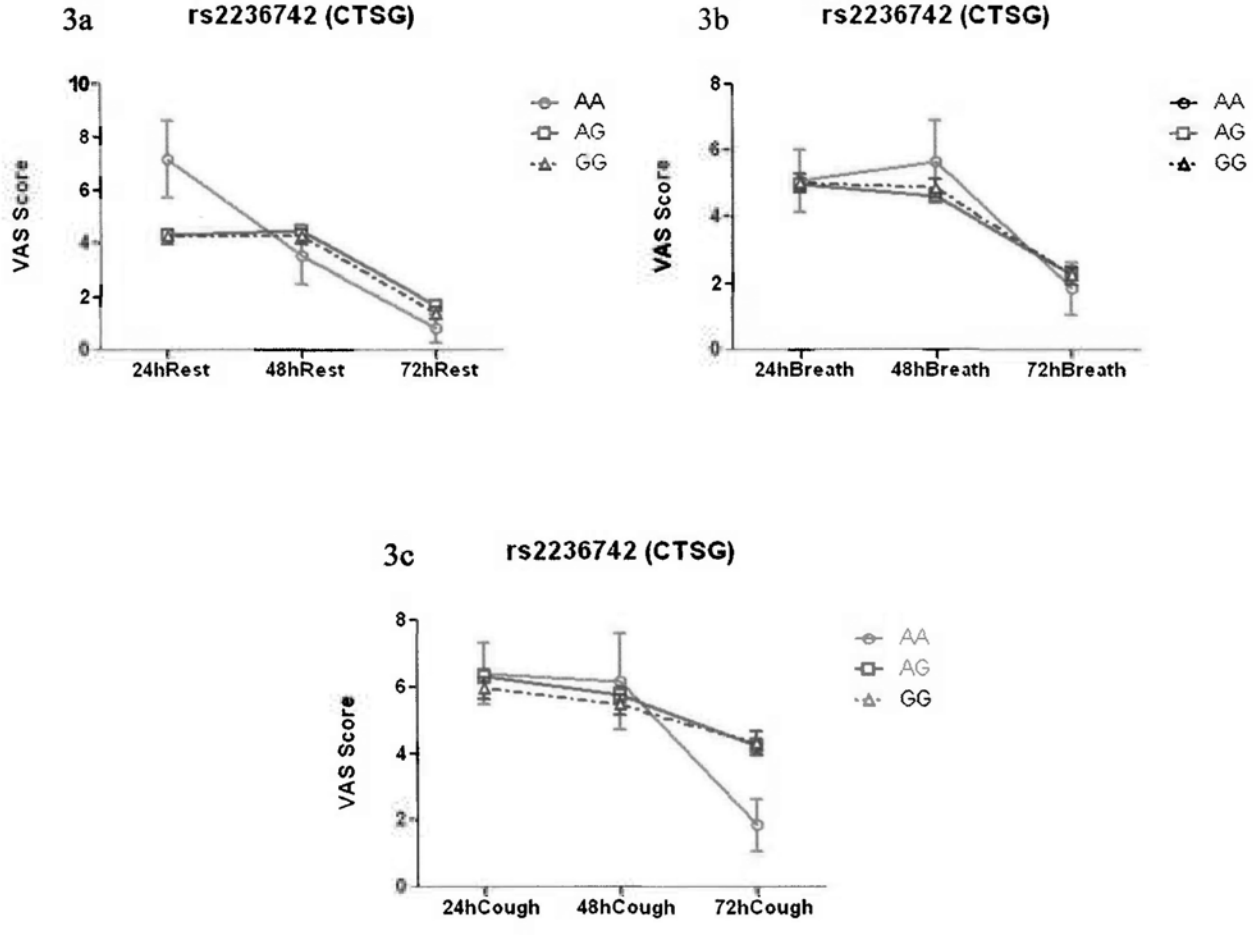

Figure 4-4. Association of cathepsin G SNP with severe acute wound pain. 4a: Genotypes of rs2236742 in cathepsin G significantly associated with the development of severe acute postoperative pain (logistic regression). Allele1=homozygous wide-type; Both=heterozygous; Allele2=homozygous minor allele; %severe acute pain=percentage of patients who developed severe acute postoperative pain (VAS $\geq$ 5). **4b:** patients carrying AA and AG had higher incidence to the development of severe acute pain than GG patients (odds ratios 12.4 [1.4-106] and 9.9 [1.1-88], respectively).

4a

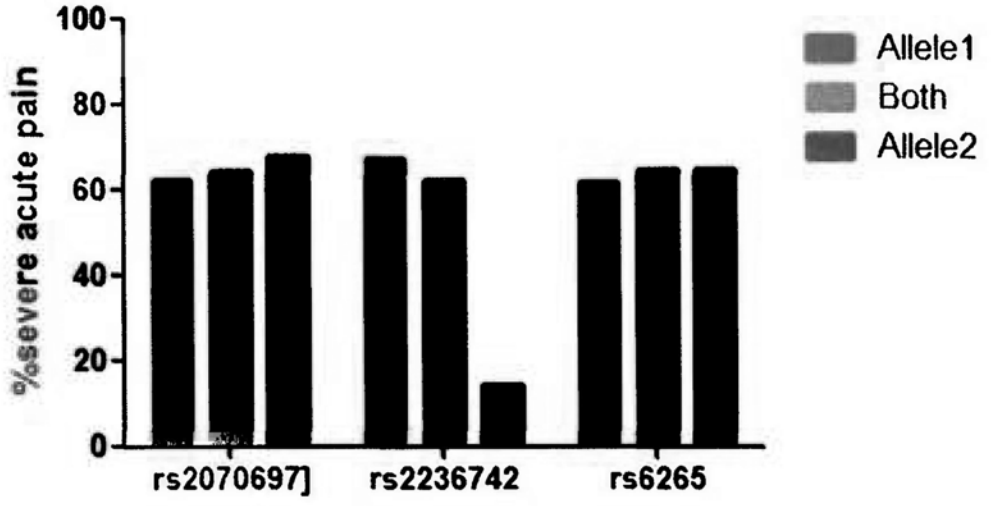

p value (χ^2 test)	0.861	0.016	0.922

4b

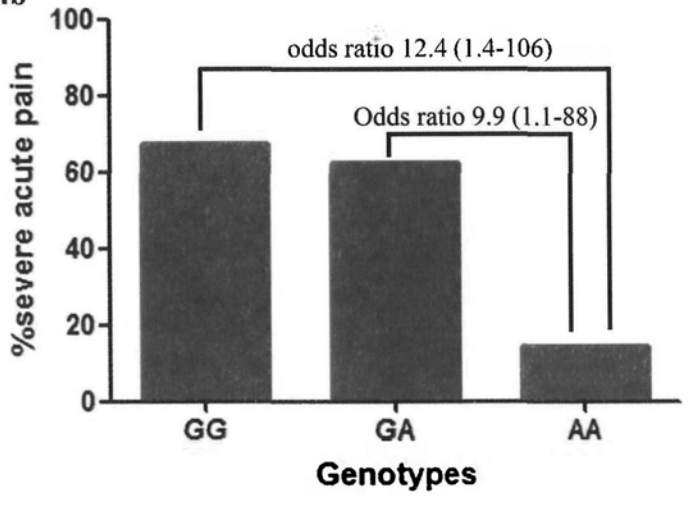

4.3.3 SNPs in cathepsin G and BDNF showed no association with persistent postoperative pain.

The effect of genotypes in these SNPs on chronic postoperative pain, 3 months after surgery was also assessed. A total of 91 patients among 230 patients (39.9%) reported chronic wound pain, 3 months after surgery. 20 patients had reported severe pain (pain score ≥ 5). One-way ANOVA was used to examine the association between cathepsin G or BDNF genotypes and the raw pain scores recorded by the mBPI scales. Logistic regression was used to detect the association between genotypes and the development of chronic postoperative wound pain (mBPI > 0) or severe chronic postoperative wound pain (mBPI ≥ 5). Pain score was similar among all three genotypes. These results showed that neither the development nor the severity of chronic postoperative pain was affected by the genotypes of cathespin G and BDNF (Figure 4-5).

Figure 4-5. No association of cathepsin G and BDNF SNPs with chronic postoperative wound pain. Genotypes in rs2070697 and rs2236742 of cathepsin G and rs6265 of BDNF were not associated with the development of chronic postoperative wound pain. Allele1, homozygous wide-type; Both, heterozygous; Allele2, homozygous minor allele; %chronic pain, percentage of patients who developed chronic postoperative wound pain on 3 month after surgery.

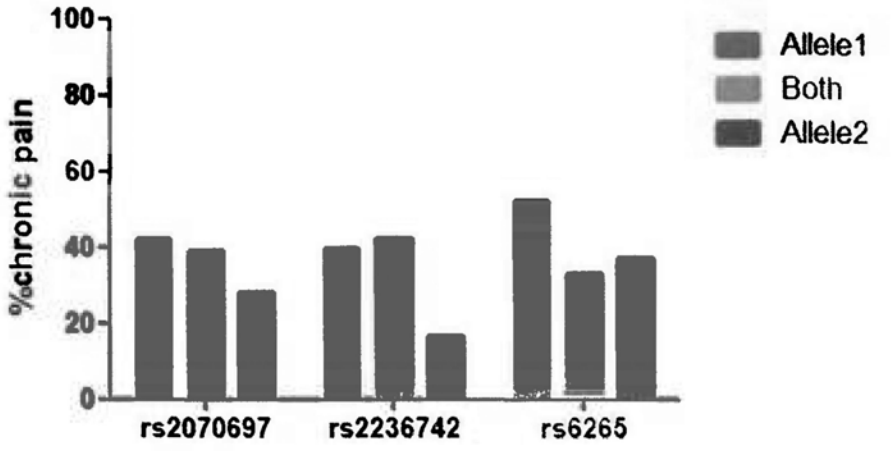

p value (χ^2 test)	0.400	0.482	0.054

Chapter 4-4 Discussion

4.4.1 Genetic polymorphisms in cathepsin G showed association with acute but not chronic postoperative pain.

When analyzed with the VAS pain scores, no difference can be found among three different genotypes of two SNPs. We then classified patients into those having severe wound pain (VAS $\geq$ 5). In patients with homozygous SNP carriers (AA) of rs2236742, there was a lower incidence of severe wound pain than the wide type patients (GG) and heterozygous genotypes carriers (GA). This result indicated that cathepsin G contributed to the development of severe acute pain after surgery. This is consistent with our animal study showing that cathepsin G may play a role in the development of acute pain via its pro-inflammatory potential (Part 3). Administration of cathepsin G inhibitor TPCK significantly reduced the paw edema induced by CFA injection and thus reversed heat hyperalgesia in animals. Therefore, my finding that genotypes of cathepsin G were associated with the development of acute postoperative pain highlighted that the pro-inflammatory regulation may be a key event during the acute postoperative period. Moreover, my result suggested that the homozygous SNP genotype at rs2236742 may represent a pain protective genotype in acute postoperative pain management. Further studies on other SNPs in linkage disequilibrium may reveal new pain protective halotypes or functional variants that

can affect cathepsin G molecular function.

There was no significant association between chronic postoperative pain and cathepsin G genotypes. This result indicated that cathepsin G was not involved in the development of chronic postoperative pain in contrast to acute postoperative pain. Our expression study suggested that cathepsin G may specifically response to chronic pain induced by CFA injection (inflammatory pain) but not after nerve injury as in chronic constriction injury model. None of the patients who have complained wound pain after 3 months report ongoing wound complication (e.g. dehiscence, infection, gapping). These results indicated that chronic postoperative pain would be more related to neuropathic pain than inflammatory pain. As a matter of fact, another gene that has been identified by our microarray analysis, the brain derived neurotrophic factor (BDNF), which plays important roles in the central sensitization of neuropathic pain (Cejas et al., 2000; Eaton et al., 2002), showed a trend of association between one of its SNPs (rs6265) and chronic postoperative pain (p=0.054). Interestingly, there is no relationship between acute postoperative pain and SNP in BDNF in our cohort (Figure 4-1). Therefore, it seems reasonable to classify postoperative pain by characterizing the genes involved (i.e. inflammatory pain specific genes *versus* neuropathic pain specific genes). As our data had suggested, anti-inflammation such as blockade of cathepsin G may be a good way to control acute postoperative pain,

while prescription to neuropathic pain that regulate BDNF expression would be benefit to the management of chronic postoperative pain.

4.4.2 Limitations of this study

We evaluated the clinical relevance of cathepsin G. Since rs2236742 is located in the intron area of cathepsin G gene, it would be difficult to link genetic polymorphism to molecular function of the protease. Therefore, analysis of other SNPs that are in linkage disequilibrium with this SNP should be performed in future studies. This study however, will help to identify the potential polymorphisms that are of functional concern. We also plan to analyses more SNPs to identify the useful haplotypes as diagnostic markers of postoperative pain.

We failed to determine the association between genotypes of cathepsin G and the development of chronic postoperative pain. Although there may be functional consequences, the results could be biased because of insufficient samples size and relatively low frequency of homozygous SNP (in rs2236742) in the current study.

4.4.3 Conclusion

In this study, we have examined the effects of genotypes of cathepsin G target SNPs on the acute and chronic postoperative pain. We recruited a cohort of 230 patients who received major abdominal surgery. The pain intensity at 24 hours, 48 hours, 72 hours and 3 months after surgery was recorded. The genotypes at rs2070697

or rs2236742 were analyzed using Taqman genotyping assay. The statistical analysis showed that the genotypes at rs2236742 were significantly associated with the development of severe acute postoperative pain. Our study showed that the genotypes of cathepsin G may be an important predictor for the development of sever acute postoperative pain.

Part 5 Conclusions and future perspectives

Chapter 5-1 Conclusions

In this study, microarray analysis was performed to identify the differential genes in the lumbar dorsal horn during development of chronic pain. The chronic pain was induced by intraplantar injection of CFA in the hind paw. Lumbar dorsal horn tissues were harvested without perfusion on day 4 after inflammation induction. The gene expression profiles of control rats and chronic pain rats were then analyzed, respectively. The differential genes were identified by comparing in rats with and without chronic pain. Bioinformatics analysis of differential genes was performed to explain the potential pain control mechanism within the spinal cord during chronic pain development. Functional studies using molecular and cellular biology methods as well as animal behavioral test to evaluate the roles of the selected new nociceptive gene in chronic pain. I found that:

1. A total of 391 genes with at least 1.5 folds of change in chronic pain rats;
2. Among all the differential genes, 188 (48%) genes were up-regulated and 203 (52%) genes were down-regulated within spinal cord during chronic pain; 169 (43%) genes belong to the known genes according to the NCBI gene database;
3. Quantitative RT PCR analysis validated the up-regulation of PDYN, CRH, AIF1L and cathepsin G;
4. A total of 25 of 169 (15%) genes were involved in the regulation of gene

expression;

5. Genes involved in endogenous pain control system were identified, including those belong to the descending pain pathways such as COMT and slc18a2, as well as the target genes of anti-nociceptive glucocorticoid receptors;
6. A total of 10 of 169 (6%) genes belonged to the proteases and protease inhibitors family;
7. Cathepsin G mRNA level was up-regulated in lumbar dorsal horn and down-regulated in DRGs during inflammation induced chronic pain, but there was no change in nerve injury induced chronic pain;
8. Cathepsin G activates p38MAPK-CREB and IκB-NFκB signaling transduction in C6 cells;
9. Cathepsin G increases the phosphorylation of p38MAPK, IκB and STAT3 in primary spinal astrocytes;
10. Cathepsin G treatment induces the gene expression of IL6 and MMP9 in C6 cells and increases the MMP9 activity in C6 cells conditioned medium;
11. Cathepsin G treatment induces p38MAPK dependent gene expression of IL6 and MMP9 in primary spinal astrocytes;
12. Blockade of cathepsin G activity reverses heat hyperalgesia response in acute and chronic phase of inflammatory pain;

13. Genotypes of rs223764 in cathepsin G were significantly associated with the development of severe acute postoperative pain.

This study suggested that transcriptional regulation is an important event during CFA induced chronic pain, not only because a large number of differential genes are identified in the study but also because considerable transcription regulators are identified in the dataset. This study also revealed that endogenous pain control system and proteases family members are regulated within lumbar dorsal horn during CFA induced chronic pain. The *in vitro* studies showed that cathepsin G exerted pro-inflammatory potentials in glial cells, suggesting it might be involved in the central sensitization mechanism of chronic pain development. Consistent with these findings, further *in vivo* studies showed that the blockade of cathepsin G produced analgesic effects not only in the acute phase but also during the chronic phase of CFA induced inflammatory pain. Finally, the clinical study suggested that the genotype in cathepsin G is associated with severe acute postoperative pain for which inflammatory response is likely to be a key mechanism. Therefore this study highlighted that cathepsin G is a new pro-nociceptive gene for inflammatory pain (Figure 5-1). The results from cellular, animal and clinical studies, suggested that cathepsin G might be a new target for the management of pain.

Figure 5-1 Pro-nociceptive role of cathepsin G in the postoprerative pain and CFA induced pain.

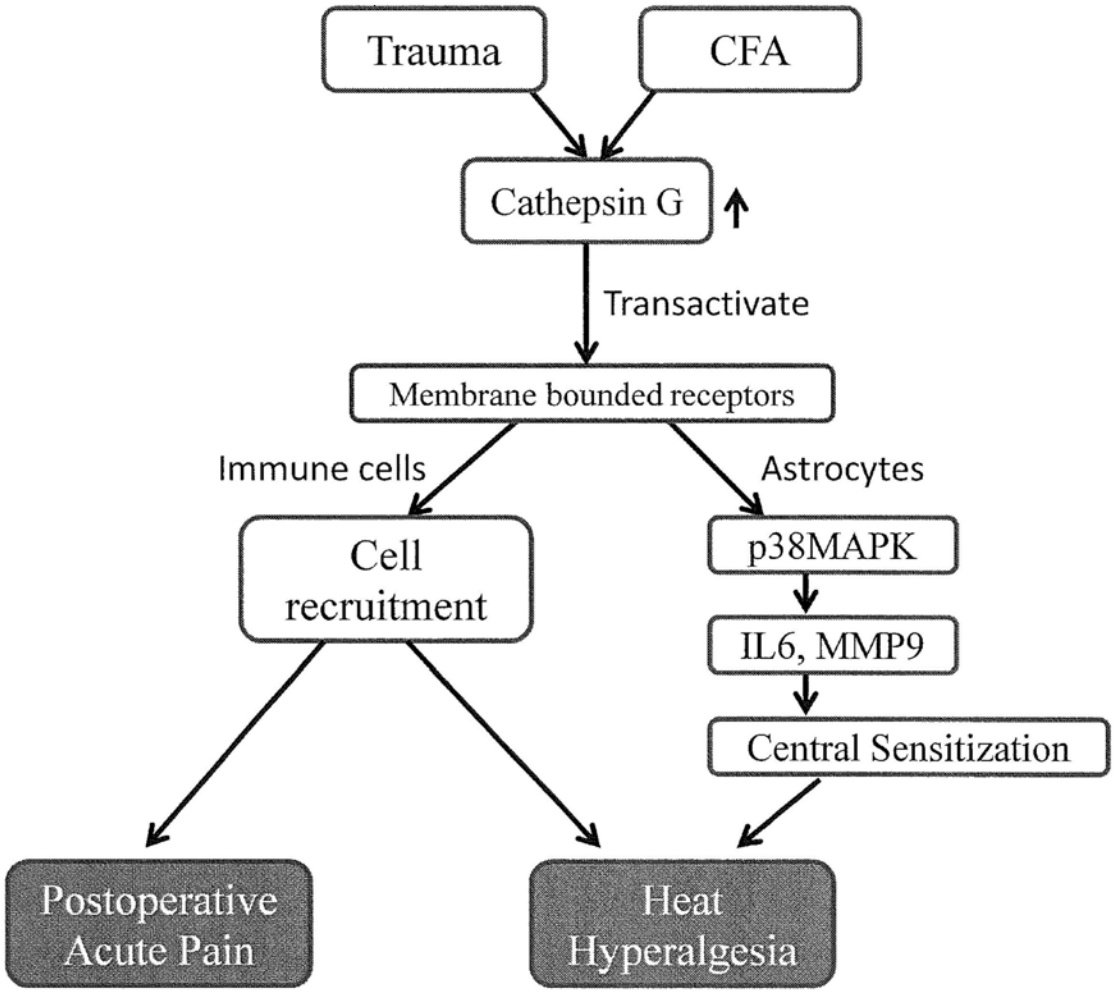

Chapter 5-2 Future perspectives

Our animal behavioral tests suggest that one of the mechanisms for blockade of cathepsin G to reverse inflammatory pain is by inhibiting inflammation in peripheral tissues. However, the pain reversal effect of cathepsin G inhibitor could be passed through a different mechanism. Given that cathepsin G exerted pro-inflammatory potentials on primary spinal astrocytes, the finding suggests that cathepsin G may have a direct effect in spinal cord that may be responsible for the analgesia during CFA induced chronic pain. To prove this, further studies are proposed:

(1) Behavioral test after intrathecal injection of purified cathepsin G;

(2) Behavioral test after intrathecal injection of cathepsin G inhibitors;

(3) Behavioral test after intrathecal co-injection of purified cathepsin G and IL6 neutralized antibody or MMP9 inhibitors.

Part 6 References

Apfelbaum JL, Chen C, Mehta SS, Gan TJ (2003) Postoperative pain experience: results from a national survey suggest postoperative pain continues to be undermanaged *Anesth Analg* **97**: 534-40

Arthur JS, Fong AL, Dwyer JM, Davare M, Reese E, Obrietan K, Impey S (2004) Mitogen- and stress-activated protein kinase 1 mediates cAMP response element-binding protein phosphorylation and activation by neurotrophins *J Neurosci* **24**: 4324-4332

Aun C, Lam YM, Collett B (1986) Evaluation of the use of visual analogue scale in Chinese patients *Pain* **25**: 215-221

Basbaum AI, Bautista DM, Scherrer G, Julius D (2009) Cellular and molecular mechanisms of pain *Cell* **139**: 267-284

Beck IM, Vanden Berghe W, Vermeulen L, Yamamoto KR, Haegeman G, De Bosscher K (2009) Crosstalk in inflammation: the interplay of glucocorticoid receptor-based mechanisms and kinases and phosphatases *Endocr Rev* **30**: 830-882

Berahovich RD, Miao Z, Wang Y, Premack B, Howard MC, Schall TJ (2005) Proteolytic activation of alternative CCR1 ligands in inflammation *J Immunol* **174**: 7341-7351

Bhat NR, Feinstein DL, Shen Q, Bhat AN (2002) p38 MAPK-mediated transcriptional activation of inducible nitric-oxide synthase in glial cells. Roles of nuclear factors, nuclear factor kappa B, cAMP response element-binding protein, CCAAT/enhancer-binding protein-beta, and activating transcription factor-2 *J Biol Chem* **277**: 29584-29592

Binshtok AM, Wang H, Zimmermann K, Amaya F, Vardeh D, Shi L, Brenner GJ, Ji RR, Bean BP, Woolf CJ, Samad TA (2008) Nociceptors are interleukin-1beta sensors *J Neurosci* **28**: 14062-14073

Cao T, Gerard NP, Brain SD (1999) Use of NK(1) knockout mice to analyze substance P-induced edema formation *Am J Physiol* **277**: R476-81

Cejas PJ, Martinez M, Karmally S, McKillop M, McKillop J, Plunkett JA, Oudega M, Eaton MJ (2000) Lumbar transplant of neurons genetically modified to secrete brain-derived neurotrophic factor attenuates allodynia and hyperalgesia after sciatic nerve constriction *Pain* **86**: 195-210

Cheng HY, Pitcher GM, Laviolette SR, Whishaw IQ, Tong KI, Kockeritz LK, Wada T, Joza NA, Crackower M, Goncalves J, Sarosi I, Woodgett JR, Oliveira-dos-Santos AJ, Ikura M, van der Kooy D, Salter MW, Penninger JM (2002) DREAM is a critical transcriptional repressor for pain modulation *Cell* **108**: 31-43

Choi JI, Svensson CI, Koehrn FJ, Bhuskute A, Sorkin LS (2010) Peripheral inflammation induces tumor necrosis factor dependent AMPA receptor trafficking and Akt phosphorylation in spinal cord in addition to pain behavior *Pain* **149**: 243-253

Clark AK, Yip PK, Grist J, Gentry C, Staniland AA, Marchand F, Dehvari M, Wotherspoon G, Winter J, Ullah J, Bevan S, Malcangio M (2007) Inhibition of spinal microglial cathepsin S for the reversal of neuropathic pain *Proc Natl Acad Sci U S A* **104**: 10655-10660

Clark AK, Yip PK, Grist J, Gentry C, Staniland AA, Marchand F, Dehvari M, Wotherspoon G, Winter J, Ullah J, Bevan S, Malcangio M (2007) Inhibition of spinal microglial cathepsin S for the reversal of neuropathic pain *Proc Natl Acad Sci U S A* **104**: 10655-10660

Constantin CE, Mair N, Sailer CA, Andratsch M, Xu ZZ, Blumer MJ, Scherbakov N, Davis JB, Bluethmann H, Ji RR, Kress M (2008) Endogenous tumor necrosis factor alpha (TNFalpha) requires TNF receptor type 2 to generate heat hyperalgesia in a mouse cancer model *J Neurosci* **28**: 5072-5081

Costigan M, Moss A, Latremoliere A, Johnston C, Verma-Gandhu M, Herbert TA, Barrett L, Brenner GJ, Vardeh D, Woolf CJ, Fitzgerald M (2009) T-cell infiltration and signaling in the adult dorsal spinal cord is a major contributor to neuropathic pain-like hypersensitivity *J Neurosci* **29**: 14415-14422

Dinkel K, Ogle WO, Sapolsky RM (2002) Glucocorticoids and central nervous system inflammation *J Neurovirol* **8**: 513-528

Eaton MJ, Blits B, Ruitenberg MJ, Verhaagen J, Oudega M (2002) Amelioration of chronic neuropathic pain after partial nerve injury by adeno-associated viral (AAV) vector-mediated over-expression of BDNF in the rat spinal cord *Gene Ther* **9**: 1387-1395

Egozi EI, Ferreira AM, Burns AL, Gamelli RL, Dipietro LA (2003) Mast cells modulate the inflammatory but not the proliferative response in healing wounds *Wound Repair Regen* **11**: 46-54

Ephraim PL, Wegener ST, MacKenzie EJ, Dillingham TR, Pezzin LE (2005) Phantom pain, residual limb pain, and back pain in amputees: results of a national survey *Arch Phys Med Rehabil* **86**: 1910-1919

Fujiwara M, Jin E, Ghazizadeh M, Kawanami O (2005) Activation of PAR4 induces a distinct actin fiber formation via p38 MAPK in human lung endothelial cells *J Histochem Cytochem* **53**: 1121-1129

Fukuizumi T, Ohkubo T, Kitamura K (2003) Spinal sensitization mechanism in vincristine-induced hyperalgesia in mice *Neurosci Lett* **343**: 89-92

Gao YJ and Ji RR (2009) c-Fos and pERK, which is a better marker for neuronal activation and central sensitization after noxious stimulation and tissue injury? *Open Pain J* **2**: 11-17

Goettl VM, Huang Y, Hackshaw KV, Stephens RL,Jr (2002) Reduced basal release of serotonin from the ventrobasal thalamus of the rat in a model of neuropathic pain *Pain* **99**: 359-366

Gopalakrishnan A, Sievert M, Ruoho AE (2007) Identification of the substrate binding region of vesicular monoamine transporter-2 (VMAT-2) using iodoaminoflisopolol as a novel photoprobe *Mol Pharmacol* **72**: 1567-1575

Gu X, Peng L, Yang D, Ma Q, Zheng Y, Liu C, Zhu B, Song L, Sun X, Ma Z (2011) The respective and interaction effects of spinal GRs and MRs on radicular pain induced by chronic compression of the dorsal root ganglion in the rat. *Brain Res* **1396**: 88-95

Hains BC, Everhart AW, Fullwood SD, Hulsebosch CE (2002) Changes in serotonin, serotonin transporter expression and serotonin denervation supersensitivity: involvement in chronic central pain after spinal hemisection in the rat *Exp Neurol* **175**: 347-362

Han YP, Yan C, Zhou L, Qin L, Tsukamoto H (2007) A matrix metalloproteinase-9 activation cascade by hepatic stellate cells in trans-differentiation in the three-dimensional extracellular matrix *J Biol Chem* **282**: 12928-12939

Hao S, Mata M, Glorioso JC, Fink DJ (2006) HSV-mediated expression of interleukin-4 in dorsal root ganglion neurons reduces neuropathic pain *Mol Pain* **2**: 6

Hazuda DJ, Strickler J, Kueppers F, Simon PL, Young PR (1990) Processing of precursor interleukin 1 beta and inflammatory disease *J Biol Chem* **265**: 6318-6322

Honma K, Kimura D, Tominaga N, Miyakoda M, Matsuyama T, Yui K (2008) Interferon regulatory factor 4 differentially regulates the production of Th2 cytokines in naive vs. effector/memory CD4+ T cells *Proc Natl Acad Sci USA* **105**: 15890-15895

Hou WY, Shyu BC, Chen TM, Lee JW, Shieh JY, Sun WZ (1997) Intrathecally administered c-fos antisense oligodeoxynucleotide decreases formalin-induced nociceptive behavior in adult rats *Eur J Pharmacol* **329**: 17-26

Houle S, Papez MD, Ferazzini M, Hollenberg MD, Vergnolle N (2005) Neutrophils and the kallikrein-kinin system in proteinase-activated receptor 4-mediated inflammation in rodents *Br J Pharmacol* **146**: 670-678

Ji RR, Kohno T, Moore KA, Woolf CJ (2003) Central sensitization and LTP: do pain and memory share similar mechanisms? *Trends Neurosci* **26**: 696-705

Kambur O and Mannisto PT (2010) Catechol-O-methyltransferase and pain. *Int Rev Neurobiol* **95**: 227-279

Karin M (1999) How NF-kappaB is activated: the role of the IkappaB kinase (IKK) complex *Oncogene* **18**: 6867-6874

Kawasaki Y, Kohno T, Zhuang ZY, Brenner GJ, Wang H, Van Der Meer C, Befort K, Woolf CJ, Ji RR (2004) Ionotropic and metabotropic receptors, protein kinase A, protein kinase C, and Src contribute to C-fiber-induced ERK activation and cAMP response element-binding protein phosphorylation in dorsal horn neurons, leading to central sensitization *J Neurosci* **24**: 8310-8321

Kawasaki Y, Xu ZZ, Wang X, Park JY, Zhuang ZY, Tan PH, Gao YJ, Roy K, Corfas G, Lo EH, Ji RR (2008) Distinct roles of matrix metalloproteases in the early- and late-phase development of neuropathic pain *Nat Med* **14**: 331-336

Kiguchi N, Kobayashi Y, Maeda T, Saika F, Kishioka S (2010) CC-chemokine MIP-1α in the spinal cord contributes to nerve injury-induced neuropathic pain. *Neurosci Lett* **484**: 17-21

King BR and Nicholson RC (2007) Advances in understanding corticotrophin-releasing hormone gene expression *Front Biosci* **12**: 581-590

Kuner R (2010) Central mechanisms of pathological pain. *Nat Med* **16**: 1258-1266

Lee KM, Kang BS, Lee HL, Son SJ, Hwang SH, Kim DS, Park JS, Cho HJ (2004) Spinal NF-kB activation induces COX-2 upregulation and contributes to inflammatory pain hypersensitivity *Eur J Neurosci* **19**: 3375-3381

Liang KC, Lee CW, Lin WN, Lin CC, Wu CB, Luo SF, Yang CM (2007) Interleukin-1beta induces MMP-9 expression via p42/p44 MAPK, p38 MAPK, JNK, and nuclear factor-kappaB signaling pathways in human tracheal smooth muscle cells *J Cell Physiol* **211**: 759-770

Liu F, Qu X, Ding X, Cai J, Jiang H, Wan Y, Han J, Xing G (2010) Decrease in the descending inhibitory 5-HT system in rats with spinal nerve ligation. *Brain Res* **1330**: 45-60

Ma W, Hatzis C, Eisenach JC (2003) Intrathecal injection of cAMP response element binding protein (CREB) antisense oligonucleotide attenuates tactile allodynia caused by partial sciatic nerve ligation *Brain Res* **988**: 97-104

Ma X, Reynolds SL, Baker BJ, Li X, Benveniste EN, Qin H (2010) IL-17 enhancement of the IL-6 signaling cascade in astrocytes *J Immunol* **184**: 4898-4906

Mao Y, Zhang M, Tuma RF, Kunapuli SP (2010) Deficiency of PAR4 attenuates cerebral ischemia/reperfusion injury in mice *J Cereb Blood Flow Metab* **30**: 1044-1052

Meisner JG, Marsh AD, Marsh DR (2010) Loss of GABAergic interneurons in laminae I-III of the spinal cord dorsal horn contributes to reduced GABAergic tone and neuropathic pain after spinal cord injury *J Neurotrauma* **27**: 729-737

Melemedjian OK, Asiedu MN, Tillu DV, Peebles KA, Yan J, Ertz N, Dussor GO, Price TJ (2010) IL-6- and NGF-induced rapid control of protein synthesis and nociceptive plasticity via convergent signaling to the eIF4F complex *J Neurosci* **30**: 15113-15123

Meng ZY (2010) Genetic determinants of postoperative pain. Master of Philosophy thesis of the Chinese University of Hong Kong

Mezyk-Kopec R, Bzowska M, Bzowska M, Mickowska B, Mak P, Potempa J, Bereta J (2005) Effects of elastase and cathepsin G on the levels of membrane and soluble TNFalpha *Biol Chem* **386**: 801-811

Milligan ED and Watkins LR (2009) Pathological and protective roles of glia in chronic pain *Nat Rev Neurosci* **10**: 23-36

Mitchell K, Yang HY, Tessier PA, Muhly WT, Swaim WD, Szalayova I, Keller JM, Mezey E, Iadarola MJ (2008) Localization of S100A8 and S100A9 expressing

neutrophils to spinal cord during peripheral tissue inflammation *Pain* **134**: 216-231

Moriuchi H, Moriuchi M, Fauci AS (2000) Cathepsin G, a neutrophil-derived serine protease, increases susceptibility of macrophages to acute human immunodeficiency virus type 1 infection *J Virol* **74**: 6849-6855

Myles PS, Troedel S, Boquest M, Reeves M (1999) The pain visual analog scale: is it linear or nonlinear? *Anesth Analg* **89**: 1517-1520

Nakae A, Nakai K, Tanaka T, Hagihira S, Shibata M, Ueda K, Masimo T (2008) The role of RNA editing of the serotonin 2C receptor in a rat model of oro-facial neuropathic pain *Eur J Neurosci* **27**: 2373-2379

Nesic O, Lee J, Johnson KM, Ye Z, Xu GY, Unabia GC, Wood TG, McAdoo DJ, Westlund KN, Hulsebosch CE, Regino Perez-Polo J (2005) Transcriptional profiling of spinal cord injury-induced central neuropathic pain *J Neurochem* **95**: 998-1014

Obreja O, Rathee PK, Lips KS, Distler C, Kress M (2002) IL-1 beta potentiates heat-activated currents in rat sensory neurons: involvement of IL-1RI, tyrosine kinase, and protein kinase C *FASEB J* **16**: 1497-1503

Oh SB, Tran PB, Gillard SE, Hurley RW, Hammond DL, Miller RJ (2001) Chemokines and glycoprotein120 produce pain hypersensitivity by directly exciting primary nociceptive neurons *J Neurosci* **21**: 5027-5035

Ossipov MH, Dussor GO, Porreca F (2010) Central modulation of pain *J Clin Invest* **120**: 3779-3787

Ossovskaya VS and Bunnett NW (2004) Protease-activated receptors: contribution to physiology and disease *Physiol Rev* **84**: 579-621

Padi SS and Kulkarni SK (2008) Minocycline prevents the development of neuropathic pain, but not acute pain: possible anti-inflammatory and antioxidant mechanisms *Eur J Pharmacol* **601**: 79-87

Pertovaara A, Almeida A (2006) Chapter 13 Descending inhibitory systems Handb Clin Neurol **81**: 179-92

Pham CT (2006) Neutrophil serine proteases: specific regulators of inflammation *Nat Rev Immunol* **6**: 541-550

Pietrobon D (2010) Insights into migraine mechanisms and CaV2.1 calcium channel function from mouse models of familial hemiplegic migraine *J Physiol* **588**: 1871-1878

Priestley JV, Michael GJ, Averill S, Liu M, Willmott N (2002) Regulation of nociceptive neurons by nerve growth factor and glial cell line derived neurotrophic factor *Can J Physiol Pharmacol* **80**: 495-505

Rafiq K, Hanscom M, Valerie K, Steinberg SF, Sabri A (2008) Novel mode for neutrophil protease cathepsin G-mediated signaling: membrane shedding of epidermal growth factor is required for cardiomyocyte anoikis *Circ Res* **102**: 32-41

Ranganath S, Ouyang W, Bhattarcharya D, Sha WC, Grupe A, Peltz G, Murphy KM (1998) GATA-3-dependent enhancer activity in IL-4 gene regulation *J Immunol* **161**: 3822-3826

Reich NC and Liu L (2006) Tracking STAT nuclear traffic *Nat Rev Immunol* **6**: 602-612

Ren K and Dubner R (2010) Interactions between the immune and nervous systems in pain *Nat Med* **16**: 1267-1276

Rengarajan J, Mowen KA, McBride KD, Smith ED, Singh H, Glimcher LH (2002) Interferon regulatory factor 4 (IRF4) interacts with NFATc2 to modulate interleukin 4 gene expression *J Exp Med* **195**: 1003-1012

Rittner HL, Machelska H, Stein C (2005) Leukocytes in the regulation of pain and analgesia *J Leukoc Biol* **78**: 1215-1222

Sabri A, Alcott SG, Elouardighi H, Pak E, Derian C, Andrade-Gordon P, Kinnally K, Steinberg SF (2003) Neutrophil cathepsin G promotes detachment-induced cardiomyocyte apoptosis via a protease-activated receptor-independent mechanism *J Biol Chem* **278**: 23944-23954

Scholz J, Broom DC, Youn DH, Mills CD, Kohno T, Suter MR, Moore KA, Decosterd I, Coggeshall RE, Woolf CJ (2005) Blocking caspase activity prevents transsynaptic neuronal apoptosis and the loss of inhibition in lamina II of the dorsal horn after peripheral nerve injury *J Neurosci* **25**: 7317-7323

Schwarzer C (2009) 30 Years of Dynorphins--New Insights on their Functions in Neuropsychiatric Diseases *Pharmacol Ther* **123**: 353-370

Sharony R, Yu PJ, Park J, Galloway AC, Mignatti P, Pintucci G (2010) Protein targets of inflammatory serine proteases and cardiovascular disease *J Inflamm (Lond)* **7**: 45, doi:10.1186/1476-9255-7-45

Shubayev VI, Angert M, Dolkas J, Campana WM, Palenscar K, Myers RR (2006) TNFalpha-induced MMP-9 promotes macrophage recruitment into injured peripheral nerve *Mol Cell Neurosci* **31**: 407-415

Song XS, Cao JL, Xu YB, He JH, Zhang LC, Zeng YM (2005) Activation of ERK/CREB pathway in spinal cord contributes to chronic constrictive injury-induced neuropathic pain in rats *Acta Pharmacol Sin* **26**: 789-798

Sounvoravong S, Nakashima MN, Wada M, Nakashima K (2004) Decrease in serotonin concentration in raphe magnus nucleus and attenuation of morphine analgesia in two mice models of neuropathic pain. *Eur J Pharmacol* **484**: 217-223

Suter MR, Wen YR, Decosterd I, Ji RR (2007) Do glial cells control pain? *Neuron Glia Biol* **3**: 255-268

Tak PP and Firestein GS (2001) NF-kappaB: a key role in inflammatory diseases *J Clin Invest* **107**: 7-11

Tsuda M, Kohro Y, Yano T, Tsujikawa T, Kitano J, Tozaki-Saitoh H, Koyanagi S, Ohdo S, Ji RR, Salter MW, Inoue K (2011) JAK-STAT3 pathway regulates

spinal astrocyte proliferation and neuropathic pain maintenance in rats *Brain* **134**: 1127-1139

Vergnolle N (2009) Protease-activated receptors as drug targets in inflammation and pain *Pharmacol Ther* **123**: 292-309

Vergnolle N, Derian CK, D'Andrea MR, Steinhoff M, Andrade-Gordon P (2002) Characterization of thrombin-induced leukocyte rolling and adherence: a potential proinflammatory role for proteinase-activated receptor-4 *J Immunol* **169**: 1467-1473

Walsh J, Tighe O, Lai D, Harvey R, Karayiorgou M, Gogos JA, Waddington JL, O'Tuathaigh CM (2010) Disruption of thermal nociceptive behaviour in mice mutant for the schizophrenia-associated genes NRG1, COMT and DISC1. *Brain Res* **1348**: 114-119

Wang XS, Mendoza TR, Gao SZ, Cleeland CS (1996) The Chinese version of the Brief Pain Inventory (BPI-C): its development and use in a study of cancer pain *Pain* **67**: 407-416

Warner FJ, Smith AI, Hooper NM, Turner AJ (2004) Angiotensin-converting enzyme-2: a molecular and cellular perspective *Cell Mol Life Sci* **61**: 2704-2713

Watkins LR, Milligan ED, Maier SF (2001) Glial activation: a driving force for pathological pain *Trends Neurosci* **24**: 450-455

Wei F, Guo W, Zou S, Ren K, Dubner R (2008) Supraspinal glial-neuronal interactions contribute to descending pain facilitation *J Neurosci* **28**: 10482-10495

Weyerbacher AR, Xu Q, Tamasdan C, Shin SJ, Inturrisi CE (2010) N-Methyl-D-aspartate receptor (NMDAR) independent maintenance of inflammatory pain *Pain* **148**: 237-246

Wilson TJ, Nannuru KC, Futakuchi M, Sadanandam A, Singh RK (2008) Cathepsin G enhances mammary tumor-induced osteolysis by generating soluble receptor activator of nuclear factor-kappaB ligand *Cancer Res* **68**: 5803-5811

Wilson TJ, Nannuru KC, Futakuchi M, Sadanandam A, Singh RK (2008) Cathepsin G enhances mammary tumor-induced osteolysis by generating soluble receptor activator of nuclear factor-kappaB ligand *Cancer Res* **68**: 5803-5811

Wilson TJ, Nannuru KC, Futakuchi M, Singh RK (2010) Cathepsin G-mediated enhanced TGF-beta signaling promotes angiogenesis via upregulation of VEGF and MCP-1 *Cancer Lett* **288**: 162-169, doi:10.1016/j.canlet.2009.06.035

Wilson TJ, Nannuru KC, Singh RK (2009) Cathepsin G recruits osteoclast precursors via proteolytic activation of protease-activated receptor-1 *Cancer Res* **69**: 3188-3195

Wilson TJ, Nannuru KC, Singh RK (2009) Cathepsin G-mediated activation of pro-matrix metalloproteinase 9 at the tumor-bone interface promotes transforming growth factor-beta signaling and bone destruction *Mol Cancer Res* **7**: 1224-1233

Woolf CJ and Costigan M (1999) Transcriptional and posttranslational plasticity and the generation of inflammatory pain *Proc Natl Acad Sci USA* **96**: 7723-7730

Wu SX, Wang W, Wang YY, Ni TS, Li YQ, Yew DT (2002) C-fos antisense oligodeoxynucleotide decreases subcutaneous bee venom injection-induced nociceptive behavior and fos expression in the rat *Neurosignals* **11**: 224-230

Xia Y and Zhai Q (2010) IL-1β enhances the antibacterial activity of astrocytes by activation of NF-κB. *Glia* **58**: 244-252

Xing J, Kornhauser JM, Xia Z, Thiele EA, Greenberg ME (1998) Nerve growth factor activates extracellular signal-regulated kinase and p38 mitogen-activated protein

kinase pathways to stimulate CREB serine 133 phosphorylation *Mol Cell Biol* **18**: 1946-1955

Yoon S, Woo SU, Kang JH, Kim K, Kwon MH, Park S, Shin HJ, Gwak HS, Chwae YJ (2010) STAT3 transcriptional factor activated by reactive oxygen species induces IL6 in starvation-induced autophagy of cancer cells. **6**: 1125-1138

Zhang J, Shi XQ, Echeverry S, Mogil JS, De Koninck Y, Rivest S (2007) Expression of CCR2 in both resident and bone marrow-derived microglia plays a critical role in neuropathic pain *J Neurosci* **27**: 12396-12406

Zhang N, Inan S, Cowan A, Sun R, Wang JM, Rogers TJ, Caterina M, Oppenheim JJ (2005) A proinflammatory chemokine, CCL3, sensitizes the heat- and capsaicin-gated ion channel TRPV1 *Proc Natl Acad Sci U S A* **102**: 4536-4541

Zhang RX, Li A, Liu B, Wang L, Ren K, Zhang H, Berman BM, Lao L (2008) IL-1ra alleviates inflammatory hyperalgesia through preventing phosphorylation of NMDA receptor NR-1 subunit in rats *Pain* **135**: 232-239

Zhang Y, Li Y, Yang YR, Zhu HH, Han JS, Wang Y (2007) Distribution of downstream regulatory element antagonist modulator (DREAM) in rat spinal

cord and upregulation of its expression during inflammatory pain. *Neurochem Res* **32**: 1592-1599

Zhang Y, Wang X, Ennis M (2010) Effects of neonatal inflammation on descending modulation from the rostroventromedial medulla. *Brain Res Bull* **83**: 16-22

Appendix 1. Down-regulated known genes in spinal dorsal horn after CFA injection.

Gene Symbol	Genbank Accession	Gene Name	Fold Change
Abca13	NM_001106020	ATP-binding cassette, sub-family A (ABC1), member 13	1.74
Abcc6	NM_031013	ATP-binding cassette, sub-family C (CFTR/MRP), member 6	1.74
Actbl2	NM_001106409	actin, beta-like 2	1.81
Adamts6	NM_001108544	ADAM metallopeptidase with thrombospondin type 1 motif, 6	1.85
Amot	XM_235733	angiomotin	2.16
Apoa2	NM_013112	apolipoprotein A-II	2.24
Arnt	NM_012780	aryl hydrocarbon receptor nuclear translocator	2.28
Asb18	NM_001108231	ankyrin repeat and SOCS box-containing 18	1.89
Bach1	NM_001107113	BTB and CNC homology 1, basic leucine zipper transcription factor 1	1.78
Bard1	NM_022622	BRCA1 associated RING domain 1	1.65
Ccdc112	NM_001109124	coiled-coil domain containing 112	2.27
Cdkn2a	NM_031550	cyclin-dependent kinase inhibitor 2A	1.51
Clec2d	AF321552	C-type lectin domain family 2, member d	1.95
Clec2d	AF321552	C-type lectin domain family 2, member d	1.62
Comt	NM_012531	catechol-O-methyltransferase	2.22
Cox8b	AI103885	cytochrome c oxidase, subunit VIIIb	2.11
Crebl2	NM_001015027	cAMP responsive element binding protein-like 2	1.74
Ctsq	BC107913	cathepsin Q	1.51
Cyr61	NM_031327	cysteine-rich, angiogenic inducer, 61	3.76
Dnase2b	NM_021664	deoxyribonuclease II beta	1.59
Dsp	BC098071	desmoplakin	2.19
Dusp1	NM_053769	dual specificity phosphatase 1	1.84
Es22	NM_031565	esterase 22	2.18
Esr2	NM_012754	estrogen receptor 2 (ER beta)	1.66
Fam129c	NM_001100908	family with sequence similarity 129, member C	1.52
Fer1l4	NM_001106534	fer-1-like 4 (C. elegans)	2.04
Fibcd1	NM_001107829	fibrinogen C domain containing 1	2.13
Foxd2	L13192	forkhead box D2	1.95
Gapdhs	NM_023964	glyceraldehyde-3-phosphatedehydrogenase,spermatogenic	2.09

Appendix 1. Down-regulated known genes in spinal dorsal horn after CFA injection. (continued)

Gata3	NM_133293	GATA binding protein 3	6.36
Gpha2	NM_133619	glycoprotein hormone alpha 2	1.58
Gpr176	S73608	G protein-coupled receptor 176	1.61
Guca1b	NM_001108198	guanylate cyclase activator 1B	1.52
Havcr1	NM_173149	hepatitis A virus cellular receptor 1	1.86
Hoxc11	XM_001068573	homeobox C11	3.04
Hs3st3b1	XM_220557	heparan sulfate (glucosamine) 3-O-sulfotransferase 3B1	1.89
Hsn2	NM_001002823	hereditary sensory neuropathy, type II	1.87
Ifi44	NM_001107729	interferon-induced protein 44	1.94
Ifit3	NM_001007694	interferon-induced protein with tetratricopeptide repeats 3	2.79
Irf7	NM_001033691	interferon regulatory factor 7	1.75
Isg15	NM_001106700	ISG15 ubiquitin-like modifier	1.97
Kcnk6	NM_053806	potassium channel, subfamily K, member 6	1.53
Klf14	NM_001135094	Kruppel-like factor 14	2.23
Klf4	NM_053713	Kruppel-like factor 4 (gut)	1.52
Lamp3	NM_001012015	lysosomal-associated membrane protein 3	1.96
LOC365778	NM_001014251	similar to RIKEN cDNA 1700034I23	2.54
LOC500300	NM_001024334	similar to hypothetical protein MGC6835	2.88
LOC683720	XR_009563	similar to keratin 6L	1.58
Mbtps2	NM_001035007	membrane-bound transcription factor peptidase, site 2	1.53
Mylk	NM_001105874	myosin light chain kinase	2.48
Nkapl	NM_001029913	NFKB activating protein-like	2.86
Nlrp1	NM_001145755	NLR family, pyrin domain containing 1	1.98
Olr193	NM_001000186	olfactory receptor 193	1.76
Olr196	NM_001000187	olfactory receptor 196	1.83
Olr375	NM_001000259	olfactory receptor 375	2.13
Olr654	NM_001000636	olfactory receptor 654	16.19
Olr687	NM_001000356	olfactory receptor 687	2.10
Olr95	NM_001001024	olfactory receptor 95	2.10
Olr962	NM_001000487	olfactory receptor 962	2.75
Phox2a	NM_053869	paired-like homeobox 2a	1.69
Ptprc	NM_138507	protein tyrosine phosphatase, receptor type, C	1.62
Rbm27	NM_001108429	RNA binding motif protein 27	1.70
Rbm47	NM_001005882	RNA binding motif protein 47	1.88
RGD1562720	NM_001109240	similar to hypothetical protein FLJ25369	1.70

Appendix 1. Down-regulated known genes in spinal dorsal horn after CFA injection. (continuned)

RGD1563060	NM_001106149	similar to AVLV472	2.45
RGD1563281	XM_001081403	similar to leucine-rich repeat domain-containing protein	1.52
Rgs1	NM_019336	regulator of G-protein signaling 1	1.63
Ropn1	NM_001025628	ropporin, rhophilin associated protein 1	7.02
Serpine1	NM_012620	serine (or cysteine) peptidase inhibitor, clade E, member 1	2.65
Slc18a2	NM_013031	solute carrier family 18 (vesicular monoamine), member 2	1.83
Slc22a25	NM_138908	solute carrier family 22, member 25	1.51
Slc2a2	NM_012879	solute carrier family 2 (facilitated glucose transporter), member 2	2.04
Svs3b	NM_001102417	seminal vesicle secretory protein 3B	2.74
Tmem82	XM_238429	transmembrane protein 82	2.15
Tox2	NM_199392	TOX high mobility group box family member 2	1.62
Ttll6	XM_220904	tubulin tyrosine ligase-like family, member 6	2.32
Upb1	NM_053845	ureidopropionase, beta	2.16
Usp18	NM_001014058	ubiquitin specific peptidase 18	1.74
Utrn	NM_013070	utrophin	1.63
V1ra16	NM_153729	vomeronasal 1 receptor, A16"	2.61
Zc3hav1	NM_173045	zinc finger CCCH type, antiviral 1	1.58
Zfp52	NM_001014158	zinc finger protein 52	1.90

Appendix 2. Up-regulated known genes in spinal dorsal horn after CFA injection.

Gene Symbol	Genbank Accession	Gene Name	Fold Change
Abca4	NM_001107721	ATP-binding cassette, sub-family A (ABC1), member 4	2.21
Ace2	NM_001012006	angiotensin I converting enzyme (peptidyl-dipeptidase A) 2	1.77
Aifl1	NM_001108578	allograft inflammatory factor 1-like	3.35
Als2cr12	NM_001014101	amyotrophic lateral sclerosis 2 (juvenile) chromosome region, candidate 12 (human)	1.76
Bdnf	NM_012513	brain derived neurotrophic factor	2.33
C1ql3	NM_001109403	complement component 1, q subcomponent-like 3	1.52
Ccnt1	NM_001108110	cyclin T1	1.84
Cd109	NM_001108771	CD109 molecule	1.57
Cdo1	NM_052809	cysteine dioxygenase, type I	1.69
Cenpf	NM_001100827	centromere protein F	4.08
Cgn	XM_227472	cingulin	1.83
Chl1	AF069775	cell adhesion molecule with homology to L1CAM	1.67
Cobl	NM_001107236	cordon-bleu homolog (mouse)	1.53
Crh	NM_031019	corticotropin releasing hormone	3.07
Cryba1	AF013248	crystallin, beta A1	2.07
Ctsg	NM_001106041	cathepsin G	6.17
Dennd2c	EV774482	DENN/MADD domain containing 2C	2.08
Dhx32	NM_001130039	DEAH (Asp-Glu-Ala-His) box polypeptide 32	1.78
Dmbx1	NM_001107961	diencephalon/mesencephalon homeobox 1	1.69
Dmgdh	NM_139102	dimethylglycine dehydrogenase	1.83
Dppa3	NM_001047864	developmental pluripotency-associated 3	1.63
Enc1	NM_001003401	ectodermal-neural cortex 1	1.78
Fgg	NM_012559	fibrinogen gamma chain	2.63
Foxa2	NM_012743	forkhead box A2	3.08
Fshr	NM_199237	follicle stimulating hormone receptor	2.05
Gjb3	NM_019240	gap junction protein, beta 3	1.59
Gpr156	NM_153295	G protein-coupled receptor 156	2.05
Gykl1	NM_134341	glycerol kinase-like 1	2.02
Hmha1	NM_001108067	histocompatibility (minor) HA-1	1.73

Appendix 2. Up-regulated known genes in spinal dorsal horn after CFA injection. (continuned)

Igfbp5	NM_012817	insulin-like growth factor binding protein 5	1.68
Irf4	NM_001106108	interferon regulatory factor 4	2.77
Itpripl1	NM_001025043	inositol 1,4,5-triphosphate receptor interacting protein-like 1	1.78
Kb15	NM_001008825	type II keratin Kb15	1.71
Kcne2	NM_133603	potassium voltage-gated channel, Isk-related subfamily, gene 2	1.70
Kcnip1	NM_022929	Kv channel-interacting protein 1	3.07
Kcnq1	NM_032073	potassium voltage-gated channel, KQT-like subfamily, member 1	1.64
LOC100364673	NM_001177905	hypercoagulability-related protein-like	2.21
LOC498222	NM_001100788	similar to specifically androgen-regulated protein	1.80
LOC687105	NM_001127591	hypothetical protein LOC687105	1.76
Mphosph6	XM_001080959	M phase phosphoprotein 6	1.84
Mttp	NM_001107727	microsomal triglyceride transfer protein	1.92
Mybl1	NM_001106632	myeloblastosis oncogene-like 1	2.13
Nccrp1	NM_001134506	non-specific cytotoxic cell receptor protein 1 homolog (zebrafish)	1.95
Npy1r	NM_001113357	neuropeptide Y receptor Y1	4.02
Nudcd1	NM_001130561	NudC domain containing 1	1.96
Olr1399	NM_001001095	olfactory receptor 1399	2.37
Omp	NM_012616	olfactory marker protein	2.09
Pdyn	NM_019374	prodynorphin	3.46
Phf17	NM_001107670	PHD finger protein 17	1.83
Pla2g2a	NM_031598	phospholipase A2, group IIA (platelets, synovial fluid)	1.80
Plekha5	XM_342781	pleckstrin homology domain containing, family A member 5	2.37
Prosapip1	NM_172022	ProSAPiP1 protein	2.18
Prss21	NM_181477	protease, serine, 21	1.55
Rabggtb	NM_138708	Rab geranylgeranyltransferase, beta subunit	1.87
Rbm3	NM_053696	RNA binding motif (RNP1, RRM) protein 3	1.51
Rbpjl	NM_001108604	recombination signal binding protein for immunoglobulin kappa J region-like	1.68
RGD1304731	NM_001106139	similar to RIKEN cDNA 5330437I02 gene	2.22

Appendix 2. Up-regulated known genes in spinal dorsal horn after CFA injection. (continuned)

RGD1307368	NM_001144850	similar to prosaposin (variant Gaucher disease and variant metachromatic leukodystrophy); Prosaposin (sphingolipid activator protein-1)	2.65
RGD1310251	NM_001024240	similar to RIKEN cDNA 2010001M09	1.80
RGD1563100	XM_001069698	similar to KIAA0089	2.00
RGD1564340	NM_001134620	similar to hypothetical protein MGC5356	1.81
RGD1565560	XM_001060544	similar to ribosomal protein S11	2.45
RGD1566386	NM_001107127	similar to Hypothetical protein A430033K04	2.08
Rhbdf2	NM_001107067	rhomboid 5 homolog 2 (Drosophila)	1.64
Rpap3	NM_001004243	RNA polymerase II associated protein 3	1.54
Rxfp3	NM_001008310	relaxin/insulin-like family peptide receptor 3	1.90
Sacs	XM_224256	spastic ataxia of Charlevoix-Saguenay (sacsin)	2.13
Scrn3	EV774910	secernin 3	1.51
Serpina5	NM_022957	serine (or cysteine) peptidase inhibitor, clade A, member 5	1.63
Sftpb	NM_138842	surfactant protein B	1.81
Sla	NM_178097	src-like adaptor	1.63
Sorcs1	XM_220080	sortilin-related VPS10 domain containing receptor 1	1.51
Spag16	NM_001134728	sperm associated antigen 16	1.82
Spint2	NM_199087	serine peptidase inhibitor, Kunitz type, 2	2.01
St6gal1	NM_147205	ST6 beta-galactosamide alpha-2,6-sialyltranferase 1	1.79
Stac3	NM_001130558	SH3 and cysteine rich domain 3	2.41
Stag1	NM_001108179	stromal antigen 1	3.03
Syt16	XM_234300	synaptotagmin XVI	1.74
Tll1	NM_001106081	tolloid-like 1	1.74
Ttc23l	XM_577993	tetratricopeptide repeat domain 23-like	2.35
Ttc8	NM_001106752	tetratricopeptide repeat domain 8	2.17
Vof16	NM_147207	ischemia related factor vof-16	1.58
Vom2r45	AF318940	vomeronasal 2 receptor, 45	1.74
Vwa3b	XM_001055017	von Willebrand factor A domain containing 3B	1.97
Zc3h6	NM_001107772	zinc finger CCCH type containing 6	2.62
Zfp382	NM_144749	zinc finger protein 382	1.57